FINGERTIP ECG SIGNAL BASED BIOMETRIC RECOGNITION SYSTEM

GÖKHAN GÜVEN

IŞIK UNIVERSITY

2016

FINGERTIP ECG SIGNAL BASED BIOMETRIC RECOGNITION SYSTEM

GÖKHAN GÜVEN

B.S., Electronics Engineering, Işık University, 2014

Submitted to the Graduate School of Işık University

In partial fulfillment of the requirements for the degree of

Master of Science

in

Electronics Engineering

IŞIK UNIVERSITY

2016

IŞIK UNIVERSITY

GRADUATE SCHOOL OF SCIENCE AND ENGINEERING

FINGERTIP ECG SIGNAL BASED BIOMETRIC RECOGNITION SYSTEM

GÖKHAN GÜVEN

APPROVED BY:

Assoc. Prof. Hakan Gürkan   Işık University

Thesis Supervisor (Thesis Co-Advisor: Assoc. Prof. Ümit Güz)   _____

Assist. Prof. Sakip Önder   Işık University   _____

Prof. Dr. Serdar Özoğuz   Istanbul Technical University   _____

APPROVAL DATE: 10.05.2016

FINGERTIP ECG SIGNAL BASED BIOMETRIC RECOGNITION SYSTEM

Abstract

The idea is the; realize biometric recognition system by using ECG signal which was began to use in the last 10 years.

Until now, ECG based biometric systems have been developed by using the database which ECG signals are taken from the subjects' chest by using patient monitor or high speed data acquisition systems. For constructing database, most researchers have used three disposable ECG electrodes on subjects' chest to extract the ECG signal. Because of that, ECG based biometric systems were being considered hard to use. For this reason, we want to make a system that is easy to carry, and easy to apply on subjects.

In most of biometric systems, ECG database have constructed by using ECG signal of the subjects that were taken by using electrodes which were located in left and right side of the heart with a reference electrode on right leg. However, in our system, the database consisted of the ECG signals which were taken by using patient's right and left thumb. The difference of our system with the others is; there is EMG noise which is in the same frequency range with ECG signal. Because of frequencies are the same, it is very hard to eliminate with filters. For this reason, database was enhanced by applying the different filters on ECG signal to reduce the noises for higher recognition rate.

First week of the dataset -which was obtained by using ECG signals of 30 people in two separate weeks- is extracted the personality information by performing AC/DCT and MFCC methods and is reserved as training dataset. ECG signals which obtained by AC/DCT methods in second week are called as test dataset. First candidate is determined by putting the AC/DCT features of an unknown person into the LDA classifier. In the meantime, same person's MFCC features put into the LDA classifier and the second candidate is determined. If these two candidates are the same, they are labeled as A and B person. If they are not the same person, then QRS frames of the proximate two candidates obtained from AC/DCT features and QRS frames of

the proximate two candidates obtained from MFCC features are sent to K-NN algorithm. QRS frames of these 4 candidates are sorted ascending according to the proximity to the QRS frame of unknown person, and nearest candidate to unknown QRS segment is labeled as A and B person. Proposed method was reached to success at rate of %96 average frame recognition.

PARMAK UCU EKG TABANLI BİYOMETRİK TANIMA SİSTEMİ

Özet

Projenin başlıca amacı, 10 yıldan beri süre gelen EKG sinyali ile yapılan biyometrik sistemlerini, farklı bir ölçüm yöntemiyle gerçekleştirmektir.

Şu ana kadar yapılan EKG tabanlı biometrik sistemlerin çoğu, hastanelerde kullanılan hasta başı monitör veya yüksek hızlı veri analiz kartları yardımıyla EKG ölçümlerinin alınarak veri kümelerinin oluşturulmasına dayanmaktadır. Bu kapsamda her bir deneğin göğsüne tek kullanımlık 3 adet elektrot takılarak kanal 1 ölçüm uçlarından EKG sinyali alınmıştır. Her bir denek için kullanılan elektrotlar hem maliyeti arttırmakta, hem de zahmetli bir iş olmaktadır. Bu cihazların pahalı olmasının yanı sıra kullanılabilirlikleri de bir hayli zordur. Bu yüzden amacımız; kolaylıkla taşınabilir, kullanımı kolay, elektrot tak çıkar derdinden kurtaracak bir sistem yaparak biyometrik tanıma sistemini gerçekleştirmek istememizdir.

Diğer biyometrik tanıma sistemlerinde, kalbin sağ ve sol tarafına yerleştirilen elektrotlar ve sağ bacağa takılan referans elektrotu ile alınan EKG sinyallerinden oluşan veri kümeleri kullanılmıştır. Sistemimizde ise sağ ve sol kol başparmaklardan alınan EKG sinyallerinin diğer parmakları da referans alarak veri kümesini oluşturmaktayız. Diğer sistemlerden farklı olarak sistemimizde, EKG sinyallerinin üstüne binen EMG gürültüsü daha fazla olmaktadır. EKG ve EMG sinyallerin frekans aralıkları iç içe olduklarından dolayı birbirinden filtreler yardımıyla ayrılması bir hayli zordur. Bu nedenle farklı filtreler uygulayarak EKG sinyallerinin gürültü oranını azaltmaya yönelik yöntemler kullandık ve EKG veri tabanlarımızı geliştirdik.

Otuz kişiden iki farklı haftada aldığımız EKG sinyalleriyle oluşturulan veri kümesinin ilk haftası AC/DCT ve MFCC metotlarına uygulanarak kişilik bilgileri çıkartılır ve eğitim veri seti olacak şekilde ayrılır. İkinci hafta aldığımız EKG sinyalleri ise AC/DCT ve MFCC metotlarından geçirilerek test veri seti olarak isimlendirilir. AC/DCT öznitelikleri çıkarılan kişi LDA sınıflandırıcıya sokularak bir aday belirlenir. Eş zamanlı olarak aynı kişinin MFCC öznitelikleri de LDA sınıflandırıcıya sokularak bir aday daha belirlenir. Eğer bu iki aday aynı ise, A veya B kişisi diye etiketlenir. Eğer birbirinden farklı iseler AC/DCT özniteliklerinden

çıkarılan en yakın iki adayın QRS bölütleri ve MFCC özniteliklerinden çıkarılan en yakın iki adayın QRS bölütleri K-NN algoritmasına gönderilir. Bu dört adayın QRS bölütleri, bilinmeyen kişinin QRS bölüdüne yakınlığına göre küçükten büyüğe sıralanır ve en yakın aday, A veya B kişisi olarak etiketler. Önerdiğimiz yöntemle ortalama bölüt tanıma oranı %96 'ya ulaşmıştır.

Acknowledgements

To my family

Table of Contents

List of Tables

List of Figures

LIST OF SYMBOLS

AC/DCT	Discrete Cosine Transform of Autocorrelation Sequence
MFCC	Mel Frequency Cepstral Coefficients
DFT	Discrete Fourier Transform
PCA	Principle Component Analysis
IMFs	Intrinsic Mode Functions
K-NN	K-Nearest Neighbors
LDA	Linear Discrimination Analysis
HMM	Hidden Markov Model
LPC	Linear Predicting Coding
SVM	Support Vector Machine
GMM	Gaussian Mixture Model
MLP	Multilayer Perception Neural Network
DWT	Discrete Wavelet Transform
RBF	Radial Basis Function
ECG	Electrocardiogram
EMG	Electromyogram
EOG	Electrooculogram
CMRR	Common Mode Rejection Ratio
FIR	Finite Impulse Response
IIR	Infinite Impulse Response
A/D	Analog Digital Converter
PCB	Printed Circuit Board
TP	True Positive
TN	True Negative

FP	False Positive
FN	False Negative
FRR	Frame Recognition Rate
ASM	Assembly Computer Language
PLL	Phase Locked Loop
MIPs	Million Instructions per Second
SMD	Surface Mounted Device
UART	Universal Asynchronous Receiver/Transmitter

Chapter 1

Introduction to Biometric Recognition System

Biometric recognition is a description of an individual based on his/her physiological and/or behavioral character [1]. Within the past 20 years, biometric recognition systems has developed based on physiological features such as face, fingerprint and retina or behavioral features like gaits. But these are not reliable systems in the terms of recognition accuracy, imitable and forgery. In the meantime, the biometric recognition systems are not described as lifetime detector. In other words, biometric systems based on recognition of fingerprint, face or retina describes the individual correctly though, it can't guarantee the individual's presence of that particular place perceptibly [2, 3].

Electrocardiogram (ECG) signals are a biological signs of heart's electrical activity and it can be measured from the skin which also is something low-cost [1, 2, 3]. For the last 20 years, ECG signal's analysis which are very important device for recognition became an active research field [2]. At the same time, ECG signals carry distinctive features depending on personal features such as age, gender, position, size and anatomy of the heart. Therefore, ECG signals are discussed to use in biometric recognition systems for its biometric size [2, 4]. In the terms of reliability, the biggest advantage of biometric recognition system based on ECG signal is the obligatory of taking these signals from a live body [3]. Besides, this universal ECG signal is almost difficult to imitate and a proof of an individual presence at that particular place. In addition to this, a technology that can imitate or produce an individual ECG signal artificially has not been developed yet. For all these reasons, biometric recognition systems based on ECG have an extensive potentials usage in governme

1

ntal enforcement such as control of computer and network access, cash point and board control systems [2].

Despite of all these superiorities, biometric recognition systems based on ECG are not used for these enforcements. The main reason why biometric recognition systems based on ECG are not used is; traditionally ECG measurement methods have been used for obtaining the ECG signal. Also, this type of measurements in this systems cause recognitions process cost much.

In the recent decade, various biometric recognition systems based on ECG and its' practices have been developed. First study in this field was done by Biel and the others in 2001 [5]. This study showed that ECG signals can be used for human recognition. By using commercials device which is used for extraction the ECG signal, 30 features that contains of temporal and amplitude are extracted on the ECG signal which is taken lead 1 placement. After that, these 30 features were reduced to 12 by using the algorithm based on the classification method which uses simple analysis of the correlation matrix. For the classification, multivariate analysis methods were used. The proposed method is; achieved the %100 recognition demonstration by using 360 features (30x12 channels) from taken the subject group which consists of 20 individuals. However, this method was lack of automatic recognition ability, because a special device was needed for feature extraction [2, 5]. Again in 2001, Irvine and the others were showed that the changes in heart beats can be used in human recognition as a biometric size [6].

In 2002, Shen and the others [7] were suggested two phased method for biometric recognition system from taken 1 channel ECG signal. In the first phase of this suggested method, autocorrelation coefficients were calculated using the template matching method for comparing two QRS distance. In the second phase, recognition process was executed using the Decision-Based Neural Network-DBNN [7] algorithm on possible subjects which was found after the template matching method. Seven features which represent temporal and amplitude values were used in this study. At the end of the experiments which performed on 20 individuals, template matching method executed %95 and DBNN method executed %80 recognition rate, when this two methods used together, it executed %100 recognition rate [2,7].

In 2003, Israel and the others [8] presented a recognition system which is using the ECG and facial signals integrated. This system could provide automatic recognition but recognition rates were low [2, 8].

In 2005, By the Israel and the others [9] ,15 features were detected from each heartbeat of ECG signals and later on it was reduced 12 features with Wilks' Lambda [9] method. This method which uses Linear Discriminant Analysis-LDA [9] for classification, was tested on database collected from 29 people and reached success on heartbeat recognition %81 and %100 in individual recognition [2, 9]. Same year, Shen [10] extended and developed his previously presented method [7] by working on far greater database which collected with EKG signals from 168 healthy people. Unlike his previously study, template matching and mean-square error were examined in the first phase and DBNN and distance classification method were examined comparatively in the second phase. 17 temporal and amplitude features were extracted in this study. The best recognition rate represented as %95.3 by using template matching and distinct classification [2, 10].

In 2006, Shen again [11] provided %95 recognition success on the same ECG database by reducing the ECG feature set which in the study he had represented in 2005 [10] from 17 to 11[2, 11].

In 2007, Wübbeler and the others [4] described a two-dimensional heart vector by using Einthoven channels (Einthoven triangles which is Lead 1, Lead 2, Lead 3) for biometric recognition. In this study, distance between the two heart vectors have been used as a feature and the distance criterion was defined for these two heart vectors as, the sum of square of first and second derivation's differences. %98.1 ECG recognition success was provided in this study [4].

In 2008, Wang and the others [2] developed a biometric recognition based on ECG without establishing specific points about ECG signals. This developed method was based on AC/DCT feature's classification which obtained by applying the autocorrelation sequence (AC) operation to windowed ECG signals ,then applying the Discrete Cosine Transform (DCT) to the result of AC operation. This method was tested in two different databases and had individual recognition success at the rate of %94.47 and %97.8 respectively [2]. Again in 2008, Chan and the others [12]

described a new error criterion based on wavelet transform for the biometric recognition based on ECG. In this method, individual ECG signals were cleared from the noise by pre-processing first. Then QRS segments were determined with the QRS identification method based on multiplication of backward differences algorithm. By using average value of obtained QRS segments, a representative exclusive QRS segment was established. Classification process was performed by using a new error criterion based on the wavelet transformation. At the rate of %89 recognition success was gained [12]. In 2008, Chuang-Chien and the others [13] represented an ECG recognition method based on a wavelet transform. In this method, a new feature set was formed from the coefficients which can be found by using wavelet transform on ECG signals. Represented method was tested on ECG signals obtained from 45 people. Database was consisted of 35 healthy and 10 arrhythmia people's ECG signals. While represented method had a %100 recognition success on healthy people's ECG signals, the rate of recognition success was %81 on people who have arrhythmia. Same year, Irvine and the others [14] represented a biometric recognition method based on ECG called Eigen Pulse. Represented method was based on traditional biometric sizes such as fingerprint, retina and commonly used Principles Component Analysis.

In 2009, Fang and Chan [3] developed a biometric recognition method based on unsupervised ECG that is based on 1 or 3 channel ECG signal's reproduction on the phase space. In this method, instead of extracting the reduced feature set, all ECG signals were transferred to multi-dimensional phase space. Reproduced phase spaces descriptions were used as distinguishing features. Individual recognition process was occurred by questioning the similarities and differences between ECG phase space descriptions. In this study, 1 channel ECG signals provide %93 success and 3 channel ECG signals provide %99 successes [3]. In 2009, Fatemian and Hatzinakos [15] offered a new biometric recognition system based on ECG by extracting the individual representative QRS segment.

 In suggested method, ECG signals went through the noise cleaning method based on discrete wavelet transform and QRS identification processes and QRS segments were extracted for every individual. Representative QRS segmentation that identifies a person was established by using the average values of the obtained QRS

segmentation. Classification and recognition systems were performed by using the correlation coefficient. At the rate of %99.61 recognition success was reached by the suggested system.

In 2010, Li and Narayanan [16] developed a new biometric recognition algorithm based on ECG signals by using the temporal and power spectrum information. In reformed method, first ECG signals of an individual were passed over QRS identification process to extract the individual's temporal information. Then heartbeat waveform of the individual was extracted and normalized in the same time and amplitude scale. For the normalized heartbeat waveform, Hermite polynomial coefficients were calculated by using the Hermite's polynomial expansion. Hermite polynomial coefficient that shows the temporal information for every individual in database is classified by using support vector machine (SVM) method. In addition to that, cepstral features are calculated for modeling the frequency information of ECG signals and modeled by GMM (Gaussian mixture model). At the rate of %98.26 recognitions was obtained by using both feature sets. Same year, Sufi and the others [17] presented a biometric recognition system based on polynomial distance measurement. Presented method was reported to be faster in comparison with other methods. Again in 2010, Loong and the others [18] offered a LPC (Linear predictive coding) based ECG biometric recognition system. In this method, first 40 coefficients of LPC spectrum of ECG signal were used as a feature set and at the rate of %99 correct recognition was indicated [18]. Same year, Ting and the others [19] presented an ECG based biometric recognition system based on Kalman filters.

In 2011, Sufi and Khalil [20] represented a method for extracting ECG feature set based on data mining techniques on compressed ECG signal. Same year, Shen and the others [21] have developed a biometric recognition system which uses ECG signals recorded on channel 1. In this research, 17 features which contains temporal and amplitude values belonging to extracted individualized cardiac cycle waveform are used, and %95.3 correct recognition rates was indicated. Again in 2011, Safie and others [22] derivate a new feature extraction technique which is called Pulse Active Ratio-PAR and new feature set were extracted for ECG signals. In proposed method, it is stated that if the length of feature vector which is extracted by using PAR method for the ECG signals is less than 20, the success of recognition system will

reduce. Therefore, length of feature vector have fixed in the range of 20 and 40. In 2011, Chen and others [23] developed a biometric recognition method based on extracting chaotic features from ECG signals. In this method, ECG signals firstly moved to phase space by using phase-space reconstruction algorithm. After that, by using Lyapunow coefficients and correlation measurement chaotic feature set was extracted. For the classification, back propagation neural network algorithm was used. In this method, %90 correct recognition rate was indicated.

In 2012, B. Vuksanovic and M. Alhamdi [24] represented a new approach for automatic analysis of single lead ECG for human recognition system. Their method firstly partitions the ECG signals into separate windows where each window includes single beat of ECG signal. After that, features which contain QRS, various temporal, amplitude and AR coefficients are extracted for each windowed ECG signals. For proposed system, three different publicly available ECG databases are used. At the rate of %95 correct recognitions was indicated by using amplitude and AR parameters for classification. In their research, %100 correct recognition rate is proposed to be achievable by using four parameters which are amplitude, time, width, AR model for classification. Same year, O.Boubarov and the others [25] developed a method for denoising and framing for recognition system. Firstly, in order to separate the muscle artifacts' noise from ECG signals, wavelet denoising with soft threshold of the wavelet coefficients was realized. After the signal is separated from noise, Hidden Markov Model (HMM) sequential probabilistic model was used for framing. Then feature extraction is performed by using principle component analysis (PCA) which is used for dimensionality reduction that concentrates the discriminative information into low number coefficients. In the classification test, ECG PCA training set from 10 persons with 10 complete cardiac cycles for each. In the end, Linear Discriminant Analysis (LDA) is proposed to achieve more discriminative features for ECG personal recognition. Again in 2012, N.Belgacem, Fethi Bereksi [26] presented a method for analyzing ECG signal, extracting the features and for real time human identification. ECG data were obtained from Lead 1 ECG records of forty students at Paris Est. University. In the research, time domain processing was performed which consist of filtering, peak detection, heartbeat waveform, framing, amplitude normalization. After that, features are extracted by using Fast Fourier Transform (FFT) of the autocorrelation (AC)

sequence of these ECG data's frames. FFT was used for reducing the extracted features from ECG signals.

In 2013, Zhidong Zhao and the others [27] presented a robust preprocessing method comprising noise elimination, heart normalization and quality measurement for eliminating the effects of noise and heart rate variability. The proposed system was independent of the heart rate, and the ECG signal was decomposed into number of intrinsic mode functions (IMFs). Then Welch spectral analysis was used for extracting the significant heartbeat signal features. Principle Component Analysis (PCA) was also used for reducing dimensionality of the feature space, and the K nearest neighbors (K-NN) method was applied for classification. Proposed method was tested on MIT-BIH ECG databases and % 95 correct recognition rates were achieved for 90 subjects.

In 2015, M. M. Tantawi and others [28] represented a discrete wavelet feature extraction method for ECG based biometric recognition system. In the proposed method, R-R intervals were extracted and decomposed into wavelet coefficient structures by using discrete bi-orthogonal wavelet transform. These structures were reduced by excluding the non-informative coefficients, and they were fed into a radial basis functions (RBF) neural network for classification. After that features were extracted by performing the AC/DCT method on ECG frames which fed into RBF network for classification. Experiment was conducted by using the four Physionet ECG databases. Same year, Fatema and Khairul [29] represented a cardioid graph based feature extraction technique for performing compressed ECG biometric. It is said that cardioid graph based method has not been implemented on compressed ECG signal before, and decompression of the compressed ECG signal is not needed to be performed before the recognition step. In their method, QRS complexes obtained by using Discrete Wavelet Transform (DWT), followed by the cardioid graph retrieval operation. Compression was conducted in three decomposition level and with the first two Daubechies wavelets. After that classification was performed on all three decomposition level using Multilayer Perception (MLP) Neural Network. Maximum compression rate of % 87.5 was achieved with the accuracy rate of % 93.75. For compression rate of % 85, the identification rate obtained as % 98.75.

Before continuing the extraction of ECG signal from body, physiological events that causing ECG signals should be known. For this reason, electrocardiography should be introduced.

Chapter 2

Biosignals

Human living cells work like little batteries. These cells in human have different ion concentrations outside and inside of their membranes that produce small electricity in range of microvolts to millivolts. When there is a disturbance on membrane, it will cause rising on action potential that is depolarization and repolarization of the cell as shown in Figure below [29].
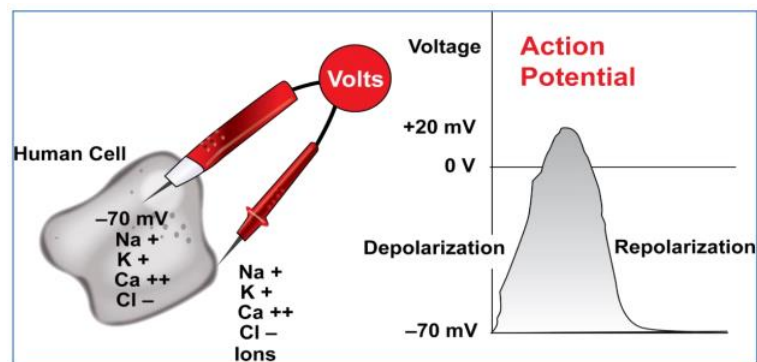
Figure 1: Human cells that polarized and depolarized [5]

The cardiac cycle begins with sinus node's depolarization which is the area of situated in the high right atrium (RA). Then a wave of electrical depolarization deploys from RA and to inter-atrial septum into the left atrium (LA). Electrically inert fibrous ring separate the atria from ventricles. For this reason; only route for transmission of electrical depolarization is through the atrioventricular (AV) node. After AV node delays the electrical signal, wave's depolarization spreads to interventricular (IVS) via the right and left bundle branches. Myocardium repolarizes after the complete heart's depolarization for being ready to depolarize again [30]. Action potential which is produced from the heart is in the Figure 2.
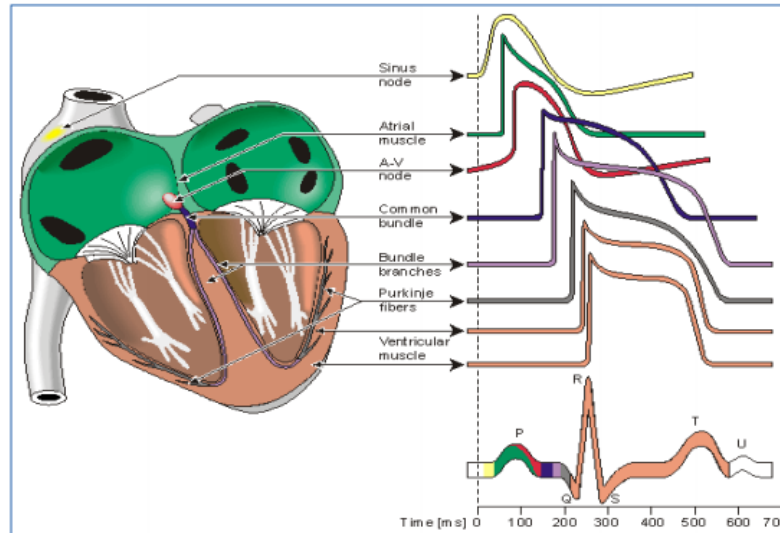
Figure 2: Action potentials produced from the heath [5] (Malmivuo and Plonsey, 1995)

2.1 Measurement Techniques

Heart's electrical activity produces currents which spread from surrounding tissue to the skin. When sensors are attached to the skin, they sense the electrical current activity and transmit them to the instrumentation amplifier. This electrical activity which represents heart's depolarization and repolarization cycles is transform into the waveform by instrumentation amplifier. Electrical current from the heart radiates to the skin in many directions. Because of this, electrodes placed to the different location of the heart position give the total picture of the heart's electrical activity. ECG records from different perspectives, which are called **leads** [52].

A lead provides heart's electrical activity between two points. Each leads consist of one positive pole and one negative pole. Polarization of the waveform which is recorded by these two points changes if the direction of the current moving from heart to the skin changes.

2.1.1 12-Lead Measurement Setup and Einthoven's triangle

A 12-lead ECG records provide 12 different view of the heart's electrical activity. 12 waveforms are obtained by placing the electrodes on to the patient's chest and limbs. These leads provide different information. Lead I, II, III and augmented vector left (aV_L), augmented vector right (aV_R) and augmented vector foot (aV_F) provide information about frontal plane of the heart. The six lead which are V_1, V_2, V_3, V_4, V_5 and V_6 provide the information of the horizontal plane of the heart [52].

10

Measurement point provides information about the heart's frontal plane forms like a triangle. Axes of the three limb leads (Lead I, II, and III) are known as Einthoven's triangle.
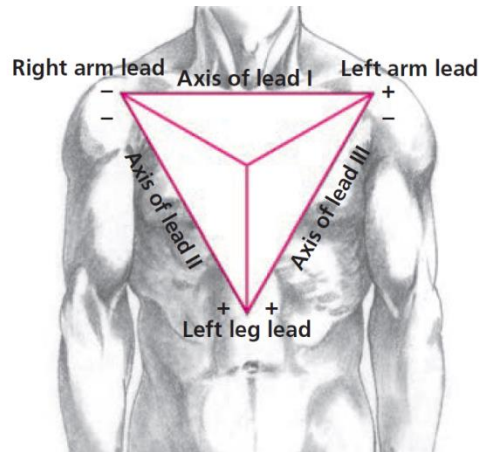
Figure 3: Einthoven's Triangle [52]

The measurement point of the lead I ECG begins with right shoulder and ends with left shoulder, and right arm lead connects to negative electrode and left arm lead connects to the positive electrode. Lead II ECG measurement point runs from negative right arm lead electrode to positive left leg lead electrode. Lead III ECG measurement point begins with negative left arm lead electrodes, and ends with positive left leg lead electrode.

2.2 Common Monitoring Problems

Waveforms which are illustrated in the figures below present the most commonly encountered monitoring problems.

2.2.1 Baseline Wandering

Patients restlessness, or electrode movements placed on the skin cause this problem. It can be seen that signal is shifted up and down, because skin electrode movements causes DC coupling on ECG signal.
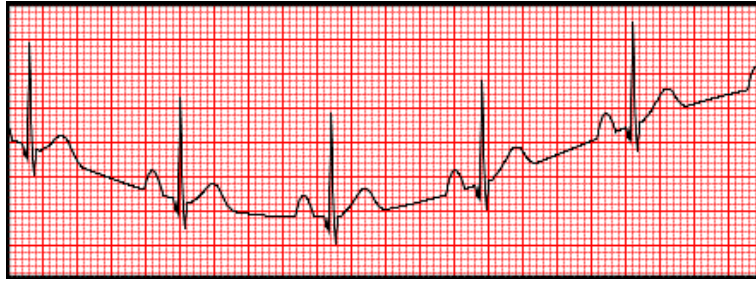
Figure 4: ECG signal which has baseline wanders [52]

For solving the problem, 0.5 Hz highpass filter should be applied on the ECG signal which has baseline wandering. It can be said that baseline wandering can be reduced by encouraging the patient to relax and by repositioning the electrodes properly.

2.2.2. Power line Noise

This type of signal is seen when ECG signal is corrupted with power line noise. In United States, the electricity changes direction 60 times per second (60 Hertz in frequency). However, Many European countries use 50 Hz AC electricity. When the ECG circuit is poorly grounded, or not having filters for this specific power line, thick ECG waveform is seen as in the Figure 5.
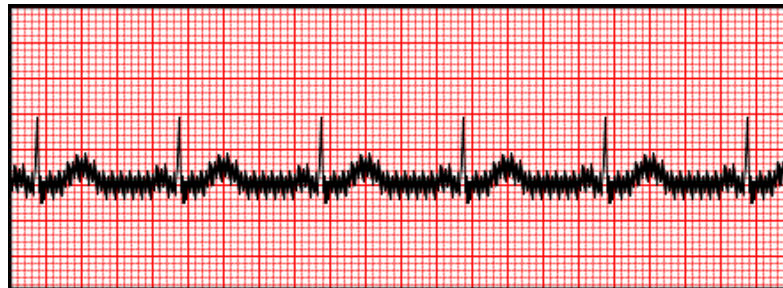
Figure 5: ECG signal which has AC interference [52]

Powerline noise is eliminated by using bandstop or notch filters. Filter specifications are changed by the frequency of powerline of the countries which ECG recorder will be used on.

2.2.3 Muscle Tremor

Not only heart's electrical activity is produced on the measurement point of ECG lead, but also muscle noise can be seen when skeletal muscles undergo tremors. This type of noisy ECG signal cannot be filtered by specific filters.
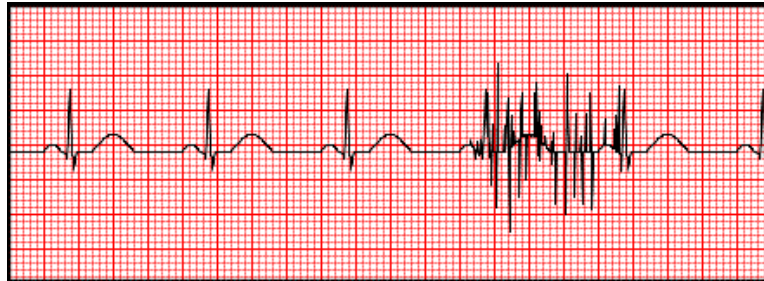
Figure 6: ECG signal which has muscle interference [52]

2.2.4 Misleaded Electrodes

Electrodes placement are important, because direction of the current flow is viewed in the recorded electrocardiogram.

Figure 7: ECG signal recorded as reversed lead [52]

2.3 ECG Waveform Components

An ECG complex represents electrical activity of the heart in every one cardiac cycle. ECG signals consist of three waveform; P wave, QRS complex, and T wave. This electrical activity can be broken down into intervals and segments which are the PR interval, the QT interval and the ST segment. Additional of these activities, u wave can sometimes present. J point in the Figure 8 marks the end of QRS complex and beginning of the ST segment [52].
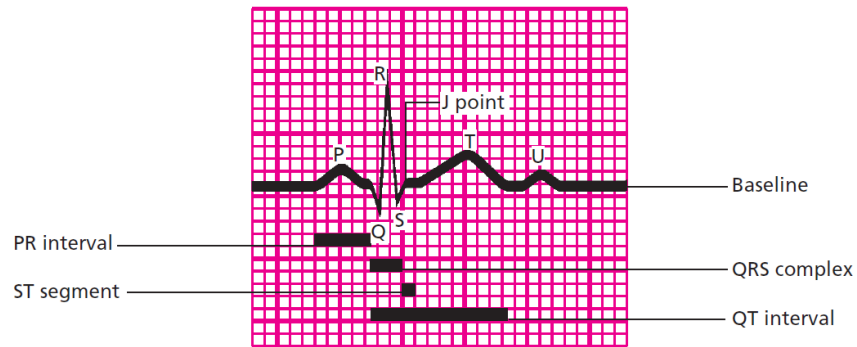
Figure 8: ECG waveform components [52]

This ECG grid shows the vertical, horizontal axis and their measurement values.
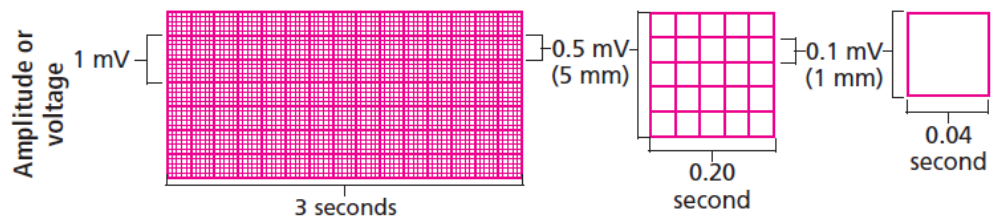
Figure 9: Understanding the ECG grid [52]

2.3.1 P wave

P wave is the first component on the normal ECG signal. P wave represents atrial depolarization, or transmission of electrical impulse through the atria [52]. Normal P wave characteristics are shown as

- Location: Precedes QRS complex
- Amplitude: 0.2 to 0.3 mV high
- Duration: 0.06 to 0.12 second
- Deviation: Positive in Lead I, II, aV_F And V_2 toV_6, negative in other leads
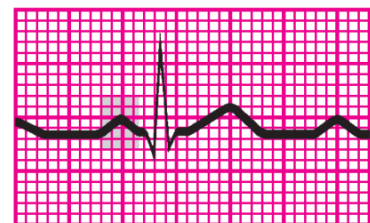
Figure 10: P wave [52]

2.3.2 PR interval

PR interval follows the atrial impulse from the atria to the AV node, bundle of His, right and left branches [52]. Normal PR interval characteristics are shown as

- Location: It starts from the beginning of the P
  wave to the beginning of the QRS complex.
- Duration: 0.12 to 0.20 second
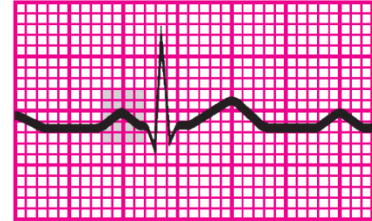
Figure 11: PR interval [52]

2.3.3 QRS complex

QRS complex tracks the P wave and it represents depolarization of ventricles. After the ventricles depolarize, the blood is ejected from ventricles and is pumped through the arteries [52]. QRS complex characteristics are shown as

Location: tracks the PR interval (beginning of the Q wave to end of S wave

- Amplitude: 0.5 mV to 3 mV high, however it differs for each lead use
- Duration: 0.06 to 0.10 second
- Deviation: positive in Lead I, II, III, aV_L, aV_F, and V_4 to V_6,
- biphasic in V_3, negative in other leads
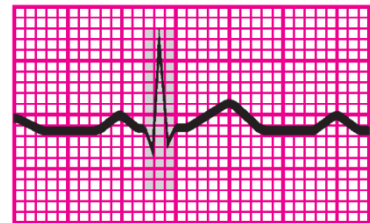
Figure 12: QRS complex [52]

2.3.4 ST segment

ST segment represents the ventricular depolarization, and the beginning of ventricular repolarization [52]. ST segment characteristics are shown as

- Location: spreads from S wave to the beginning of T wave.
- Deviation: usually on baseline, may change between -0.05 mV to 0.1 mV in some Leads
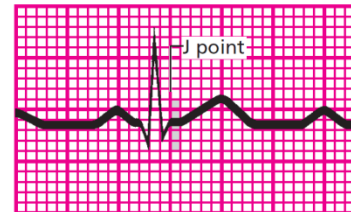
Figure 13: ST segment [52]

2.3.5 T wave

T wave represents the ventricular recovery, or period of repolarization [52]. T wave characteristics are shown as

- Location: tracks the ST segment
- Amplitude: vary between 0.05 mV to 0.5 mV
- Deviation: Positive in Lead I, II, and V_2 to V_6 , negative in aV_R ,vary in leads III, and V_1
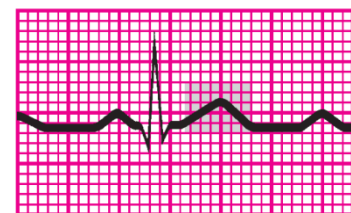
Figure 14: T wave   [52]

2.3.6 QT interval

QT interval is the time needed for ventricular depolarization and repolarization. QT interval changes according to heart rate. QT interval is shorter when heart rate is increased [52]. QT interval characteristics are shown as

- Location: spreads from beginning of QRS complex to end of T wave
- Duration: vary according to gender, age, and heart rate. It usually varies between 0.36 to 0.44 second.
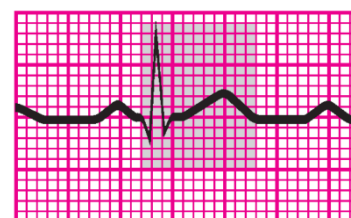
Figure 15: QT interval [52]

Chapter 3

Analog Filters

Analog filters are the basic building blocks which have been used as a signal processing in electronics. They are separated into active and passive filters. Passive analog filters only consist of resistors, capacitors and inductors, and they are unity gain. Active filters are the other type of analog electronic filter which use active components such as operational amplifier (op-amp). Active filters have been used because of high performance and predictability. It does not need inductor which is expensive compared to other electronic components. The specification for building active filters are included as

- The range of desired frequency with the shape of frequency response is needed to be known. This shows us which filter type is needed such as highpass, lowpass, bandpass or bandreject filter.
- Dynamic range of the active components is needed to be known. Op-amp should not saturate at expected input signal.
- The allowable ripple on passband or stopband, and the shape of frequency curve near the cut-off frequency is needed to be known. This shows us which filter topology will be used such as Chebyshev filter, Butterworth filter, Bessel filter, Elliptic filter, and Linkwitz-Riley filter [33].

3.1 Fundamentals of Analog Filters

The most common simple low-pass filters are the passive RC low-pass filters. By using Laplace transform, transfer function of the filter can be easily found and symbolized as H(s) [33]. Transfer function is known as system response of the filter.

$$H(s) = \frac{1/RC}{s + 1/RC} = \frac{1}{1 + sRC} \tag{3.1}$$

Where s is the complex variable, $s = \sigma + j\omega$

To normalize the presentation of transfer function

$$s = \frac{s}{\omega_c}\Big|_{s=j\omega} = \frac{j\omega}{\omega_c} = j\frac{f}{f_c} = j\Omega \quad \text{where } \omega_c \text{ is the cut} - \text{off frequency} \tag{3.2}$$

$$H(s) = \frac{1}{1 + s} \tag{3.3}$$

By replacing s with $j\omega$, and giving values on ω, system response of that given frequencies are found simply. For example

$$H(s) = \frac{1}{1+s} \quad \rightarrow \quad H(j\omega) = \left|\frac{1}{1 + j\omega}\right| \tag{3.4}$$

$$\text{For } \omega = 0 \quad H(j\omega) = 1 \tag{3.5}$$

$$\text{For } \omega = 1 \quad H(j\omega) = \left|\frac{1}{1+j}\right| = 0.7071 \tag{3.6}$$

$$\text{For } \omega = 5 \quad H(j\omega) = \left|\frac{1}{1+j5}\right| = 0.1916 \tag{3.7}$$

$$\text{For } \omega = 100 \quad H(j\omega) = \left|\frac{1}{1+j100}\right| = 0.010 \tag{3.8}$$

It can be seen that if higher frequencies is applied on the system above, it will eliminate that frequencies with the percent of frequency response.
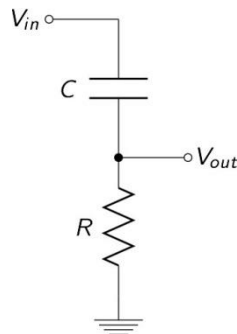
Figure 16: Passive Low-Pass Filter

Low-pass filter's gain and phase response can be optimized for satisfying following three criteria

1. A maximum passband flatness
2. An immediate passband to stopband transition
3. A linear phase response

The formula below is the transfer function which must allow for complex poles

$$H(s) = \frac{H_0}{(1 + a_1 s + b_1 s^2)(1 + a_2 s + b_2 s^2) \dots (1 + a_n s + b_n s^2)} \qquad (3.9)$$

$$H(s) = \frac{H_0}{\pi_i(1 + a_i s + b_i s^2)} \qquad (3.10)$$

Where H_0 is the passband DC gain, a_i and b_i are the filter coefficients.
Coefficients of predetermined filters are available; Butterworth, Chebyscheff and Bessel etc.

The Butterwort coefficients: It is a type of coefficient that gives us flat frequency response as possible in the passband. It is also known as **maximum flat magnitude filter**.

The plot in Figure 17 is for the Butterworth low-pass filter of order 1 through 5, with cut-off frequency $\omega_0 = 1$
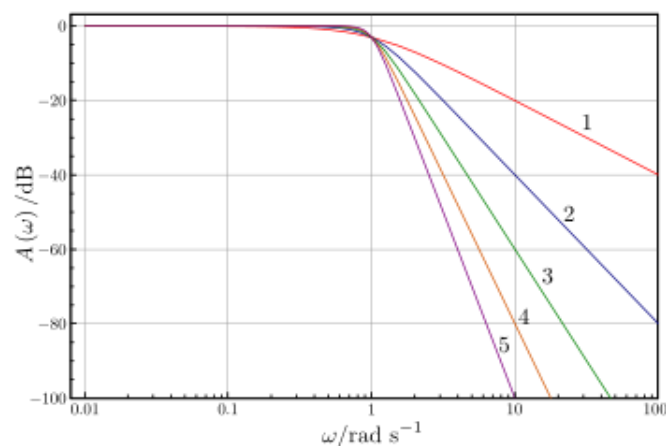
Figure 17: Butterworth Lowpass Filter Frequency Response **[46]**

19

The Chebyshev coefficients: Sharping the transition from passband to stopband Chebyscheff filter are the filters that passband ripples are more than Butterworth filter.
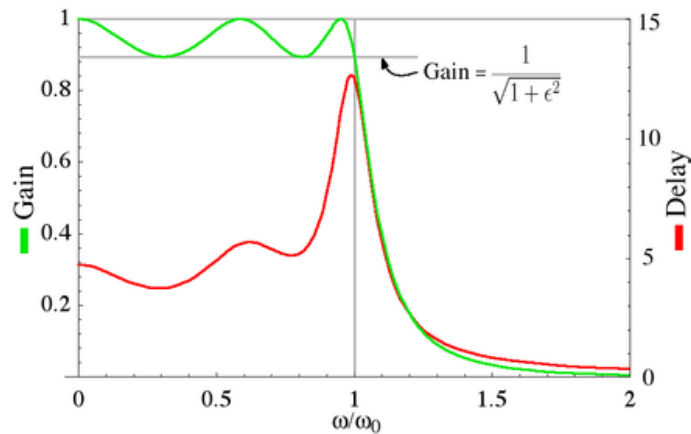
Figure 18: Chebyshev Lowpass Filter Gain and Group delay **[47]**

The Bessel coefficients: Linearizing the phase response.

3.2 Lowpass Filter Design

3.2.1 First-order lowpass filter design

Transfer function of first order filter is given below

$$H_1(s) = \frac{H_0}{(1 + a_1 s)} \tag{3.11}$$
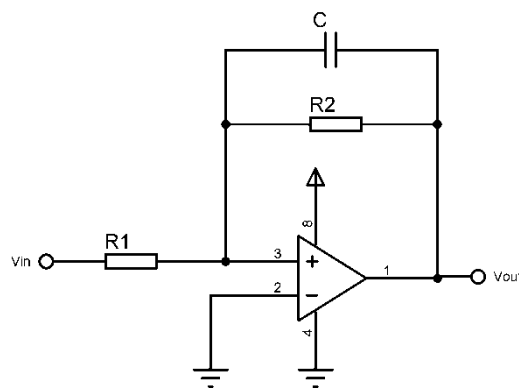
Figure 19: First order inverting lowpass filter

20

Transfer function of the inverting lowpass filter is given as

$$H(s) = \frac{H_0}{(1 + \omega_c R_2 Cs)}, \qquad where \ H_0 = -\frac{R_2}{R_1} \quad , \quad a_1 = \omega_c R_2 C \tag{3.12a}$$

$$or \quad R_1 = \frac{a_1}{2\pi f_c C} \quad , \quad R_1 = -\frac{R_2}{H_0} \tag{3.12b}$$

To find the dimension of the circuit, specify the cut-off frequency f_c and the dc gain H_0 , and the capacitor C, and then solve for resistors R_1 and R_2.

H_0, f_c represent the filter's gain and cut-off frequency, respectively. By giving value to the capacitor, resistors' value are easily found for a specific cut-off frequency. Inverting filters mean that output and input signals have 90 degree phase shift compared with each other.
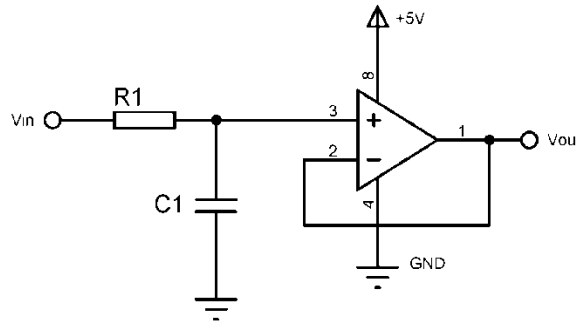
Figure 20: First order unity gain non-inverting lowpass filter

Transfer function of the unity gain non-inverting lowpass filter is

$$H(s) = \frac{H_0}{(1 + \omega_c R_1 C_1 s)}, \qquad where \quad H_0 = 1 \quad , \quad a_1 = \omega_c R_1 C_1 \tag{3.13a}$$

$$or \quad R_1 = \frac{a_1}{2\pi f_c C_1} \tag{3.13b}$$

21

3.2.2 Second order unity gain lowpass filter design

Transfer function of second order filter is given as

$$H_i(s) = \frac{H_0}{(1 + a_i s + b_i s^2)} \tag{3.14}$$
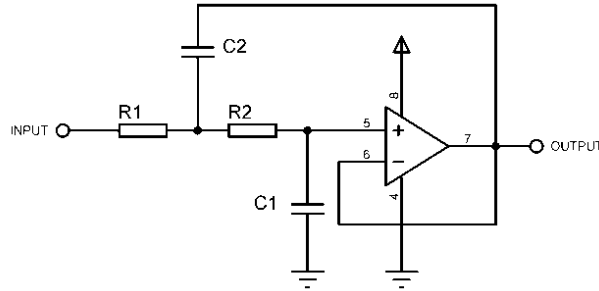
Figure 21: Second order unity gain Sallen Key topology Lowpass filter

$$H(s) = \frac{H_0}{(1 + \omega_c C_1 (R_1 + R_2)s + \omega^2 R_1 R_2 C_1 C_2 s^2)} \tag{3.15a}$$

Where $\qquad H_0 = 1$, $a_1 = \omega_c C_1 (R_1 + R_2)$, $\qquad b_1 = \omega^2 R_1 R_2 C_1 C_2$ \qquad (3.15b)

Given $C_1 \ and \ C_2$,

$$R_{1,2} = \frac{a_1 C_2 \pm \sqrt{a_1{}^2 C_2{}^2 - 4 b_1 C_1 C_2}}{4 \pi f_c C_1 C_2} \tag{3.16}$$

For obtaining the real values under square root, C_2 must satisfy the equation (3.17) [33]

$$C_2 \geq C_1 \left[\frac{4 b_1}{a_1{}^2} \right] \tag{3.17}$$

3.3 Highpass Filter Design

3.3.1 First-order inverting highpass filter design
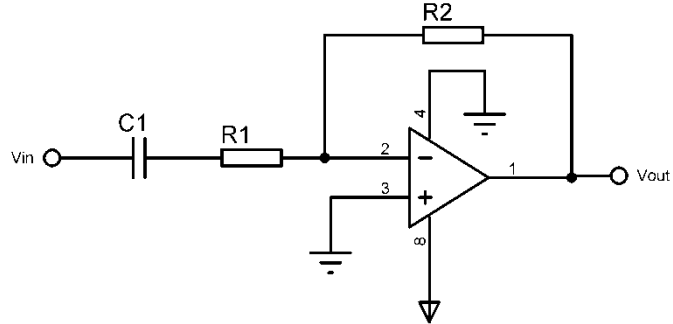
Figure 22: First order inverting highpass filter

Transfer function of second order highpass filter is given as

$$H(s) = \frac{-\dfrac{R_2}{R_1}}{\left(1 + \dfrac{1}{\omega_c R_1 C_1 s}\right)}, \qquad H_0 = -\frac{R_2}{R_1} \quad , \quad a_1 = \frac{1}{\omega_c R_1 C_1} \tag{3.18a}$$

Given C_1 , H_0 , and ω_c we can solve for R_1 and R_2 as

$$R_2 = -R_1 H_0 \tag{3.18b}$$

3.3.2 Second-order unity gain highpass filter design
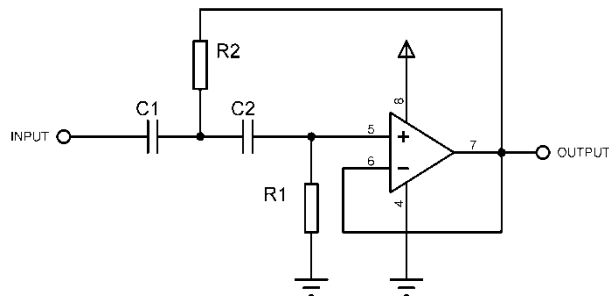
Figure 23: Second order unity gain Sallen Key topology Highpass filter

For $C_1 = C_2 = C$, the transfer function of the filter simplifies to

$$H(s) = \frac{H_0}{\left(1 + \frac{2}{\omega_c C R_1}\frac{1}{s} + \frac{1}{\omega^2 R_1 R_2 C^2}\frac{1}{s^2}\right)} \tag{3.19a}$$

Where

$$H_0 = 1 \;,\;\; a_1 = \frac{2}{\omega_c R_1 C} \;\;,\;\;\;\; b_1 = \frac{1}{\omega^2 R_1 R_2 C^2} \tag{3.19b}$$

Given C, R_1 and R_2 values can be found as

$$R_1 = \frac{1}{2\pi f_c a_1 C} \;\;,\;\; R_2 = \frac{a_1}{4\pi f_c C b_1} \tag{3.20}$$

The order of the filter can be increased by connecting second and first order filters as cascades. For example; to design 5th order low pass filter, first order and second order filter coefficients should be calculated and connected them in cascades as the block diagram in Figure 24.
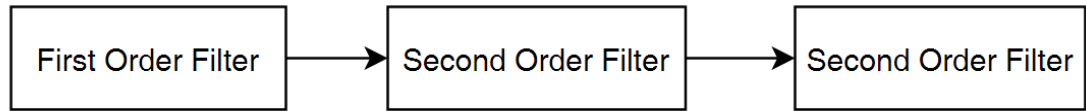
Figure 24: Block Diagram of 5th order filter

3.4 Designing 5th order Lowpass Filter

Let's design 5th order lowpass filter by using equations in the previous sections. Firstly, for designing 5th order lowpass filter, there need 1 first order and 2 second order low pass filter circuit connected in cascade.

For 5th order Butterworth filter, Normalized denominator polynomials in factored form are written below

$$(1+s)(1+0.618s+s^2)(1+1.618s+s^2) \tag{3.21}$$

It can separated as

$$a_0 = 1 \;,\;\;\;\; a_1 = 0.618 \;\;\;\; b_1 = 1 \;\;\;\;,\;\;\;\; a_2 = 1.618 \;\;\;\; b_2 = 1 \tag{3.22}$$

24

Let's design 150 Hz lowpass filter by using Butterworth coefficients above

For the first coefficient which is $a_0 = 1$, let's give C_1 as $100\ nF$, transfer function of the first order filter can be written as

$$H(s) = \frac{1}{(1 + a_0 s)} = \frac{1}{(1 + 2\pi f_c R_1 C_1 s)} \qquad where\ R_1 = \frac{a_1}{2\pi f_c C_1} \tag{3.23}$$

$$R_1 = \frac{a_1}{2\pi f_c C_1} = \frac{1}{2\pi 150 \times 100 \times 10^{-9}} = 1.061 \times 10^{-4} \cong 10\ k\Omega \tag{3.24}$$
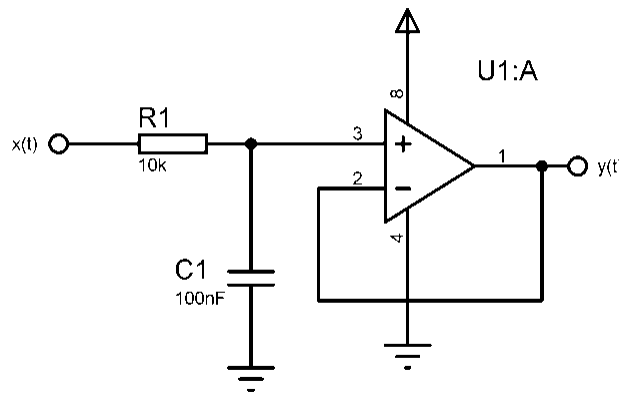
Figure 25: First order lowpass filter

For the second coefficients which are $a_1 = 0.618 \qquad b_1 = 1$, let's give C_1 as $100\ nF$, Second order filter function can be written as

$$H(s) = \frac{1}{(1 + 0.618 s + s^2)} = \frac{H_0}{(1 + \omega_c C_1 (R_1 + R_2)s + \omega_c^2 R_1 R_2 C_1 C_2 s^2)} \tag{3.25}$$

So

$$R_{1,2} = \frac{a_1 C_2 \pm \sqrt{a_1^2 C_2^2 - 4 b_1 C_1 C_2}}{4\pi f_c C_1 C_2} \qquad C_2 \geq C_1 \left[\frac{4 b_1}{a_1^2}\right] \tag{3.26}$$

$$C_2 \geq 100 * 10^{-9} \left[\frac{4}{(0.618)^2}\right] \quad , \quad C_2 \geq 1.047\ uF \quad \text{Let's give } C_2 \text{ as } 2\ uF \tag{3.27}$$

25

$$R_{1,2} = \frac{0.618 \times 2 \times 10^{-6} \pm \sqrt{(0.618)^2(2 \times 10^{-6})^2 - 4(100 \times 10^{-9})(2 \times 10^{-6})}}{4\pi(100 \times 10^{-9})^2(2 \times 10^{-6}) \times 150} \tag{3.28}$$

$$R_1 = 5.541 \text{ k}\Omega \cong 5.6 \text{ k}\Omega \quad , \quad R_2 = 1.015 \text{ k}\Omega \cong 1 \text{ k}\Omega \tag{3.29}$$
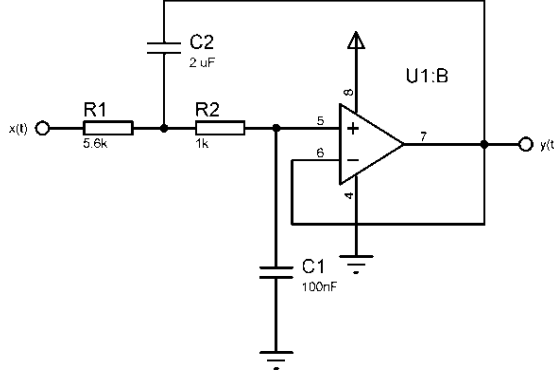
Figure 26: Second order lowpass filter

For the third coefficients which are $a_2 = 1.618 \quad b_2 = 1$, let's give C_1 as $100 \ nF$, Transfer function can be given as

$$H(s) = \frac{1}{(1 + 1.618s + s^2)} = \frac{H_0}{(1 + \omega_c C_1(R_1 + R_2)s + \omega_c{}^2 R_1 R_2 C_1 C_2 s^2)} \tag{3.30}$$

So

$$R_{1,2} = \frac{a_1 C_2 \pm \sqrt{a_1{}^2 C_2{}^2 - 4b_1 C_1 C_2}}{4\pi f_c C_1 C_2} \qquad C_2 \geq C_1 \left[\frac{4b_1}{a_1{}^2}\right] \tag{3.31}$$

$$C_2 \geq 100 * 10^{-9} \left[\frac{4}{(1.618)^2}\right] \quad , \quad C_2 \geq 152 \ nF \quad \text{Let's give } C_2 \text{ as } 160 \ nF \tag{3.32}$$

$$R_{1,2} = \frac{1.618 \times 160 \times 10^{-9} \pm \sqrt{(1.618)^2(160 \times 10^{-9})^2 - 4(100 \times 10^{-9})(160 \times 10^{-9})}}{4\pi(100 \times 10^{-9})^2(160 \times 10^{-9}) \times 150} \tag{3.33}$$

$$R_1 = 10.0406 \text{ k}\Omega \cong 10 \text{ k}\Omega \quad , \quad R_2 = 6.762 \text{ k}\Omega \cong 6.8 \text{k}\Omega \tag{3.34}$$
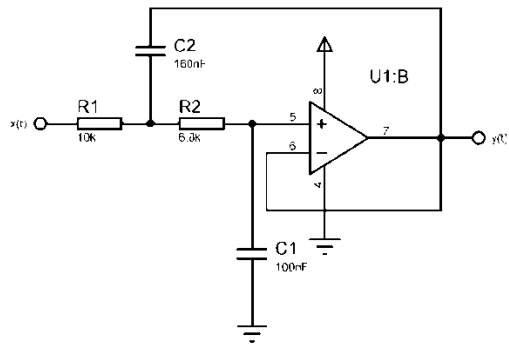
Figure 27: Second order lowpass filter
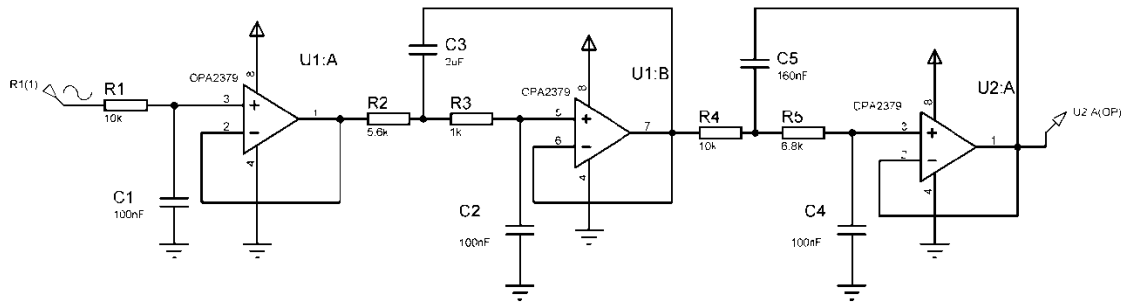
Figure 28: 5th order lowpass filter circuit which has 150 Hz cut-off frequency
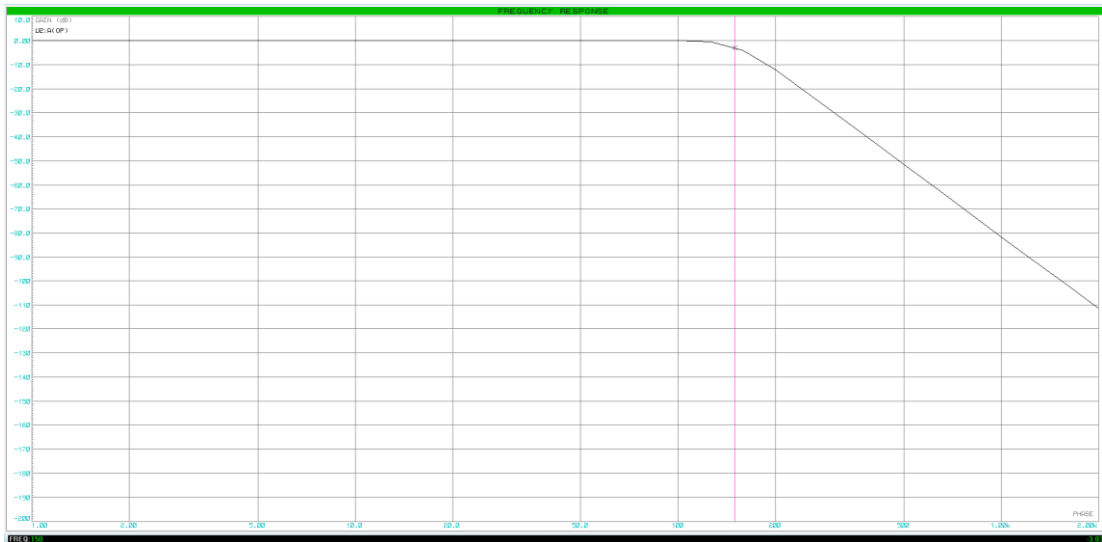
Figure 29: Frequency response of 5th order lowpass filter which has 150 Hz cut-off frequency

ECG signal is applied on analog 5th order Butterworth lowpass filter which has a unity gain and 150 Hz cut-off frequency. The important point is second and higher order analog filters should be used after the amplification of the signal. If they are used before the amplification, desired ECG signal will be eliminated because of these filters. Higher order lowpass filter is used for eliminating the EMG (electromyogram) which is called the muscle signal, and higher frequency components. EMG signals frequency range is between 10 Hz to 500 Hz, and amplitude range is 0, 1 mV to 1 mV. The reason for using 5th order low-pass filter is to eliminate as much as EMG signal to take the ECG signal clearly from thumbs. If ECG measurement location is far from heart, the amount of EMG noises will increase and will cause deformation on the ECG signal. After using analog filter, the other type of noises such as power-line noise (50 Hz in Europe), baseline wander are needed to be eliminated. For this reason, digital filters are used.

Chapter 4

Digital Filters

Analog filters have a continuous-time signal at both its input $x(t)$ and output $y(t)$. Both $x(t)$ and $y(t)$, t represents the continuous signals which have infinite number of values. Analog filter designing requires sophisticated mathematical knowledge, and the most processes such as CMRR and slew rate of the op-amps or tolerance of resistors and capacitors affect frequency response of the analog filter. Rather than hard process of analog filters, digital filters can be easily applied without needing for resistors and capacitors. By using modern sampling, or digital signal processing tools, analog filters can be easily replaced with digital filters. Advantages of digital filters over analog filter are shown as

- They can be easily built and tested because of being software program
- They only require the arithmetic operations such as multiplication, addition and subtraction
- They don't drift for the reason of high temperature, humidity or require high precision electronic components.-They have high performance to cost ratio.
- Their working performance does not suffer from aging or manufacturing variations.

4.1 Fundamental of Digital Filters

Finite Impulse Response (FIR) filters can be designed by using frequency response specifications. Impulse response of digital filter which determines the coefficients of the FIR filter can be found by taking inverse Discrete Fourier Transform on frequency response of the filters. It is essential for understanding basics of FIR filters.

Before designing digital filters, Nyquist criteria should be known. The maximum frequency component of the signal should be known before sampling process. For example; if F_{max} is 500 Hz of desired signal, sampling frequency should be at least 1 kHz. These specifications came from Nyquist criteria. For reconstruction of the desired signal, Nyquist frequency should at least two times higher than maximum frequency of the desired signal. Or in mathematical terms

$f_s \geq 2f_c$, where f_s is the sampling frequency, and f_c is the highest frequency of the desired signal

If highest frequency of the desired signal is higher than sampling frequency, aliasing occurs. Aliasing means that higher frequency component of the desired signal gets on the lower frequencies of the signal from starting the point of $f_s/2$. Therefore, desired signal loses information and gets deformation. Block diagram for designing digital filter is shown in Figure 30
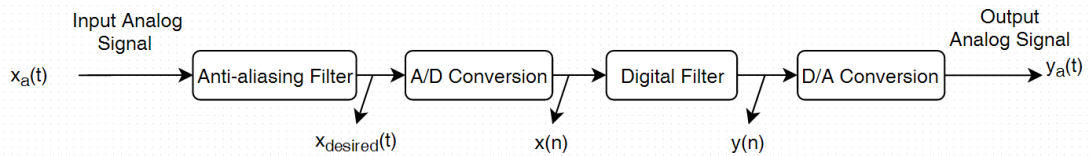
Figure 30: Block diagram of Digital Filtering Process

Anti-aliasing signal is simply an analog lowpass filter which is shown in analog filter design. It is used for elimination of higher frequency component of the signal not to lose the desired information. Desired signal is sampled by f_s on A/D conversion block. After analog signal transferred to the digital signals which consist of finite numbers, digital filter is applied on. For reconstruction of desired analog signal, filtered signal is applied on D/A conversion block [35].

30

4.1.1 FIR Lowpass Filter

Let's begin with designing the lowpass digital filter. Frequency response of the ideal lowpass filter is shown in Figure 31
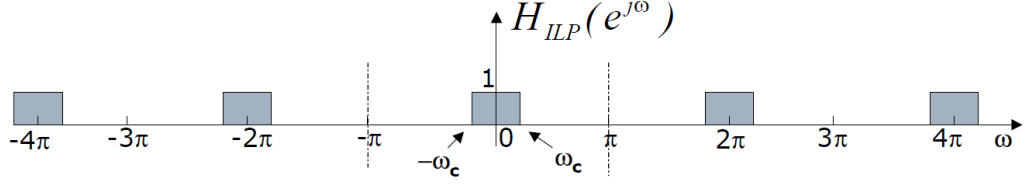
Figure 31: Ideal Digital Lowpass filter [34]

Frequency response of ideal digital lowpass filter is limited in $-\pi < H_{ILP}(e^{j\omega}) < \pi$. The reason can be shown with an example. If F_{max} of the desired signal is 500 Hz, Nyquist frequency should be at least 1 KHz. From this information, let's sample highest frequency of desired signal [34]

$$x_a(t) = \cos(2\pi 500 t) \ , F_s = 1000 \tag{4.1}$$

$$x_{sampled}(n) = \cos\left(2\pi \frac{500}{1000} n\right) = \cos(\pi n) \tag{4.2}$$

So sampled signal is limited in $-\pi < x_{sampled} < \pi$ where n is integer number

$$H_{ILP}(e^{j\omega}) = \begin{cases} 1 & for & -\omega_c \le \omega \le \omega_c \\ 0 & for & -\pi \le \omega \le -\omega_c \quad and \quad \omega_c \le \omega \le \pi \end{cases} \tag{4.3}$$

$$H_{ILP}(e^{j\omega}) = H_{ILP}\left(e^{j(\omega-2k\pi)}\right) ; \quad k = \pm 1, \pm 2, \dots, \pm\infty \tag{4.4}$$

Let's find the impulse response of the H_{ILP} by taking the inverse Discrete Fourier Transform

$$h_{ILP}(n) = \mathcal{F}^{-1}\{H_{ILP}(e^{j\omega})\} \tag{4.5}$$

$$h_{ILP}(n) = \frac{1}{2\pi} \int_{-\pi}^{\pi} H_{ILP}(e^{j\omega}) e^{j\omega n} d\omega = \frac{1}{2\pi} \int_{-\omega_c}^{\omega_c} e^{j\omega n} d\omega \tag{4.6}$$

$$h_{ILP}(n) = \frac{1}{2\pi j n}(e^{j\omega_c n} - e^{-j\omega_c n}) = \frac{\sin\omega_c n}{\pi n} \tag{4.7}$$

Consider the ideal lowpass filter characteristic with the cutoff frequency $\omega_c = \frac{\pi}{6}$, and let's draw discrete impulse response of ideal lowpass filter
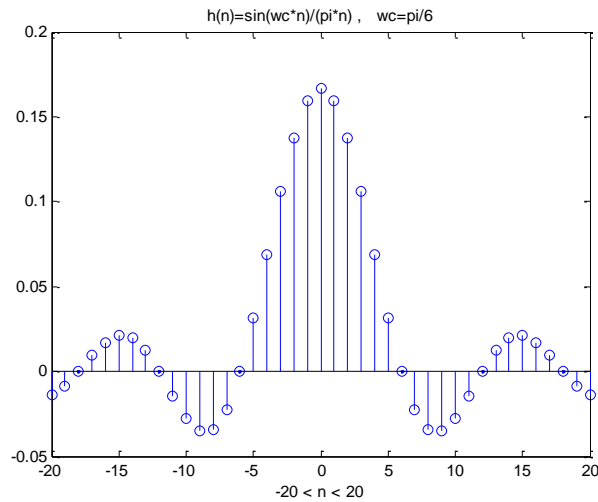
Figure 32: Impulse response of ideal lowpass filter

Matlab code for ideal low pass impulse response

```
close all
n=-20:1:20;
wc=pi/6;
x=sin(wc*(n+.0001));
h=x./(pi*(n+.0001));
stem(n,h)
title('h(n)=sin(wc*n)/(pi*n) , wc=pi/6');
xlabel(' -20 < n < 20 ');
```

But impulse response of the ideal digital lowpass filter is infinite duration and extends symmetrically to infinity on both sides of $n = 0$. For this reason, the ideal lowpass filter can not realize possibly with such a system with infinite duration [34].

Therefore, we could

1. Truncate the expression of $h_{ILP}(n)$ at some reasonable value of n
2. Start $h_{ILP}(n)$ at time zero. so, shift all the coefficient by the same number n.

By doing these, $h_{ILP}(n)$ will be finite duration number and can be easily applied on.

Discrete Fourier transform of

$$h_{ILP}(n) = \frac{sin\omega_c n}{\pi n} \tag{4.8}$$

32

Given as

$$H_{ILP}(e^{j\omega}) = \sum_{-\infty}^{\infty} h_{ILP}(n)e^{-j\omega n} \tag{4.9}$$

This formula can be reviewed as the Fourier series expansion of $H_{ILP}(e^{j\omega})$, which is the periodic square wave form with $2\omega_c$ duty cycle. Because $H_{ILP}(e^{j\omega})$ is symmetrical around zero (n=0), we can express

$$H_{ILP}(e^{j\omega}) = h_{ILP}(0) + 2\sum_{-\infty}^{\infty} h_{ILP}(n)\cos(\omega n) \tag{4.10}$$

Now, let's truncate the expression in both ends. Truncated impulse response is given by

$$h_t(n) = h_{ILP}(n)[u(n+N) - u(n-N)] \tag{4.11}$$

From the expression above, the Fourier transform of $h_t(n)$ is obtained as

$$H_t(e^{j\omega}) = h_{ILP}(0) + 2\sum_{n=1}^{N} h_{ILP}(n)\cos(\omega n) \tag{4.12}$$

We have

$$H_t(e^{j\omega}) = \frac{\omega_c}{\pi} + \frac{2}{\pi}\sum_{n=1}^{N} \frac{sin\omega_c n}{n}\cos(\omega n) \tag{4.13}$$

Let's assume $\omega_c = {\pi}/{2}$, we can obtain frequency response of the truncated impulse response

$$H_t(e^{j\omega}) = \frac{1}{6} + \frac{2}{\pi}(cos\omega - \frac{1}{3}cos3\omega + \cdots + \frac{1}{N}cosN\omega) \tag{4.14}$$

33

Let's draw it by using Matlab to understand better
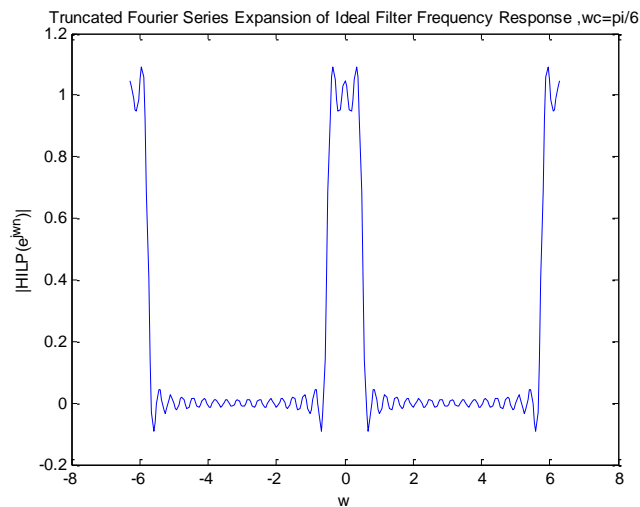
Figure 33: Frequency response of Truncated Impulse Response from $n = \pm 20$, $-2\pi < \omega < 2\pi$

Matlab code for plotting truncated impulse response

```
w=-2*pi:pi/64:2*pi;
wc=pi/6;
h=wc/pi;
n=1;
while n<20
x=sin(wc*(n+.0001));
x1=x./(pi*(n+.0001));
x2=2*x1*cos(w*n);
h=h+x2;
n=n+1;
end
figure, plot(w,h);
title('Truncated Fourier Series Expansion of Ideal Filter Frequency
Response,wc=pi/6');
xlabel('w');
ylabel('|HILP(e^j^w^n)|');
```

For realizable frequency response truncated impulse response should be shifted to the right by N, so the realizable impulse response is given as

$$h(n) = h_t(n - N) \tag{4.15}$$

Since

$$\mathcal{F}\{h_t(n - N)\} = e^{-jN\omega} H_t(e^{j\omega}) \tag{4.16}$$

34

It can be obtained as

$$\mathcal{F}\{h(n)\} = e^{-jN\omega} H_t(e^{j\omega}) \tag{4.17}$$

$$H(e^{j\omega}) = \left(h_{ILP}(0) + 2\sum_{n=1}^{N} h_{ILP}(n)\cos(\omega n)\right)e^{-jN\omega} \tag{4.18}$$

$$H(e^{j\omega}) = \left(\frac{\omega_c}{\pi} + \frac{2}{\pi}\sum_{n=1}^{N} \frac{sin\omega_c n}{n}\cos(\omega n)\right)e^{-jN\omega} \tag{4.19}$$

From this formula, with given ω_c, the design of truncated lowpass filter is simple. The lowpass filter transfer function is also used for designing highpass, bandpass and bandstop filters [34].

4.1.2 FIR Highpass Filter
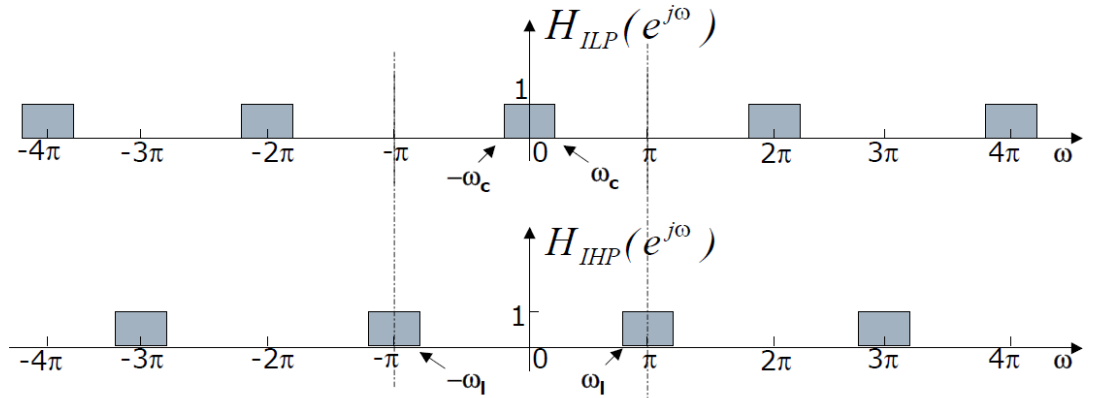
Figure 34: Frequency Response of Highpass filter and Lowpass filter **[34]**

The relation between the frequency responses of lowpass and highpass filters is given as

$$H_{HP} = H_{LP}\left(e^{j(\omega-\pi)}\right) \quad , \quad \omega_c = \pi - \omega_l \tag{4.20}$$

The frequency response of ideal lowpass filter known as

$$H_{ILP}(e^{j\omega}) = \sum_{-\infty}^{\infty} h_{ILP}(n)e^{-j\omega n} \tag{4.21}$$

So using the relation, it can be written as

$$H_{HP} = H_{LP}\left(e^{j(\omega-\pi)}\right) = \sum_{-\infty}^{\infty} h_{ILP}(n)e^{-j(\omega-\pi)n} = \sum_{-\infty}^{\infty} h_{ILP}(n)e^{-j\omega n}e^{j\pi n} \qquad (4.22)$$

$$H_{HP} = \sum_{-\infty}^{\infty} (-1)^n h_{LP}(n)e^{-j\omega n} \ , where \ e^{j\pi n} = (-1)^n \qquad (4.23)$$

So we concluded the equation as [9]

$$h_{HP}(n) = (-1)^n \ h_{LP}(n) \qquad (4.24)$$

4.1.3 FIR Bandpass Filter
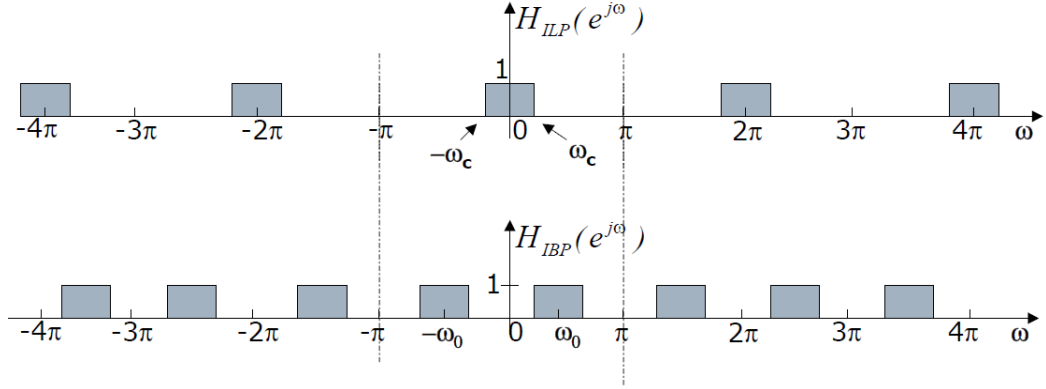
Figure 35: Frequency Response of Bandpass filter and Lowpass filter [34]

The relation between the frequency responses of lowpass and bandpass filters is given as

$$H_{IBP}(e^{j\omega}) = H_{ILP}\left(e^{j(\omega-\omega_0)}\right) + H_{ILP}\left(e^{j(\omega+\omega_0)}\right) \qquad (4.25)$$

By using that equation above

$$H_{IBP}(e^{j\omega}) = \sum_{-\infty}^{\infty} h_{ILP}(n)e^{-j(\omega-\omega_0)n} + \sum_{-\infty}^{\infty} h_{ILP}(n)e^{-j(\omega+\omega_0)n} \qquad (4.26)$$

$$H_{IBP}(e^{j\omega}) = \sum_{-\infty}^{\infty} h_{ILP}(n)e^{-j\omega n}e^{j\omega_0 n} + \sum_{-\infty}^{\infty} h_{ILP}(n)e^{-j\omega n} \ e^{-j\omega_0 n} \qquad (4.27)$$

$$H_{IBP}(e^{j\omega}) = \sum_{-\infty}^{\infty} h_{ILP}(n)e^{-j\omega n}(e^{j\omega_0 n} + e^{-j\omega_0 n}) = \sum_{-\infty}^{\infty}(2h_{ILP}(n)cos\omega_0 n)e^{-j\omega n} \qquad (4.28)$$

We concluded the equation as [34]

$$h_{IBP}(n) = 2h_{ILP}(n)cos\omega_0 \qquad (4.29)$$

4.1.4 FIR Bandstop Filter
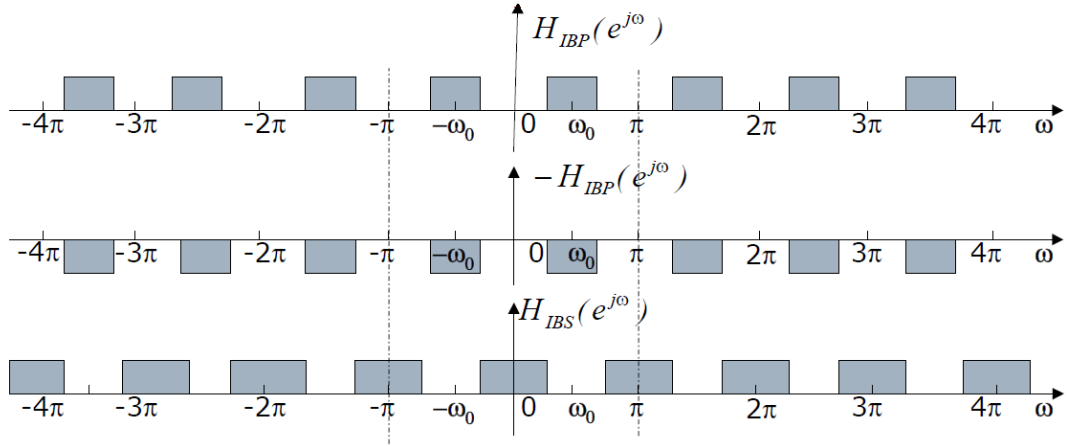
Figure 36: Frequency Response of Bandpass and Bandstop Filters **[34]**

The relation between the frequency responses of lowpass and bandstop filters is given as

$$H_{IBS}(e^{j\omega}) = 1 - H_{IBP}(e^{j\omega}) \qquad (4.30)$$

By taking the inverse Discrete Fourier Transform of both sides, we obtain the equation as [9]

$$h_{IBS}(n) = \delta(n) - h_{IBP}(n) \qquad (4.31)$$

$$h_{IBS}(n) = \delta(n) - 2h_{ILP}(n)cos\omega_0 n \qquad (4.32)$$

4.2 FIR and IIR Notch Filter Design

Let's focus on z-plane in Figure 37 to design FIR notch filter. Zeros of the filters on unit circle should have known that corresponds to the frequency which should be eliminated. The zeros of the filter must be symmetrical with respect to the origin of z-plane to make the coefficients of FIR notch filter realizable. The reason of symmetric zeros will be explained with an example. [34].
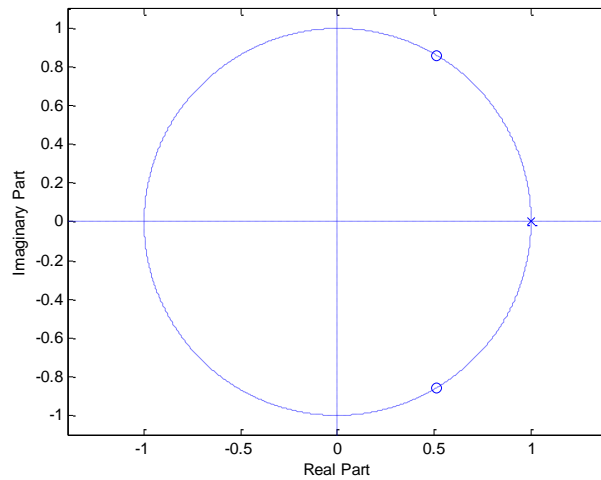
Figure 37: Zeros and Poles of FIR notch filter on z-plane

Let's design a FIR notch filter which eliminates 50 Hz frequency in the digital signal while the sampling frequency of the signal is 1000 Hz.

The zero of the z-plane should be located in $\omega_c = \frac{2\pi 50}{1000} = \frac{\pi}{10}$. So the $H(z)$ will be

$$H(z) = \left(1 - e^{j\frac{\pi}{10}}z^{-1}\right), \quad where \ z = e^{j\omega} \tag{4.33}$$
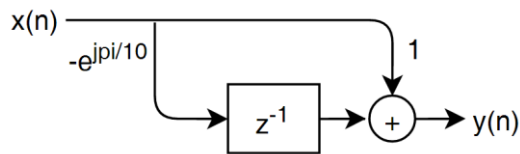
Figure 38: Block diagram of FIR notch filter (not realizable)

$H(z)$ Function consists of complex numbers. That complex numbers are multiplied with complex conjugate to make it real number.

So it can be written as

$$H(z) = \left(1 - e^{j\frac{\pi}{10}}z^{-1}\right)\left(1 - e^{-j\frac{\pi}{10}}z^{-1}\right) = 1 - 2\cos\left(\frac{\pi}{10}\right)z^{-1} + z^{-2} \qquad (4.34)$$

$$H(z) = 1 - 1.9021z^{-1} + z^{-2} \quad \rightarrow \quad y(n) = x(n) - 1.9021x(n-1) + x(n-2) \qquad (4.35)$$
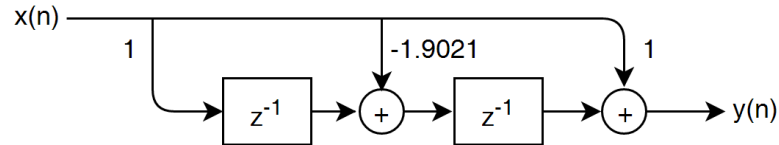
Figure 39: Block diagram of FIR notch filter (realizable)
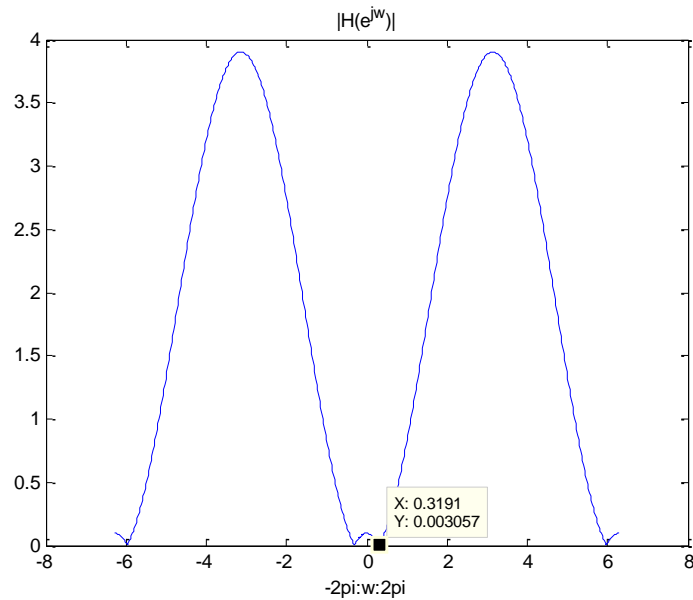
Figure 40: Frequency response of FIR notch filter

$$\omega_c = \frac{\pi}{10} = 0.314 \cong 0.3191 \qquad (4.36)$$

Matlab code

```
w=-2*pi:pi/128:2*pi;
h=1-2*cos(pi/10).*exp(-j.*w)+exp(-2*j.*w);
h=abs(h);
plot(w,h);
title('|H(e^j^w)|');
xlabel('-2pi:w:2pi');
```

Quality factor of filter is seen from the frequency response of the FIR notch filter is not good. It does not only reject 50 hz, but also reject the frequencies which close to 50 hz. Therefore, FIR digital filter shouln't be used. For this reason , Infinite Impulse Response (IIR) notch filter which has high quality factor is used[34]. Let's design an IIR notch filter by using the equation 4.34

$$H(z) = \frac{\left(1 - e^{j\frac{\pi}{10}}z^{-1}\right)\left(1 - e^{-j\frac{\pi}{10}}z^{-1}\right)}{\left(1 - ae^{j\frac{\pi}{10}}z^{-1}\right)\left(1 - ae^{-j\frac{\pi}{10}}z^{-1}\right)} \quad where \quad 0 < a < 1 \tag{4.37}$$

The value of a corresponds to poles of the filter on the z-plane . The more a closes to 1, the more quality factor of IIR filter increases. Therefore, frequency rejection of IIR filter will be narrow ,and frequency of 50 Hz on the digital signal will be rejected. Let's look at frequency response of the IIR notch filter.
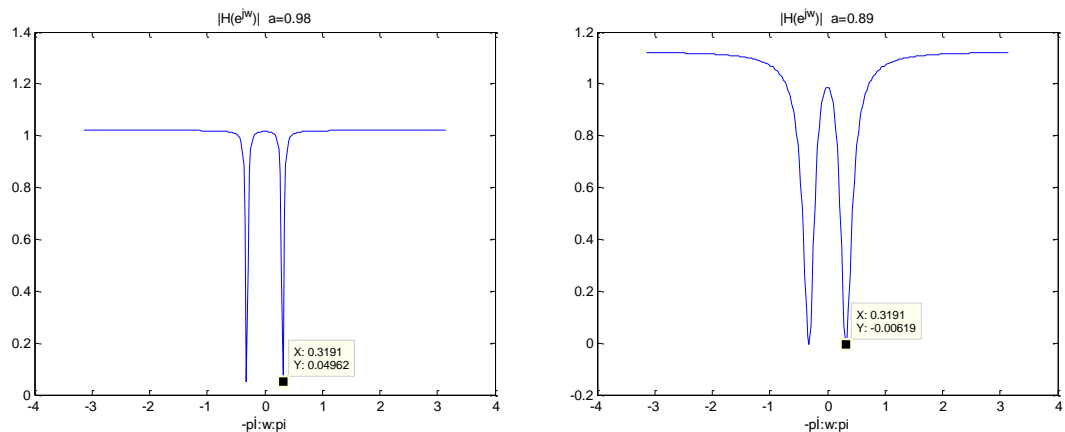
Figure 41: Frequency response of IIR notch filter where , $\omega_c = \frac{\pi}{10}$, $a = 0.98$, $and\ a = 0.89$

Matlab code is given for the notch filter which has $\omega_c = \frac{\pi}{10}$ and a=0.98 given as

```
clc
clear all
close all
w=-pi:pi/128:pi;
a=0.98;
Hb=(1-exp(j*pi/10).*exp(-j.*w)).*(1-exp(-j*pi/10).*exp(-j.*w));
Ha=(1-a*exp(j*pi/10).*exp(-j.*w)).*(1-a*exp(-j*pi/10).*exp(-j.*w));
H=Hb./Ha;
plot(w,H);
title('|H(e^j^w|  a=0.98');
xlabel('-pİ:w:pi');
```

$$H(z) = \frac{\left(1 - e^{j\frac{\pi}{10}}z^{-1}\right)\left(1 - e^{-j\frac{\pi}{10}}z^{-1}\right)}{\left(1 - 0.98e^{j\frac{\pi}{10}}z^{-1}\right)\left(1 - 0.98e^{-j\frac{\pi}{10}}z^{-1}\right)} = \frac{1 - 1.9021z^{-1} + z^{-2}}{1 - 1.8641z^{-1} + 0.9604z^{-2}} \tag{4.38}$$

$$H(z) = \frac{b_0 + b_1 z^{-1} + b_2 z^{-2}}{a_0 + a_1 z^{-1} + a_2 z^{-2}} \tag{4.39}$$

$$where\ b_0 = 1\,, b_1 = -1.9021\,, b_2 = 1,\ a_0 = 1\ ,\ a_1 = -1.8641,\quad a_2 = 0.9604 \tag{4.40}$$

$$y(n) - 1.8641y(n-1) + 0.9604y(n-2) = x(n) - 1.9021x(n-1) + x(n-2) \tag{4.41}$$
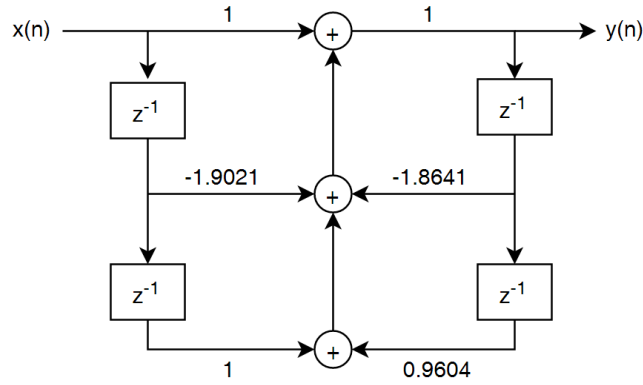
Figure 42: Block diagram of 50 Hz IIR notch filter , a=98

Now, we have the IIR notch filter coefficients which have 50 hz cut-off frequency. Thus, we can apply filter coefficients on digital signal which is sampled with 1000 Hz. These coefficients are calculated for eliminating the 50 hz frequency on digital signal which is sampled with 1000 Hz. If the coefficients are applied on a digital signal which has 2 kHz sampling frequency, cut-off frequency of the digital filter will be shifted and 25 Hz will be eliminatd. Therefore, this filter coefficients should be used on 1 khz sampled digital signal. IIR notch filter function is written as [34]

$$y(n) = x(n) - 1.9021x(n-1) + x(n-2) + 1.8641y(n-1) - 0.9604y(n-2) \tag{4.42}$$

Where

$x(n)$ corresponds to current sample of the signal

$x(n-1),\ x(n-2)$ corresponds to previous samples of the signal

$y(n)$ corresponds to current output of the filtered signal

$y(n-1), and\ y(n-2)$ corresponds to previous outputs of the filtered signal

4.2.1 IIR and FIR Notch Filter Application on Matlab

$$y(n) = x(n) - 1.9021x(n-1) + x(n-2) + 1.8641y(n-1) - 0.9604y(n-2) \qquad (4.43)$$

The output of the digital signal can be directly found by multiplying and adding of sampled signal x(n) by using the formula above, or the filtered signal can be found by using MATLAB " filter() " function.

```
Matlab code
n=0:500;
x=cos(2*pi*50/1000.*n);
b0=1 ; b1=-1.9021 ; b2=1;
a0=1 ; a1=-1.8641 ; a2=0.9604;
b=[b0 b1 b2];
a=[a0 a1 a2];
y=filter(b,a,x);
figure
plot(n,x,'r');
title('IIR NOTCH FILTER');
xlabel('n');
ylabel('Magnitude');
hold on
plot(n,y,'b');
ylim([-2 2])
legend('50 Hz signal','filtered signal')
```
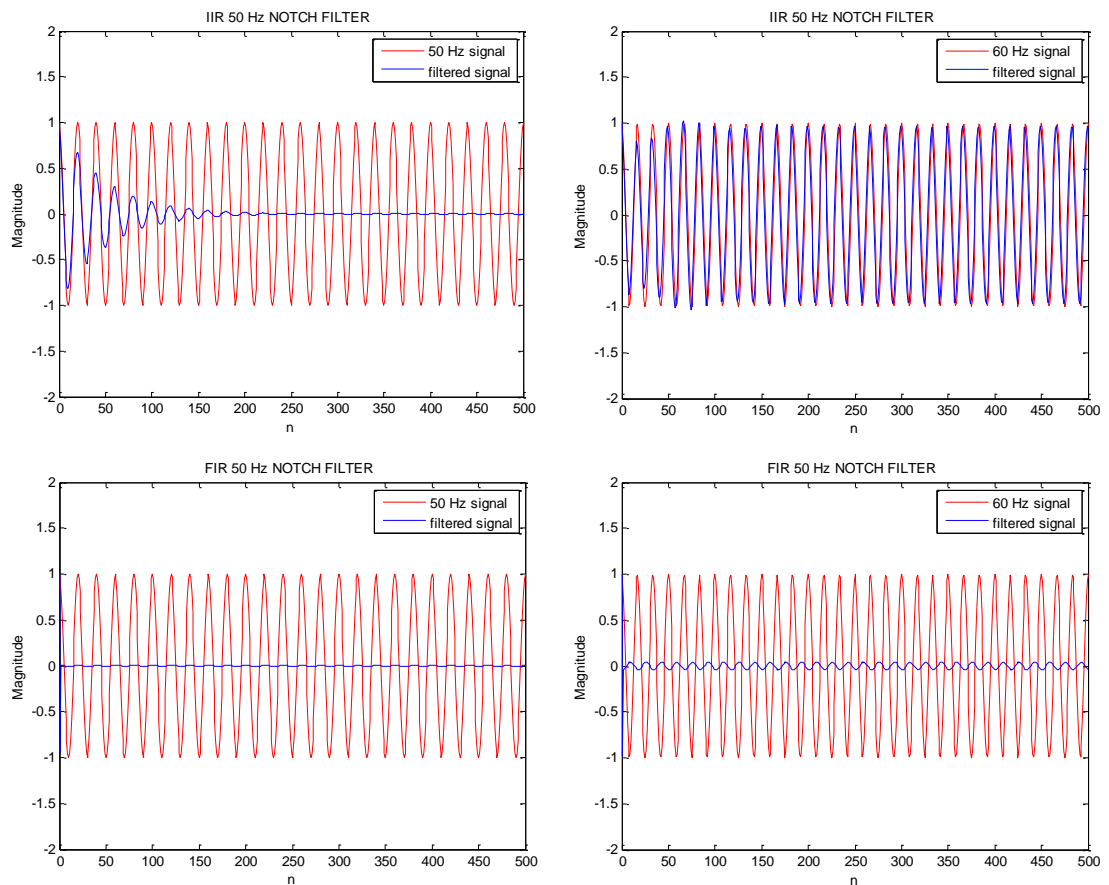

Figure 43: Comparison of original and filtered signals by using FIR and IIR Notch Filters

42

Input and output comparison of IIR and FIR filters are shown ib Figure 43. It can be seen that IIR 50 hz notch filter removes the 50 hz signal without changing the 60 Hz frequency. But FIR 50 Hz notch filter removes also 50 and 60 Hz. For this reason, IIR filters are used on ECG signal not to change the desired frequencies on the ECG.

4.2.2 IIR Notch Filter Application on dsPICs

MicroC compiler has been used for programming the dsPIC30F3011. Filter function on MicroC has been used for filtering the signal. Example of MicroC program to do IIR filtering is written [35].

```
        const unsigned int
         BUFFER_SIZE  = 8;
        const unsigned int
         FILTER_ORDER  = 2;
        const unsigned int
 COEFF_B[FILTER_ORDER+1] = {                    // Coefficient is written in Q1.15 format
0x3F9A, 0x8646, 0x4000};                        // decimal format  [1   -1.9021   1 ];
        const unsigned int
 COEFF_A[FILTER_ORDER+1] = {                    // decimal format  [1   -1.8641   0.9604];
0x4000, 0x88B1, 0x3D77};
        const unsigned int
         SCALE_B      = -1;
        const unsigned int
         SCALE_A      = -1;
        unsigned inext;                         // Input buffer index
        unsigned int input[BUFFER_SIZE];        // Input buffer
        unsigned int output[BUFFER_SIZE];       // Output buffer
        unsigned int CurrentValue;

        input[inext] = ADCBUF0;                 // Fetch sample

        CurrentValue = IIR_Radix( SCALE_B,  //Scale the coefficients in the range of 0 to 1
                      SCALE_A,               //
                      COEFF_B,               // b coefficients of the filter
                      COEFF_A,               // a coefficients of the filter
                      FILTER_ORDER+1,        // Filter order + 1
                      input,                 // Input buffer
                      BUFFER_SIZE,           // Input buffer length
                      output,                // Input buffer
                      inext);                // Current sample
        output[inext] = CurrentValue;
 inext = (inext+1) & (BUFFER_SIZE-1);           // if(inext<=BUFFER_SIZE){
                                                //inext=inext+1;
                                                //else
                                                // inext=0;  };
```

The coefficients is obtained in the previous example as

$$b_0 = 1, b_1 = -1.9021, b_2 = 1, \ a_0 = 1 \ , \ a_1 = -1.8641, \ \ a_2 = 0.9604 \qquad (4.44)$$

43

dsPIC microprocessors work with Q1.15 fixed point fractional numbers. Q1.15 number consists of 1 integer bit and 15 fractional bits. However, the IIR filter coefficients which were found in the previous section were decimal numbers. Therefore, the coefficients must be translated into Q1.15 format. Matlab code to transfer decimal number to Q1.15 format is given as

Matlab code

```
a_SCALE=2^-1;    % a coefficient scaled in the range of 0 to 1  scaling coef= -1
a=[1 -1.8641 0.9604].*a_SCALE;
b_SCALE=2^-1; %   b coefficient scaled in the range of 0 to 1  scaling coef= -1
b=[1 -1.9021 1].*b_SCALE;
a_new=convert_onedotfifteen(a)    %coefficients are converted Q1.15 format
b_new=convert_onedotfifteen(b)    %coefficients are converted Q1.15 format

function [Q15] = convert_onedotfifteen(numbers)
template = numbers;
if template > 0
decimal = round((2^15)*template);

else
decimal = abs(round(((2^15)+1)*template));
decimal = bitcmp(decimal,16) + 1;
end

Q15=dec2hex(decimal);
end
```

Results are

a_new=[0x4000, 0x88B1, 0x3D77];

b_new=[0x4000, 0x8646, 0x4000];

In the Matlab program, "a" and "b" coefficients are scaled in the range of 0 to 1 by multiplying 2^{-1} for translating to the Q1.15 format. If the coefficients are close to 1, filter resolution will increase. For example if we have the coefficients $b_0 = 0.02$, $b_1 = 0.4$, $b_2 = 0.02$, we should multiply the scaling factor of 2^2 for increasing the resolution. The important point is; scaled coefficients should always be in the range of 0 to 1. Now we can write the Q1.15 format coefficients on MicroC program and filter the signals on dsPIC processor.

Chapter 5

Design of Fingertip ECG Measurement System

5.1 Block Diagram of Fingertip ECG Measurement System
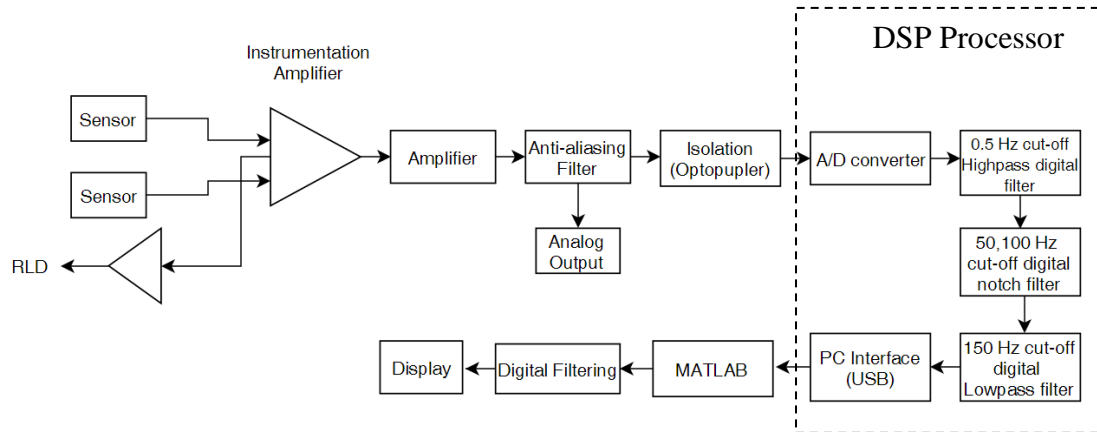
Figure 44: Block diagram of ECG Circuit

Traditionally, ECG signal from lead 1 is measured using three electrodes [31]. However, the circuit in Figure 44 is working with two Plessey sensors as differential mode, and one copper surface on the PCB as an RLD input. Instrumentation amplifier and operational amplifier which are used for amplification have an high CMRR (must greater than 80 dB) in order to amplify small signals such as ECG, EMG, and EOG signals which is the range of millivolts [31]. For the patient protection, isolation and protection circuitry are used to limit through the electrodes to safe levels [29]. Therefore, Plessey sensors have an internal input resistor up to 20 Gohm for preventing high current flow to the patients.

Instrumentation amplifier is used for differentiating the signals from the left and right side of the heart and extracting the ECG signal. ECG signals vary from the 1 millivolt to 5 millivolts. Due to the range of millivolts, the ECG signal is needed to be amplified in order to have better interpret. Therefore, the gain should be 1000 which converts the ECG signal in the range of 1 Volt to 5 Volt [29].

Anti-aliasing filter is used for eliminating the high frequency component on the ECG not to disturb the desired digital signal. Anti-aliasing filters are known as lowpass filters and their cut-off frequencies are determined by the sampling frequency of analog digital converter. If the sampling frequency of ADC is 1000 Hz, and lowpass filter is considered as ideal filter, cut-off frequency of lowpass filter should be maximum 500 Hz. 5th order lowpass filter that has 150 Hz cut-off frequency is used on the ECG circuit.

6th order highpass digital filter with 0.5 Hz cut-off, 6th order lowpass digital filter with 150 Hz cut-off and second order notch filter with 50 and 100 Hz cut-off are used on after analog digital conversion of ECG signal. The reason why highpass, notch, and lowpass filter are used after AD converter is; for being easily modifiable on the Software side. Highpass filter is used for eliminating the DC coupling from body movements. Notch filter is used for eliminating the powerline noise. Low-pass filter is used for reducing EMG noise on ECG.

Opto-coupler is used as a protection the current flow from computer to the patient. The second advantage of using opto-coupler is to reduce the powerline interference (50 Hz) on ECG. It separates the ground of power source which is computer's USB with the ground of battery. There is also second ground which needs to be separated from the battery. In order to reduce the powerline noise, right leg cannot be directly connected to ground of battery. If right leg or any part of the body is connected to ground of battery, it will also cause power line noise. Main reason is; human body works like an antenna and absorb all kind of noise such as RF, powerline noise etc. However, powerline noise on ECG coming from human body is much smaller than desired ECG signal. It can be neglectable, and there is also one way to eliminate this noise. That way is to use right leg drive for separating the body with battery ground. It can be called as virtual ground too. By using right leg drive and opto-coupler, power-line noise can be easily eliminated without using notch filter.

Let's examine the circuit part by part.

5.1.1 Power Supply of ECG circuit
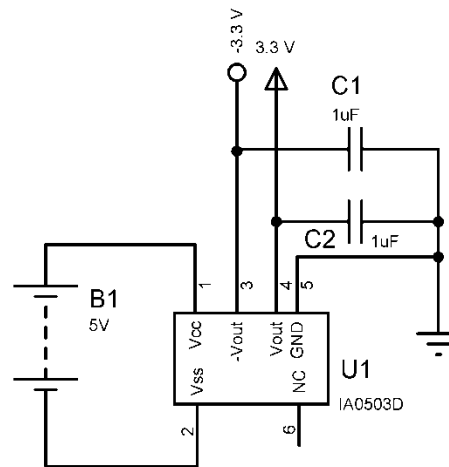
Figure 45: Power supply of ECG circuit

IA0503D DC-DC voltage converter is used as a power supply of the circuit. It converts 5 Volt DC voltages into 3.3 Volts and -3.3 Volts in order to feed the op-amp positive and negative voltage.

5.1.2 Instrumentation Amplifier

PS25201A is an ECG sensor which senses and amplifiers action potentials. It can be used as contact and non-contact mode. AD627BRZ instrumentation amplifier is used for extraction ECG signal from left and right finger. Gain calculation of instrumentation amplifier is done in appendix C. ECG signals are very small (in 1 mV - 5 mV range). For this reason, total gain of the output of AD627BRZ is settled to 1000 which is desired for increasing the resolution of the signal while converting it to digital. Because human skin can create DC voltage offset, OPA2379 is used as an integrator to compensate this DC offset by feedback the signal to the reference pin of the instrumentation op-amp. Instrumentation amplifier is fed by +5 V and -5 V not to cut the negative signal output. When the voltage of the negative input of the instrumentation amplifier is greater than positive input, amplifier creates negative signal output. But if the amplifier is fed +5 to 0 Volt, it will clip the negative voltage output. For example; if the ECG signal is negative polarized, desired ECG signal will be clipped and it cannot be seen at the output. R12 and R13 resistors are also used for

this reason to ensure the signal in the range of 0 to 5 V. These resistors give the positive feedback on ECG signal to increase the signal level to 2.5 V.
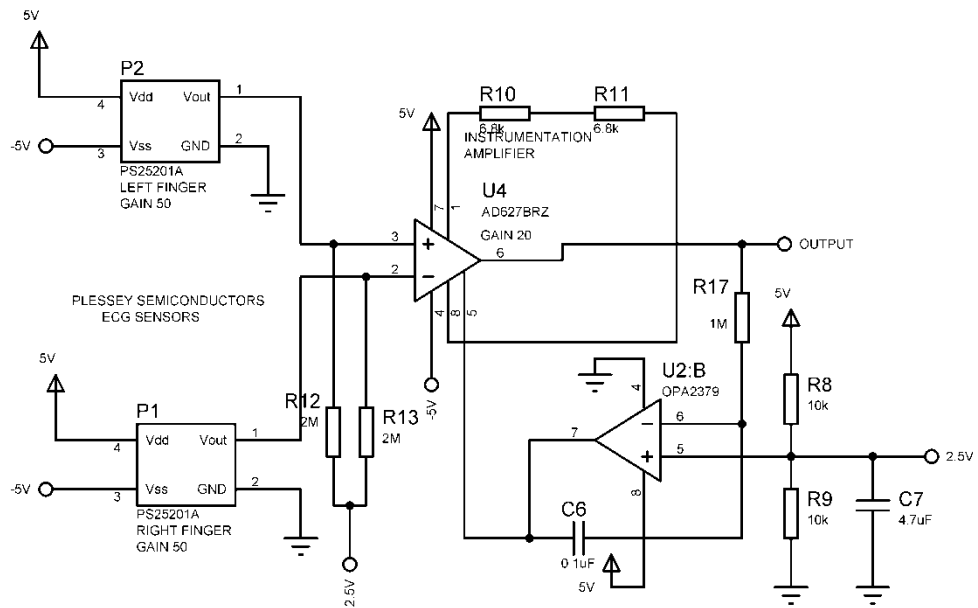
Figure 46: Instrumentation Amplifier for ECG signal extraction

Instrumentation amplifier can be used without right leg drive in the Figure 46. ECG circuit can work without analog and digital filters, and right leg drive. Let's look at the outputs of the circuit when we touch the ground and without touching the ground rather than using right leg drive. In the outputs below, analog and digital filters are not included.
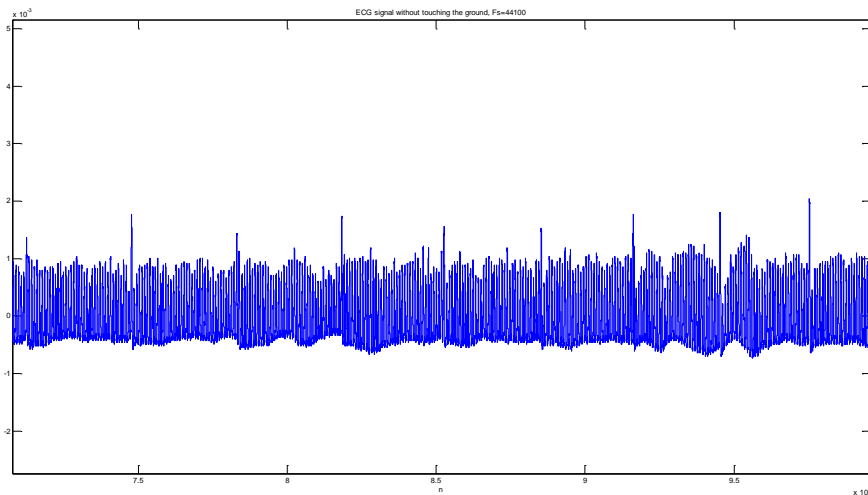
Figure 47: Fingertip ECG signal while not touching the ground
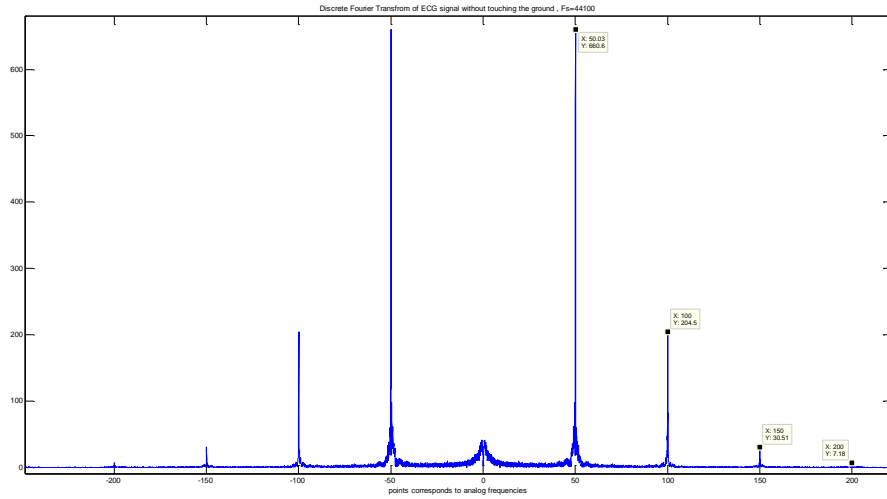
Figure 48: Discrete Fourier Transform of ECG signal while not touching the ground
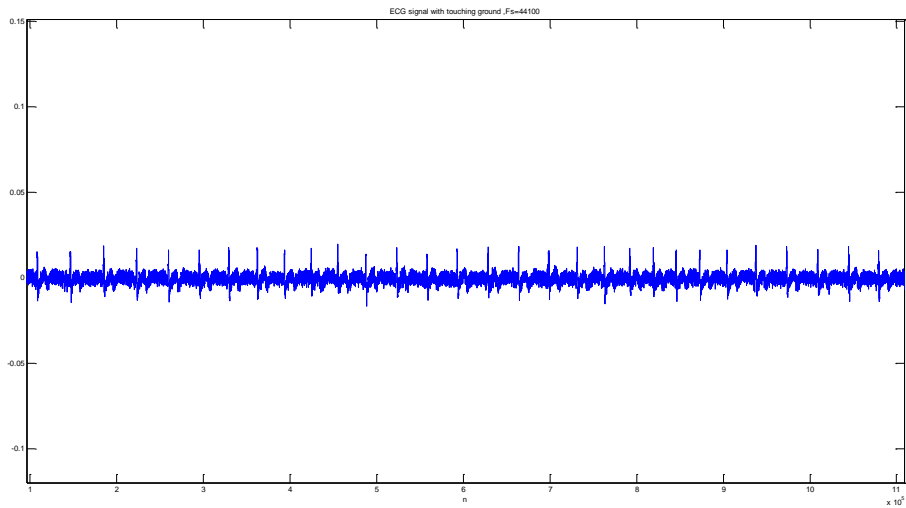
Figure 49:Fingertip ECG signal while touching the ground
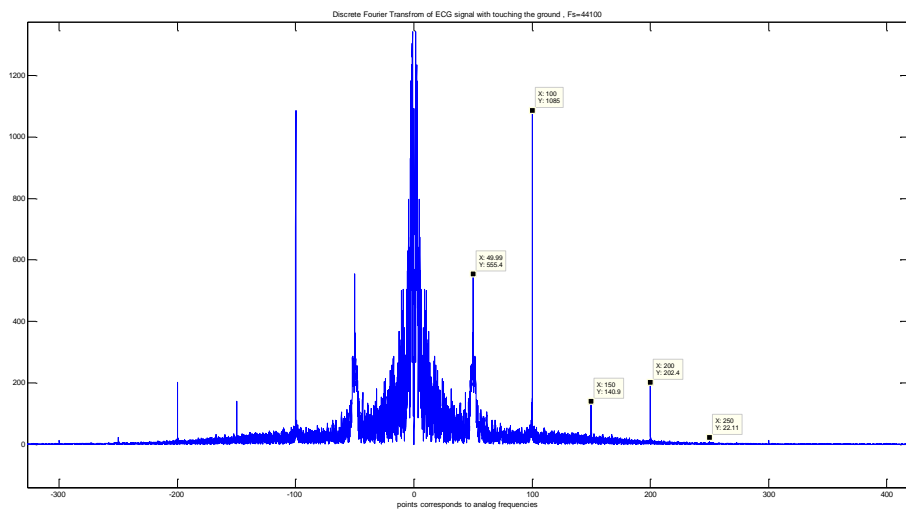
Figure 50: Discrete Fourier Transform of ECG signal while touching the ground

The result is obvious that ECG signal taken from patient while not touching the ground has more noise. Magnitude of powerline noise (50 Hz) and its harmonics are higher than desired frequencies of the ECG signal which is in the range of 0-150 Hz in the figure 47. On the figure 49, noise level is decreased by touching the ground. Grounding or using right leg drive is more important for reducing the noise level on ECG signal.

5.1.3 Right Leg Drive Circuit

In most modern ECG systems, the patients are not grounded at all. Instead of grounded, right leg drive is connected to the right leg of the patient. Two resistor of the instrumentation amplifier R_g is used to sense the common-mode voltage on the body, inverting, amplifying, and feeding the right leg. The negative feedback drives the common-mode voltage to low value. [32] The body's displacement current does not flow to ground but rather to the op-amp circuit. For this reason, this reduces the interference as far as the ECG amplifier is concerned. [32]
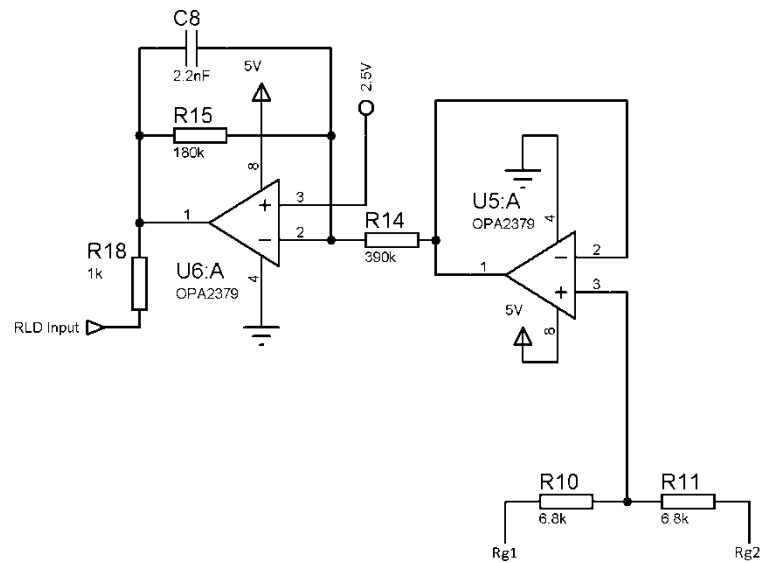
Figure 51: Right Leg Drive Circuit

5.1.4 5th order Lowpass filter

Calculation is made in the section of analog lowpass filter design. 5th order lowpass filter which has 150 Hz cut-off is used for removing the unwanted frequencies while converting the signal to digital. 5th order lowpass filters specifications are written as

- Passband flatness of the filter is high.
- 0 dB in passband cut-off frequency (150 Hz)
- 50 dB in stopband cut-off frequency (500 Hz)
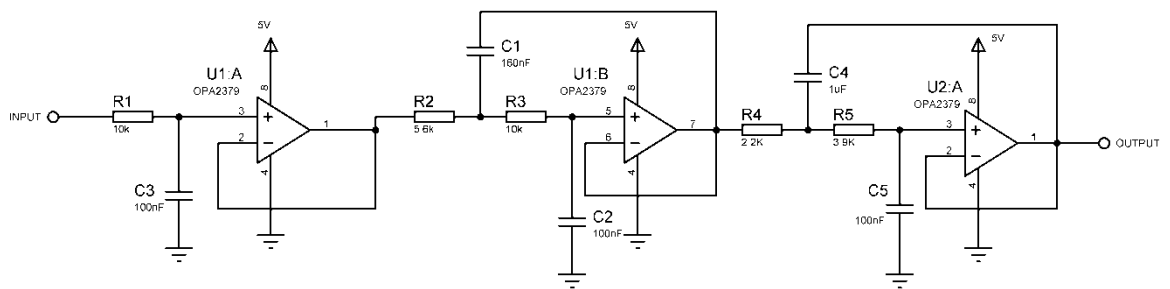
Figure 52: 5th order lowpass filter (150 Hz cut-off frequency)

The important point in this section is; operational amplifier is fed in the range of 5 Volt to 0 Volt. The reason is; Plessey sensors perform sinusoidal signal in the range of 5 Volt to -5 Volts when patient does not touch sensors. For this reason, if the operational amplifier is fed with 5V to -5V, there will be a 10 V sinusoidal signal in the output of the analog filter. Inputs of the microcontroller work with the range of 0-5 Volt, so 10 volt sinusoidal signal will break down the microcontroller's A/D converter pin.

5.1.5 Opto-coupler

PS2501 model opto-coupler have been used in the circuit. Opto-coupler is essential for reducing powerline interference on ECG. Only using optocoupler, powerline interference which comes from power supply can easily be reduced without the need of analog bandstop or notch filters. In order to reduce 50 Hz ground noise, the ground of power supply needs to be separated with the ground of battery. Especially, ground of AC power supply have to be seperated with the instrumentation amplifier and opamp which have high gains. We have found that 50 hz noise are also being amplified while the process of ECG amplification.

51

The circuit in Figure 53 is the example of ground loop separation. Ground of input signal are seperated with the ground of battery.
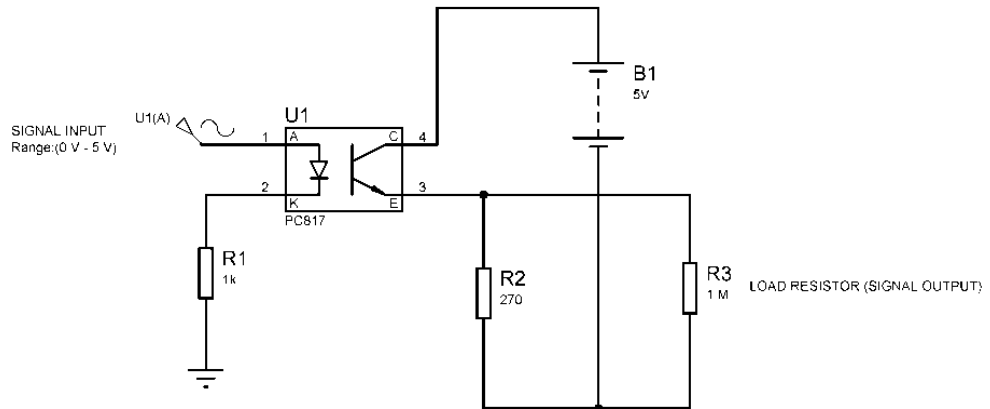
Figure 53: Ground loop separation with opto-coupler

5.2 Schematic of Fingertip ECG Circuit
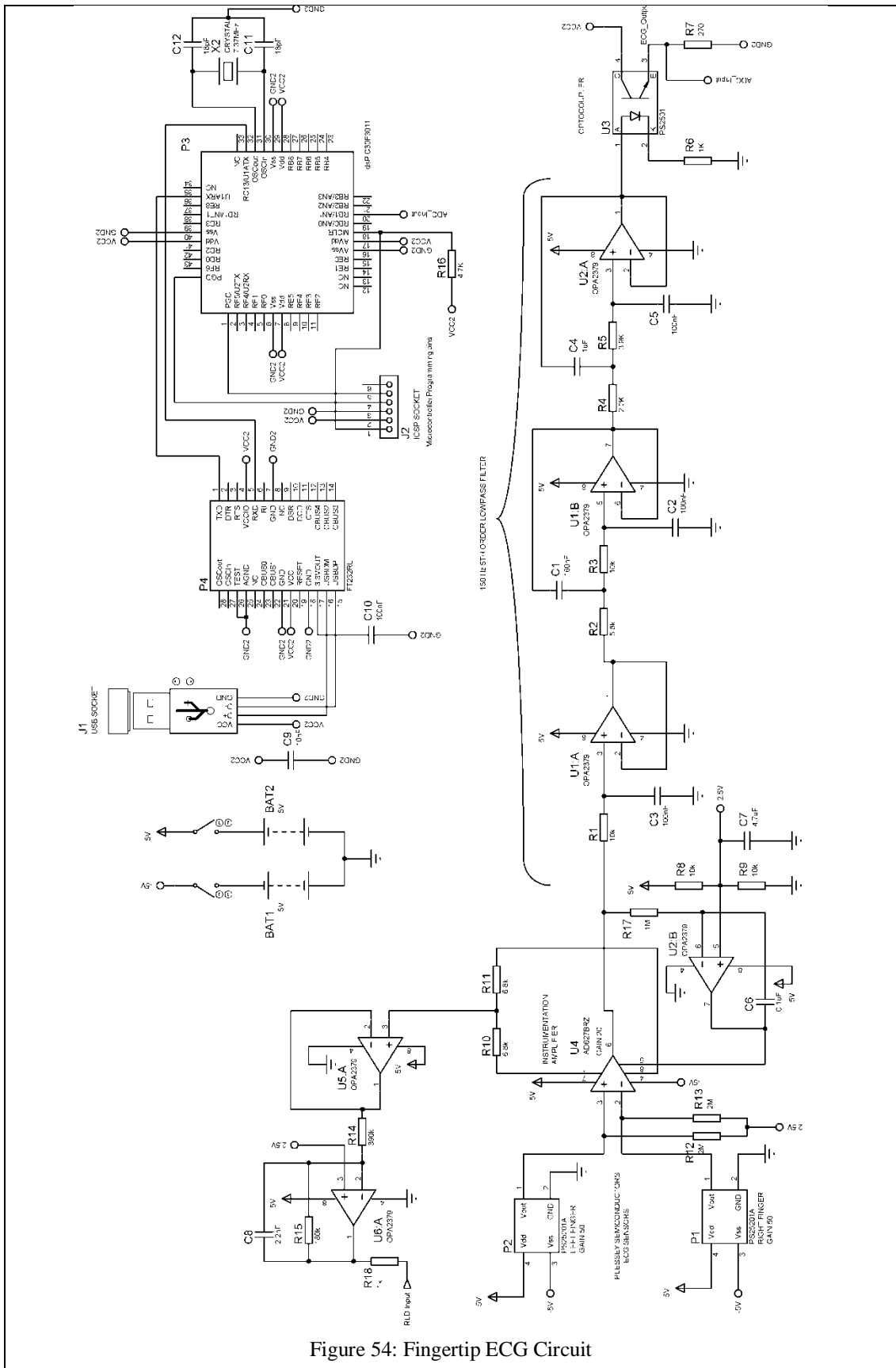
Figure 54: Fingertip ECG Circuit

Schema of the fingertip ECG circuit is given in Figure 54. It contains differential amplifier, operational amplifier, right leg drive, Plessey sensors, 5th order low-pass filter, opto-coupler (isolator), and dsPIC and USB port.

REFERENCE	COMPONENT	QUANTİTY	UNIT PRICE
P1,P2	PS25201 Plessey Sensor	2	23.66 $
U4	AD627BRZ	1	9.32 $
U1,U2,U5,U6	OPA2379AID	3	2.32 $
P3	dsPIC30F3011-30I/PT	1	5.43 $
P4	FT232RL-REEL SSOP-28	1	4.61 $
J1	Mini USB B-type socket	1	0.45 $
J2	6 pin connector	1	0.09 $
R12,R13	2 $M\Omega$,%1 1206[3225metric]	2	0.22 $
R10,R11	6.8 $k\Omega$,%1 1206	2	0.22 $
R17	1 $M\Omega$,%1 1206	1	0.22 $
R1,R3,R8,R9	10 $k\Omega$,%1 1206	4	0.22 $
R2	5.6 $k\Omega$,%1 1206	1	0.22 $
R4	2.2 $k\Omega$,%1 1206	1	0.22 $
R5	3.9 $k\Omega$,%1 1206	1	0.22 $
R6	1 $k\Omega$,%1 1206	1	0.22 $
R7	270 Ω ,%1 1206	1	0.22 $
R16	4.7 $k\Omega$,%1 1206	1	0.22 $
R14	180 $k\Omega$,%1 1206	1	0.22 $
R15	390 $k\Omega$,%1 1206	1	0.22 $
C2,C3,C5,C6, C1	100 $nF \pm$ %10 1206	5	0.50 $
C1	160 $nF \pm$ %10 1206	1	0.50 $
C4	1 $uF \pm$ %10 1206	1	0.50 $
C7	4.7 $uF \pm$ %10 1206	1	0.50 $
C9	10 $nF \pm$ %10 1206	1	0.50 $
C8	2.2 $nF \pm$ %10 1206	1	0.50 $
C11,C12	18 $pF \pm$ %10 1206	1	0.50 $
X2	7.37Mhz, 18pF crystal 30ppm	1	0.55 $
BAT1,BAT2	3.6 V LIR2477 battery holder	2	1.44 $
BAT1,BAT2	3.6 V LIR2477 rechargeable 180 mAh coin battery	2	3.98 $
U3	PS2501 Optocoupler	1	0.06 $
Total price	-	-	86.91 $

Table 1: Components of the ECG circuit with unit prices

Component price for the ECG circuit is given in Table 1.

5.3 dsPIC microC Program

USB interface between Fingertip Circuit with computer by using MicroC is given in the below. This is an example program of fingertip ECG circuit which has notch filter. In the realized circuit, all of digital filters were included on dsPIC processor.

```
// Device setup:
//    Device name: P30F3011
//    Device clock: 117.920000 MHz
//    Sampling Frequency: 1000 Hz
//    Filter setup:
//    Filter kinds: IIR
//    Filter type: 2th order 50 Hz, 100 Hz Notch filter
//    Filter window: Rectangular

 #include <built_in.h>
 const unsigned int
 BUFFER_SIZE = 8;
const unsigned int
 FILTER_ORDER = 3;
const signed int
 COEFF_B[FILTER_ORDER+1] = {           //IIR Notch filter 50 Hz b coefficients
    0x3F9A, 0x8706, 0x3F9A};
const signed int
 COEFF_A[FILTER_ORDER+1] = {           //IIR Notch filter 50 Hz a coefficients
    0x4000, 0x8706, 0x3F33};
const unsigned int
 SCALE_B     = -1; //
const unsigned int
 SCALE_A     = -1; //

 const signed int
 COEFF_D[FILTER_ORDER+1] = {           //IIR Notch filter 100 Hz b coefficients
    0x3F9A, 0x9917, 0x3F9A};
const signed int
 COEFF_C[FILTER_ORDER+1] = {           //IIR Notch filter 100 Hz a coefficients
    0x4000, 0x9917, 0x3F33};

const unsigned int
 SCALE_D     = -1;
const unsigned int
 SCALE_C     = -1;

unsigned int inext;                    // Input buffer index
unsigned int input[BUFFER_SIZE];       // Input buffer
unsigned int output[BUFFER_SIZE];      // Output buffer

unsigned int inext2;                   // Input buffer index
unsigned int input2[BUFFER_SIZE];      // Input buffer
unsigned int output2[BUFFER_SIZE];     // Output buffer

// This is ADC interrupt handler.
// Analogue input is sampled and the value is stored into input buffer.
// Input buffer is then passed through filter.

void ADC1Int() org 0x2A {              // ADC interrupt handler
unsigned int CurrentValue;

 input[inext] = ADCBUF0;               // Fetch sample

 CurrentValue = IIR_Radix( SCALE_B,    //
                SCALE_A,       //
                COEFF_B,       // b coefficients of the filter
                COEFF_A,       // a coefficients of the filter
                FILTER_ORDER+1,// Filter order + 1
                input,         // Input buffer
                BUFFER_SIZE,   // Input buffer length
                output,        // Input buffer
                inext);        // Current sample

 output[inext] = CurrentValue;

 inext = (inext+1) & (BUFFER_SIZE-1);     // inext = (inext + 1) mod BUFFER_SIZE;

 input2[inext2] = CurrentValue;        // Fetch sample

 CurrentValue = IIR_Radix( SCALE_D,    //
                SCALE_C,       //
                COEFF_D,       // b coefficients of the filter
                COEFF_C,       // a coefficients of the filter
```

```
                    FILTER_ORDER+1,// Filter order + 1
                    input2,      // Input buffer
                    BUFFER_SIZE,  // Input buffer length
                    output2,     // Input buffer
                    inext2);     // Current sample

 output2[inext2] = CurrentValue;

 inext2 = (inext2+1) & (BUFFER_SIZE-1);// inext = (inext + 1) mod BUFFER_SIZE;

IFS0.F11 = 0;                    // Clear AD1IF  to clear ADCBUF interrupt flag

 }


// This is Timer1 interrupt handler.
// It is used to start ADC at
// periodic intervals.

void Timer1Int() org 0x1A {          // Timer1 interrupt handler



//void Soft_UART_Break();
ADCON1.F1  = 1;                 // Start sampling
ADCON1.F15 = 1;                 // Start conversion
IFS0.F3   = 0;                  // Clear TMR1IF

 delay_us(10);
 Soft_UART_Write(output2[inext2]>>8); // send high bytes of 10 bit sampled signal to USB
 delay_us(10);
 Soft_UART_Write(Lo(output2[inext2]));// send low bytes of 10 bit sampled signal to USB


} //~
// Main program starts here.
// Firstly, hardware peripherals are initialized and then
//  the program goes to an infinite loop, waiting for interrupts.
void main() {
 Soft_UART_Init(&PORTC, 14, 13,38400, 0);  //UART pins configurations
 inext  = 0;                // Initialize buffer index
 inext2=0;
 Vector_Set(input, BUFFER_SIZE, 0);  // Clear input buffer
 Vector_Set(output, BUFFER_SIZE, 0);  // Clear output buffer
 Vector_Set(input2, BUFFER_SIZE, 0);  // Clear input buffer
 Vector_Set(output2, BUFFER_SIZE, 0); // Clear output buffer

 // ADC setup
 TRISB  = 0xFFFF;              // Use PORTB for input signal
 ADCON1 = 0x00E2;                // Auto-stop sampling, unsigned integer out
 ADCON2 = 0x0000;
 ADCON3 = 0x0227;                // Sampling time= 3*Tad, minimum Tad selected
 ADPCFG = 0x0000;               // Configure PORTB as ADC input port  '0'
                    //config as Analog, '1' as Digital. all PORTB = Analog
 ADCHS  = 0x0001;               // Sample input on RB1
 ADCSSL = 0;               // No input scan
 ADPCFG = 0x0000;                // Configure PORTB as analog ADC input port

 // Interrupts setup
 IFS0   = 0;
 IFS1   = 0;
 IFS2   = 0;
 INTCON1 = 0x8000;               // Nested interrupts DISABLED
 INTCON2 = 0;                // Configure PORTB as analog ADC input port
 IEC0   = 0x0808;             // Timer1 and ADC interrupts ENABLED
 IPC0.F12= 1;                  // Timer1 interrupt priority level = 1
 IPC2.F13= 1;                  // ADC interrupt priority level = 2


 PR1    = 0x7328;              //Sampling = 1000 Hz. Value of PR1 is dependent
                    //on clock. OSC=118.92 Mhz
 T1CON  = 0x8000;                // Timer1 ON, internal clock FCY, prescaler 1:1

 while(1){      };            // Infinite loop, wait for interrupts
      }                // close main program
```

5.4 Matlab Program

USB interface between Fingertip Circuit with computer by using Matlab is given as

```matlab
clc
clear all
close all

fclose('all');                % close all open files
delete(instrfindall);         % Reset Com Port
delete(timerfindall);         % Delete Timers


Baudrate=38400;

portNum=2;
wrongPort=1;

while wrongPort
    s = serial(['COM' num2str(portNum)]);
    try
set(s,'BaudRate', Baudrate, 'DataBits', 8, 'Parity', 'none','StopBits', 1,
'FlowControl', 'none');
        fopen(s);             %go to catch if can't open
        wrongPort=0;          % found the right one - exit while loop!
    catch
        delete(s);
        clear s
      %  instrreset            %close any wrongly opened connection
        wrongPort =1 ;         % keep trying...
    end
    portNum=portNum+1;
      if portNum==16
          error('Device is not connected')
      end
end

Fs=1000;
i=1;

Second=60;          % Record Time 60 second

 while i<(Fs*2*Second)
  dat(i)=fread(s,1);
  i=i+1;
  end
 k=1;

  for i=1:2:Fs*(2*Second)-2
x=uint8(dat(i));               % x is high byte which is sent by UART
y=uint8(dat(i+1));             % y is low byte which is sent by UART
bytepack=uint16(x);
bytepack=bitshift(bytepack,8);
% Put them together (here, 'y' is placed in lower 8 bits)
z=bitor(bytepack,uint16(y));
data(k)=z;                % 10 bits data array is constructed by lower and higher 8 bits
%sent by UART
k=k+1;
  end

x=double(data);
figure
plot(x);
title('Fs=1000 Original Signal');
figure
N=1000000;
plot(linspace(-pi,pi,N),fftshift(abs(fft(x,N))));
title('Fs=1000 DFT of ECG signal without using digital filter');

Wo = 50/(Fs/2);                    % BW = Wo/35;
BW=2*pi*(2/Fs);                    % BW= 2 Hz
figure
[b,a] = iirnotch(Wo,BW);
K4=filtfilt(b,a,x);               % K4 is the filtered ECG signal by using 50 Hz notch
```

57

```matlab
%filter;

Wo=100/(Fs/2);
[b,a ]=iirnotch(Wo,BW);
K4=filtfilt(b,a,K4);               % K4 is the filtered ECG signal by using 100 Hz notch
%filter;

% Wo=150/(Fs/2);
% [b,a ]=iirnotch(Wo,BW);
% K4=filtfilt(b,a,K4);              % K4 is the filtered ECG signal by using 150 Hz
notch filter;
% plot(K4);
% title('Notch 50, 100, 150 Hz signal output');

figure
Wn=2*pi*(150/(Fs));
[b,a] = butter(6,Wn,'low');
K5=filtfilt(b,a,K4);               % K5 is the filtered ECG signal by using 150 Hz 6th
%order lowpass filter;

figure
Wn=2*pi*(0.5/(Fs));
[b,a] = butter(6,Wn,'high');
K5=filtfilt(b,a,K4);               % K5 is the filtered ECG signal by using 0,5 Hz 6th
%order highpass filter;
plot(K5);
title('0,5 Hz high pass filtered ECG signal');

figure
plot(linspace(-pi,pi,N),fftshift(abs(fft(K5,N))));
title('Frequency Spectrum of filtered ECG signal output');


smoothcoef=30;                          % size of the smoothing coefficients
b= ones(1,smoothcoef)/smoothcoef;
smoothed=filter(b, 1,K5);               % ECG signal that filtered with smoothing
operation
figure
plot(smoothed);
xlabel('Smoothed ECG Signal');


save('filtered_data.mat', 'K5');        % Filtered ECG signal
save('smoothed_data.mat', 'smoothed');  % Smoothed ECG signal
fclose(s);
delete(s)
clear s
```

5.5 Matlab Outputs of the ECG circuit
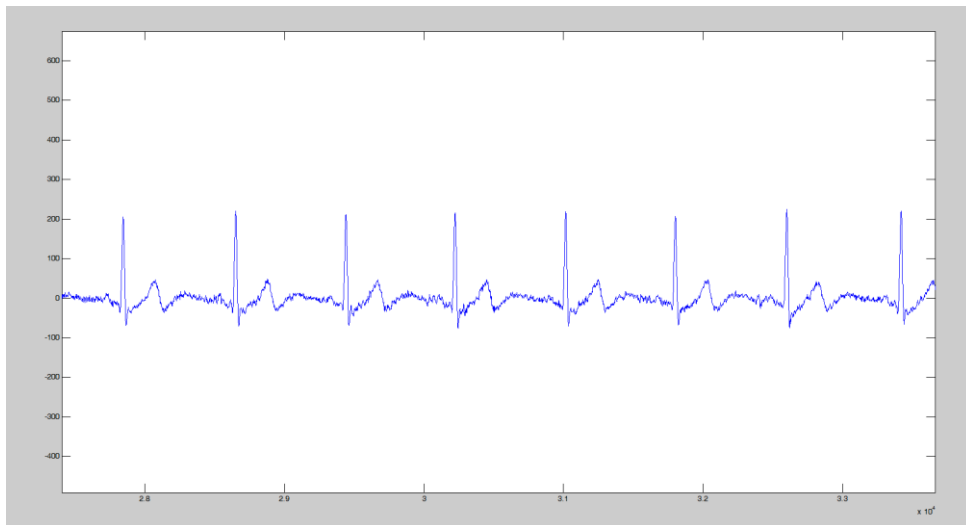
Figure 55: Fingertip ECG signal output which filtered with lowpass, highpass and notch filters
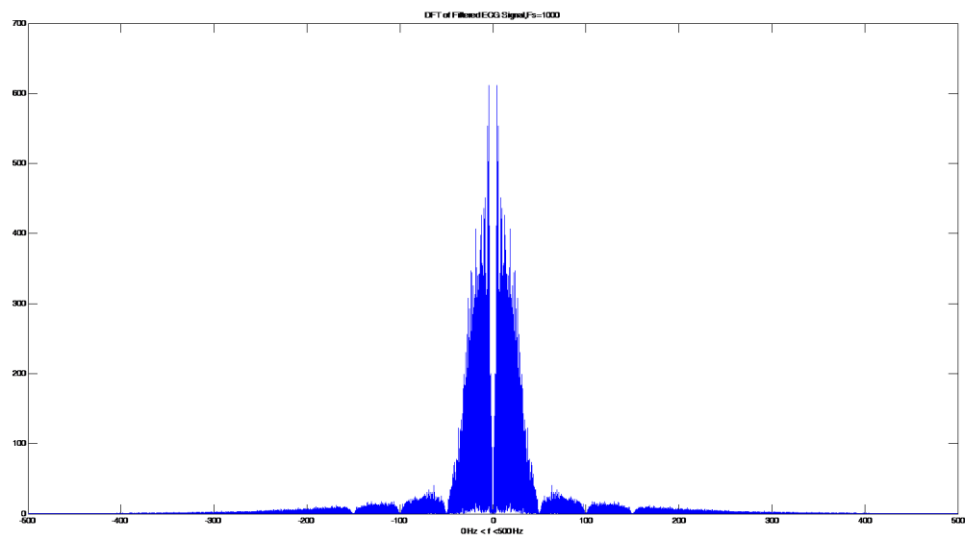
Figure 56: Discrete Fourier Transform of the filtered ECG signal
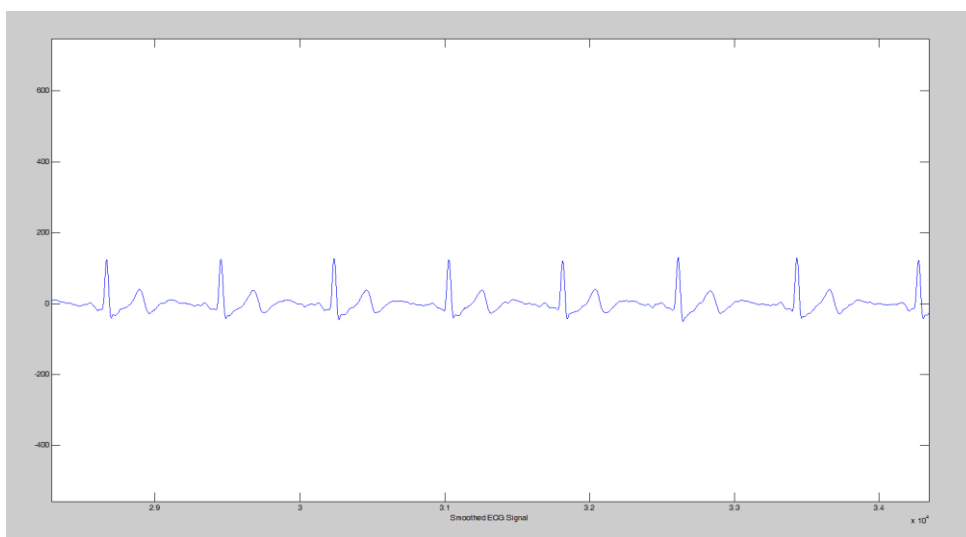
Figure 57: Fingertip ECG which is performed smoothing operation

59
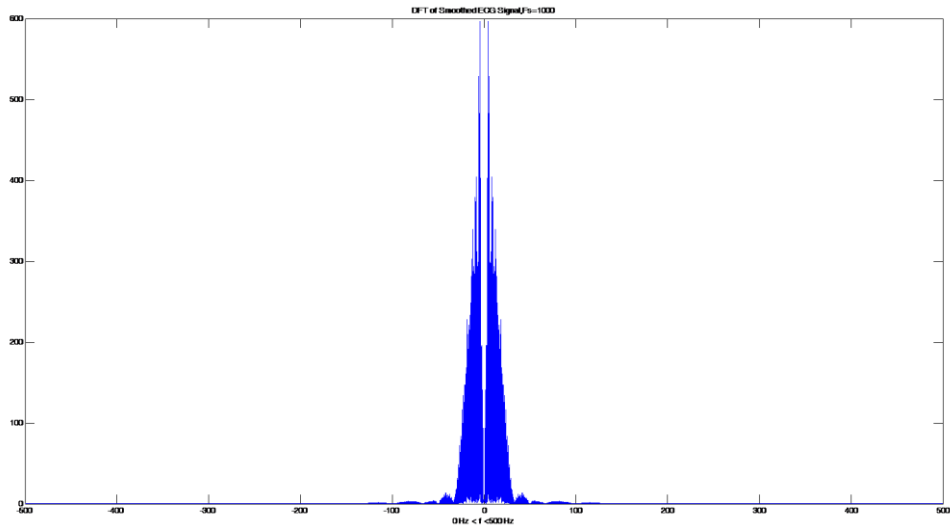
Figure 58: Discrete Fourier Transform of the smoothed ECG signal

Matlab output of the ECG signal and their frequency spectrums are given in figures above. After dsPIC microcontroller quantized the ECG signal with 10 bits at 1 KHz and sent it to USB port, digital filter is used on ECG in Matlab. Digital filter with the same frequency response can be used in both microcontroller and PC side. It does not change the ECG signal. To guarantee the best signal, it can be performed in both sides. However, smoothing operation should be only used in one side.

5.6 Basics for designing PCB of Fingertip ECG

Design of the project has been done by using PROTEUS. There are two programs within the PROTEUS. One of them is ISIS which the project's circuit diagram can be designed in it. The other one is the ARES. It is used for transferring the circuit diagram to PCB (Printed Circuit Board) board [36].
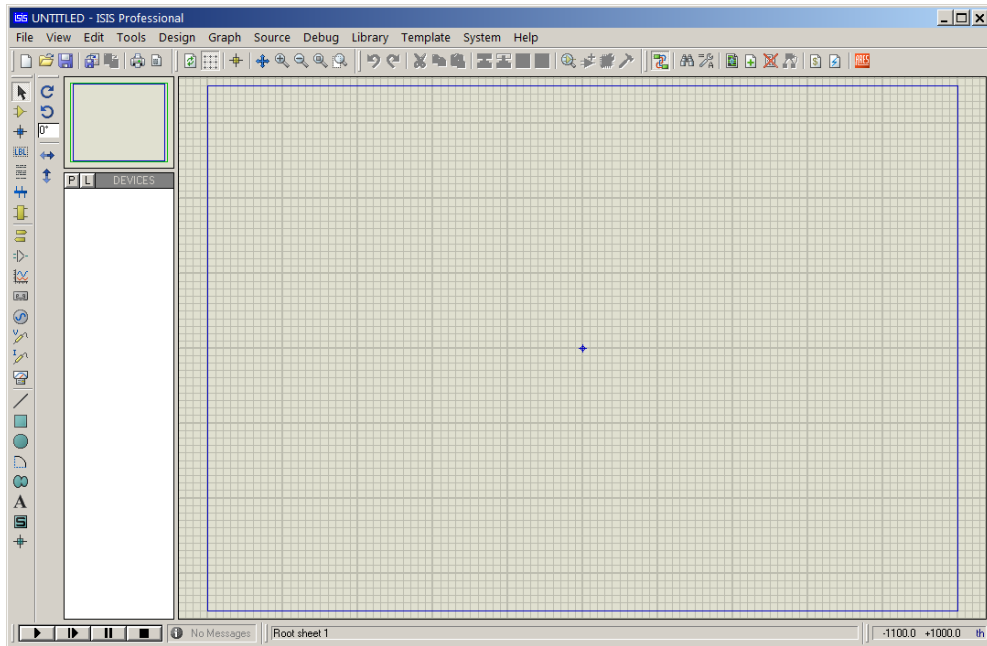
Figure 59: Circuit Design Program

For designing PCB board of Fingertip ECG circuit, program called PROTEUS is used. Usage of PROTEUS will be written as well.

PROTEUS is simulating software which helps us to attach many components to each other, and helps us to simulate the hardware on the computer. It has special libraries which contain resistors, capacitors, LEDs, LCDs, ICs, op-amp, microcontrollers etc. We can find everything which is needed. This program will completely ensure our project's success. Here are the basic steps

- Find our components from library by pressing the pick button from the left side of the program in Component Mode.
- Place the components, and connect them accordingly.
- Change the value of our components like resistor, capacitor by pressing on them twice.
- Load the hex file into microcontroller by pressing on it twice.
- Simulate the circuit

If there is no component which is searched for in the library of Proteus, User defined component can be designed and can applied on PCB board. In ECG project, there wasn't PS25201B Plessey sensor, dspic30f3011, and op-amp (OPA2379, AD627BRZ) in the Proteus library. Therefore, shell library which cannot use on simulation was designed. Here are the steps for designing component

- Left side of the Proteus, press the button called 2D Graphics Box.
- Draw a square which will be your component's case.
- Press the Device Pin Mode on the left side of the program, and choose the default.
- How many pin you want to on your components, place them on component's case. Then give pin number and name by clicking twice.
- After that take them into square by using left click of your mouse, and press the Make Device button.
- Give a name, and if you have PCB packaging for the component, choose it by pressing Add button.
- After your choice, your component will be placed in library as USERDVC (user device). You can choose them by writing their name to Component Menu.

You can make PCB package by opening the software called as ARES in PROTEUS.

Here are the steps for making package

- Draw a case for your component by choosing 2D Graphics Box Mode.
- Choose which pad you want on your component, and then place it according to their pin number by considering the dimension of your component. You do not need to give them pin number, because ARES will understand pins' number by looking the order which you follow when you place the pads.
- Take them into square by using left click of your mouse, and then give a name for your package.
- After giving name, the package to our component which we create before can be defined.

These are the basics for creating component and package. The important point is after using the component which is user defined, the property of component by pressing "edit component" is needed to change. Then the "Exclude from PCB Layout" option is need to be unclicked. We designed Fingertip ECG PCB Board by using user define components. After attaching them according to schematic of our circuit, "NETLİST Transfer to Ares" button which is located above of the PROTEUS is chosen. It will carry the schematic to ARES. In ARES, the "Layer Selection" button which is located on the bottom of the program is pressed. Then Board Edge is chosen and a board which is square or rectangle is drawn. After that, that board is taken into square by using the right click of mouse, and the "Auto Placer" which places the components of our hardware is chosen. After choosing the right position for the components on the board, the "Auto Router" which combines pins of the components by considering the schematic of hardware is pressed. These are the basics for creating PCB board by using PROTEUS. Now, PCB Board can be pressed.

PCB Board of ECG circuit can be seen as
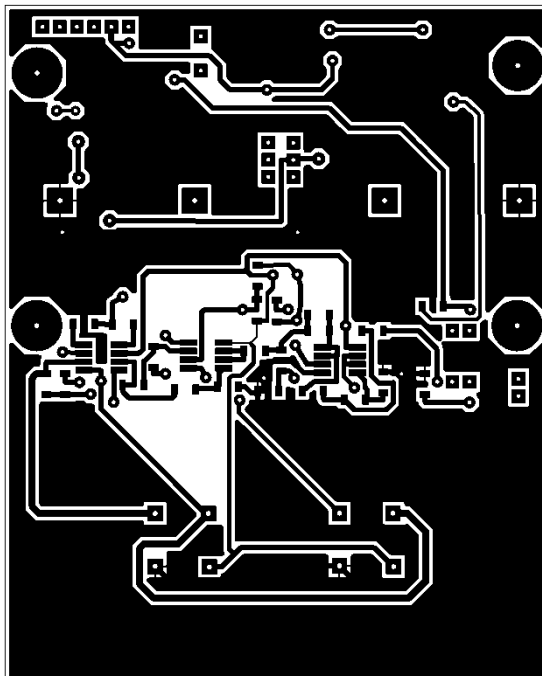
Figure 60 : PCB board top copper
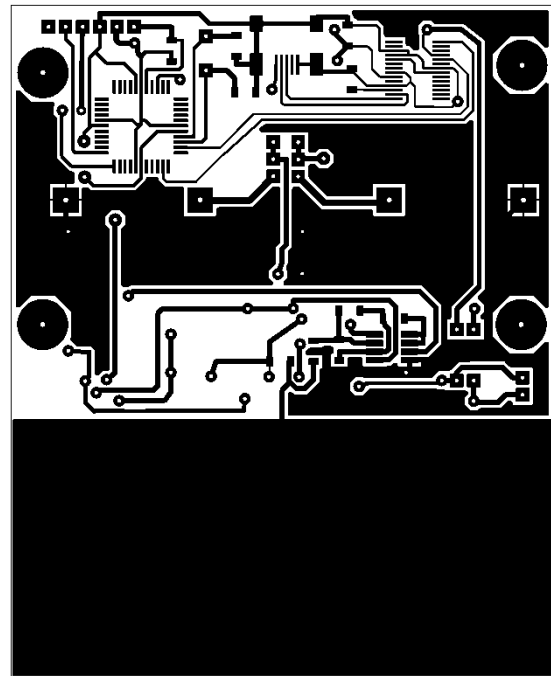
Figure 61: PCB board bottom copper
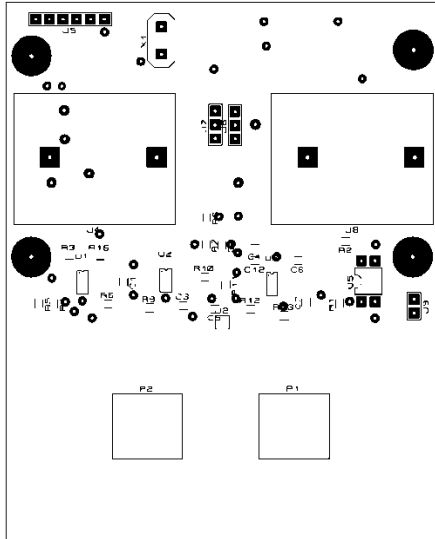
Figure 62: PCB board top component side
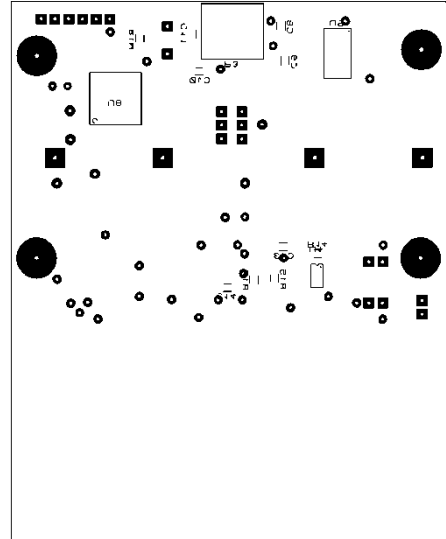
Figure 63: PCB board bottom component side
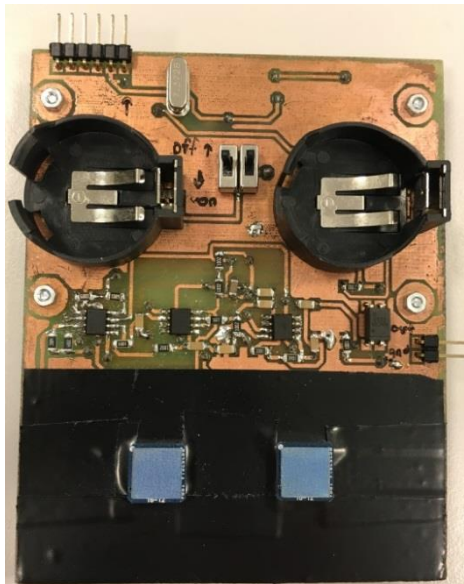
Figure 64: PCB board top side 1
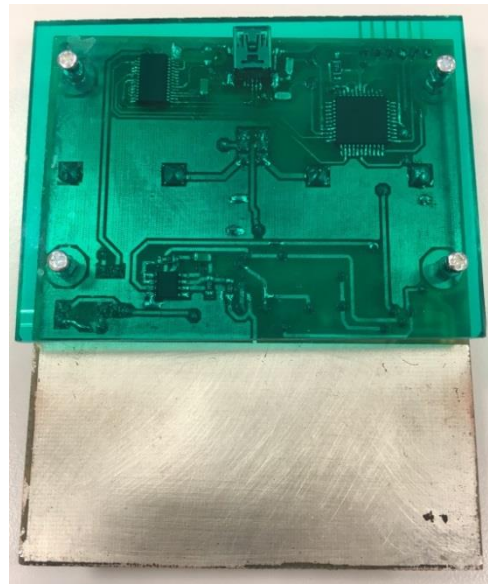
Figure 65: PCB board bottom side

Figure 66: PCB board top side 2

Figure 67: PCB board top side 3

Chapter 6

Introduction to Feature Extraction and Classification

Until now, past studies about biometric recognition systems based on ECG signal, physiological events which causing ECG signal, analog and digital filters, and design of Fingertip ECG circuit have been mentioned in the previous chapters. From now on, we will focus on feature extraction and classification methods, our proposed method, experimental works, and recognition rate which have been achieved by using proposed method.

6.1 Features related to ECG Based Biometric Systems and Feature Extraction Methods

Features related to ECG signals and feature extraction methods basically separated into 4 different groups

- Temporal and Amplitude features: These features indicate temporal and amplitude information at the important location of waveforms from ECG signals.
- Features based on Transform methods: These are the feature sets which are found by using linear transform methods such as Karhunen Loeve Transform (KLD), Fourier Transform (FT), Discrete Cosine Transform (DCT), Legendre Transform (LT) and Discrete Wavelet Transformation (DWT).
- Features based on parametric methods: These are the features obtained by using Linear Prediction Method (LPC) and Neural Network Methods.
- Features based on frequency information: These are the features which are found in the frequency domain.

In our project, both features based on Transform methods and features indicating frequency information are used. AC/DCT [2] method was used for extracting the features based on transform methods. Mel-frequency cepstral coefficients (MFCC) which are commonly used for speech recognition was utilized for extracting features indicating the frequency information. Both methods are briefly explained.

6.1.1 AC/DCT Based Features

These are the features which are found by applying Discrete Cosine Transform (DCT) on autocorrelation of the ECG frames which contain more than one QRS segments [2].

Firstly, ECG signal is separated into frames which include more than one QRS segments. After that, autocorrelation coefficients related to these frames are obtained by the following manner

$$\hat{r}(m) = \sum_{i=0}^{N-|m|-1} x(i)x(i+m), \quad m = 0,1,2,\dots,L \tag{6.1}$$

These obtained $\hat{r}(m)$ coefficients are normalized with $\hat{r}(0)$ by dividing it.

$$r(m) = \frac{\hat{r}(m)}{\hat{r}(0)} \tag{6.2}$$

After that, $c(u)$ DCT coefficients are obtained by applying Discrete Cosine Transform (DCT) on $\hat{r}(m)$ autocorrelation coefficients.

$$c(u) = \alpha(u) \sum_{m=0}^{L} r(m)cos\left[\frac{\pi(2m+1)u}{2N}\right] \tag{6.3}$$

$$\alpha(u) = \begin{cases} u = 0 \, for & \sqrt{1/N} \\ u \neq 0 \, for & \sqrt{2/N} \end{cases} \tag{6.4}$$

Obtained $c(u)$ coefficients in this manner are called AC/DCT coefficients [2]. In the following figures, AC/DCT feature vectors related to two different ECG signals are given in Figure 68.
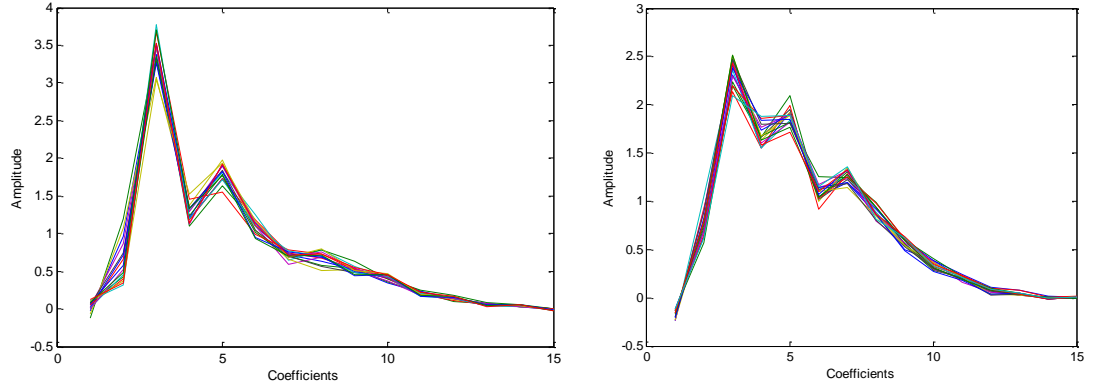
Figure 68: AC/DCT coefficients of two different person by using Fingertip ECG circuit

6.1.2 Mel-Frequency Cepstrum Coefficient Based Features

Mel-Frequency Cepstral Coefficient (MFCC) features which are commonly used on speech recognition, speaker recognition and such speech processing applications are the features that show acoustical characteristics of speaker. This coefficient which models the behavior of the auditory systems called as "Mel", uses a non-linear frequency scale [41].

$$f_{mel} = 1125 ln \left(1 + \frac{f}{700}\right)$$ (6.5)

In the equation above, real and Mel frequency values are represented as f and f_{mel} respectively.

First step for the calculation of MFCC features is to pass the signal through a window function which divides the signal into length of N segments. Then, Fourier Transform applied on length of N windowed signal segment which represented by $x(n)$ [41].

$$X_a(k) = \sum_{n=0}^{N-1} x(n) e^{-j2\pi nk/N}, 0 \le k < N$$ (6.6)

After that, obtained frequency spectrum is separated into bands by using Mel-frequency filter bank in Figure 69

67
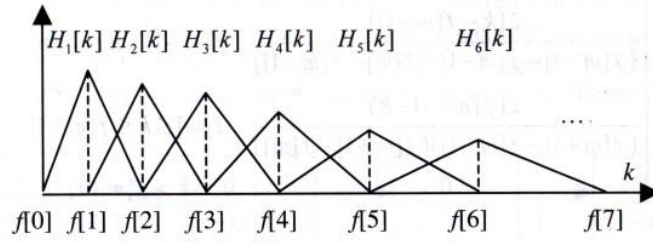
Figure 69: Mel-frequency filterbank [24]

Mel-frequency filter bank that includes M numbers triangular structure is defined as [41]

$$H_m(k) = \begin{cases} 0 & k < f(m-1) \\ \dfrac{2(k - f(m-1))}{(f(m+1) - f(m-1))(f(m) - f(m-1))} & f(m-1) \le k \le f(m) \\ \dfrac{2(f(m+1) - k)}{(f(m+1) - f(m-1))(f(m) - f(m-1))} & f(m) \le k \le f(m+1) \\ 0 & k > f(m+1) \end{cases}, \quad m = 1,2,\dots,M \tag{6.7}$$

Here, $f(m)$ presents the Mel threshold values for the scale of each Mel filter bank structure, and it calculated as below [41]

$$f(m) = \left(\frac{N}{F_s}\right) f_{mel}^{-1}\left(f_{mel(low)} + m \frac{f_{mel(high)} - f_{mel(low)}}{M+1}\right), \quad m = 0,1,2,\dots,M \tag{6.8}$$

At this equation

$$f_{mel(low)} = 1125 ln\left(1 + \frac{f_{low}}{700}\right), f_{mel(high)} = 1125 ln\left(1 + \frac{f_{high}}{700}\right) \tag{6.9}$$

$$f_{mel}^{-1} = 700\left(exp\left(\frac{f}{1125}\right) - 1\right) \tag{6.10}$$

Is obtained in the form of equation above. F_s which is located at this equation represents the sampling frequency related to signal, and f_{low} and f_{high} represents the lower and higher frequencies at the filter bank, respectively.
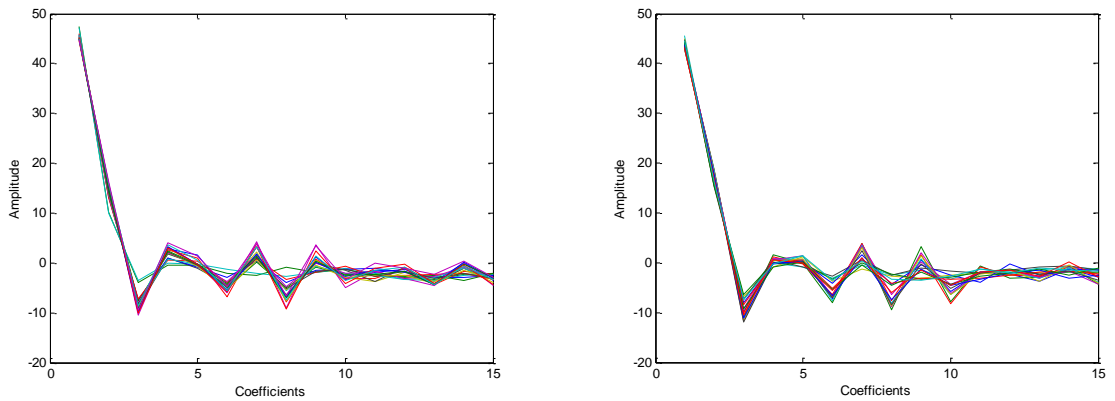
Figure 70: MFCC feature vectors taken from two different person by using Fingertip ECG circuit

After that, logarithmic energy at the output of each filter in filter bank is calculated as below

$$S(m) = ln\left[\sum_{k=0}^{N-1} |X_a(k)|^2 H_m(k)\right], \qquad 0 < m \leq M \tag{6.11}$$

MFCC features which represented with $c(n)$ are found by applying Discrete Cosine Transform (DCT) on obtained logarithmic energy for each filter outputs [41].

$$c(n) = \sum_{m=0}^{M-1} S(m) cos\left(\frac{\pi n(2m-1)}{2M}\right), \qquad 0 \leq n < M \tag{6.12}$$

In this project, MFCC coefficient vectors, for each ECG signals containing 15 coefficients were obtained by applying MFCC feature extraction algorithm which is described with details above. At the figure above, MFCC vector obtained from two different people were presented.

6.2 Methods for Classification

At this project, two different supervised classification methods are used. First of these was Linear Discriminant Analysis (LDA) based on classification method. And second one was K-nearest neighbors algorithm based on classification method. Both classification methods are explained below briefly.

6.2.1 Linear Discriminant Analysis based Classification Method

Linear Discriminant Analysis (LDA) is being defined as feature vectors which are separated into K different groups by using linearly discriminating functions.

Linear discriminant function for two different groups is defined as below:

$$y(x) = w^T x + \omega_0 \tag{6.13}$$

Here, w and x terminologies represent weight vector and feature vector respectively. And ω_0 terminology is defined as first condition value. If $y(x) \geq 0$, feature vector is appointed to C_1 class. Otherwise, this feature classifies as C_2 [42].

Case of existing K different classes, linear discrimination functions is defined as

$$y_k(x) = w_k^T x + \omega_{k0}, \qquad k = 1,2,\dots,K \tag{6.14}$$

If it provides $j \neq k$ and $y_k(x) > y_j(x)$ conditions, group of feature vector is determined as C_k [42]. In the given equation above, number of K different discriminant functions including

$$\widetilde{W} = [\widetilde{w}_1 \quad \widetilde{w}_2 \quad \cdots \quad \widetilde{w}_K] \tag{6.15}$$

$$\widetilde{w}_k = [\omega_{k0} \quad w_k^T]^T, k = 1,2,\ldots,K \tag{6.16}$$

$$\tilde{x} = [1 \quad x^T]^T \tag{6.17}$$

Are reformatted as below

$$y(x) = \widetilde{W}^T \tilde{x} \tag{6.18}$$

In the given equation, $\widetilde{W}$ is called weight matrix and it is obtained by reducing square error function given below [42].

$$E_D(\widetilde{W}) = \frac{1}{2} Tr\left\{(\tilde{X}\widetilde{W} - T)^T(\tilde{X}\widetilde{W} - T)\right\} \tag{6.19}$$

T matrix seen in the equation above shows the class labels of feature vectors located in training set. Each row of T matrix comprised of transpose of t vector which is defined as target vector. The most common method is binary method for representing the class labels. In this method, class which includes feature vector is presented as 1, others are 0. For example; If class of feature vectors are determined as 2 in the group of 5 different classes, target vector is found as $t = [0 \quad 1 \quad 0 \quad 0 \quad 0]^T$ [25]. For A training set including number of N feature vector

$$\{x_n, t_n\}, \quad n = 1,2,\ldots,N \tag{6.20}$$

T And X matrixes are generated in the form of

$$T = \begin{bmatrix} t_1^T \\ t_2^T \\ \vdots \\ t_N^T \end{bmatrix}, \tilde{X} = \begin{bmatrix} \tilde{x}_1^T \\ \tilde{x}_2^T \\ \vdots \\ \tilde{x}_N^T \end{bmatrix} \tag{6.21}$$

Derivative of $E_D(\widetilde{W})$ is taken respect to $\widetilde{W}$ terminology of sqaure error function and if it eqauls to zero, $\widetilde{W}$ weight matrix is obtained as [42]

$$\widetilde{W} = (\tilde{X}^T\tilde{X})^{-1}\tilde{X}^T T \tag{6.22}$$

A probabilistic model can be obtained by distribution of feature vectors which is located in the linear discriminant function described above and training set of linear decision boundaries. In this model, posterior probability value $p(C_k|x)$ is obtained related C_k class which displays C_k $p(x|C_k)$ value of conditional class probability and $p(C_k)$ first condition value of class probability by using Bayesian theorem [42].

Case of existing two different classes, $p(C_1|x)$ value of posterior probability related to C_1 class is obtained as

$$p(C_1|x) = \frac{p(x|C_1)p(C_1)}{p(x|C_1)p(C_1) + p(x|C_2)p(C_2)} = \frac{1}{1 + \exp(-a)} = \sigma(a) \tag{6.23}$$

$\sigma(a)$ Which is seen in the equation above is called as logistic sigmoid function. And term of a is called as logist function, and it calculated as the ratio of the probability two conditional classes [42].

$$a = ln\frac{p(x|C_1)p(C_1)}{p(x|C_2)p(C_2)} = ln\frac{p(C_1|x)}{1 - p(C_1|x)} \tag{6.24}$$

Case of existence of number of K different classes $p(C_k|x)$ is calculated by using Bayesian theorem as below [42]

$$p(C_k|x) = \frac{p(x|C_k)p(C_k)}{\sum_j p(x|C_j)p(C_j)} = \frac{\exp(a_k)}{\sum_j \exp(a_j)} \tag{6.25}$$

Exponential expression in the equation above is called as softmaks function. And term of a_k is defined as [42]

$$a_k = \ln(p(x|C_k)p(C_k)) \tag{6.26}$$

If it provides $j \neq k$ and $a_k \gg a_j$ conditions, it will be obtained as $p(C_k|x) \cong 1$ and $p(C_j|x) \cong 0$ [42].

If feature vectors located at training sets represent Gaussian distribution for each class, and all classes have the same covariance matrixes, $p(x|C_k)$ will be expressed in the form of

$$p(x|C_k) = \frac{1}{(2\pi)^{D/2}} \frac{1}{|\Sigma|^{1/2}} exp\left\{-\frac{1}{2}(x - \mu_k)^T \Sigma^{-1}(x - \mu_k)\right\} \tag{6.27}$$

71

x And μ_k terms represent feature vector and mean value of feature vectors located at C_k class, respectively. In the same equation $\sum$ and $|\sum|$ terms represent covariance matrix of this feature vector and determinant of covariance matrix, respectively. Covariance matrix $\sum$ is obtained as [42].

$$cov(x) = \Sigma = E[(x - \mu)(x - \mu)^T] \tag{6.28}$$

Case of two different classes' existence, posterior probability value related to C_k class is obtained as below

$$p(C_k|x) = \sigma(w^T x + \omega_0) \tag{6.29}$$

Here, w and ω_0 terms are calculated as

$$w = \Sigma^{-1}(\mu_1 - \mu_2) \tag{6.30}$$

$$\omega_0 = -\frac{1}{2}\mu_1^T\Sigma^{-1}\mu_1 + \frac{1}{2}\mu_2^T\Sigma^{-1}\mu_2 + ln\frac{p(C_1)}{p(C_2)} \tag{6.31}$$

Case of existence of K different classes, posterior probability value of C_k class is defined as a softmax function, and is obtained as below

$$p(C_k|x) = \frac{p(x|C_k)p(C_k)}{\sum_j p(x|C_j)p(C_j)} = \frac{\exp(a_k)}{\sum_j \exp(a_j)} \tag{6.32}$$

Here, a_k term is calculated as below

$$a_k(x) = w_k^T x + \omega_{k0} \tag{6.33}$$

In the equation above, w_k and ω_{k0} terms are obtained as below

$$w_k = \Sigma^{-1}\mu_k \tag{6.34}$$

$$\omega_{k0} = -\frac{1}{2}\mu_k^T\Sigma^{-1}\mu_k + lnp(C_k) \tag{6.35}$$

6.2.2 K-Nearest Neighbors Classification Method

K-Nearest Neighbors algorithm (K-NN) is supervised and it is a classification algorithm which is directly based on the examples in the training set. For this classification algorithm, feature vectors related to signal from the training set and class labels are recorded in the system. For this reason, it is also called memory-based classification [43].

Feature vector q which is n dimensional located at example set and n dimensional M number feature vector f_i located at training set is defined as

$$q = [q_1 \quad q_2 \quad \cdots \quad q_n] \tag{6.36}$$

$$f_i = [f_{i_1} \quad f_{i_2} \quad \cdots \quad f_{i_n}] \qquad i = 1,2,\dots,M \tag{6.37}$$

And similarities between each f_i vector and q vector are calculated by using various distance measurements. Some of the distance measurement techniques are Euclidean, Manhattan and Mahalanobis.

$$d_{Euclidean} = \sqrt{(q - f_i)(q - f_i)^T} \tag{6.38}$$

$$d_{Manhattan} = \|q - f_i\|_1 = \sum_{s=1}^{n} |q_s - f_{i_s}| \tag{6.39}$$

$$d_{Mahalanobis} = \sqrt{(q - f_i)C^{-1}(q - f_i)^T} \tag{6.40}$$

Here, C term represents correlation matrix between q and f_i vectors.

Distance obtained by using equation above, line up to small to large, and k numbers f_i vector which is nearest to q feature vector is obtained. It can be clearly seen in the figure below, k number f_i feature vector which is nearest to q vector is labelled into different classes [43].
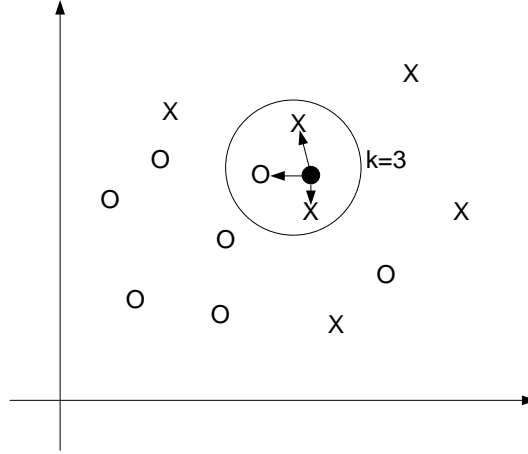
Figure 71: 3-N nearest Neighbors Classification

Two different strategies are applied for class determination process. First of these is majority voting system. In this system, unknown feature vector is assigned into the class which forms the majority in k number example set, and classification process is finished. Second method is the inverse distance-weighed voting system. In this system, inverse distance-weighed score between unknown feature vector and k-nearest feature vector for each class are obtained as below

$$V(C_j) = \sum_{m=1}^{k} \frac{1}{d(q, f_m)} L(f_m, C_j) \qquad j = 1, \dots, N \tag{6.41}$$

In the equation above, N, q, f_m, $d(q, f_m)$, and $V(C_j)$ represents number of classes, unknown feature vector, k-nearest feature vector at the training set, distance between f_m feature vector and q feature vector, and the score value for C_j class, respectively.

$L(f_m, C_j)$ function is defined as [43]

$$L(f_m, C_j) = \begin{cases} 1 & f_m \in C_j \\ 0 & f_m \notin C_j \end{cases} \tag{6.42}$$

As a result, class which gives the maximum score value is defined and labeled as class of q feature vector [43].

Chapter 7

Proposed Method

7.1 Preprocessing Stage

Preprocessing stage is the most important part for the biometric recognition systems. Because preprocessing stage plays an important role for preparing the signal which used on feature extraction and classification. In the given block diagram, preprocessing stage consists of three parts

- Filtering operation
- Normalization
- Framing
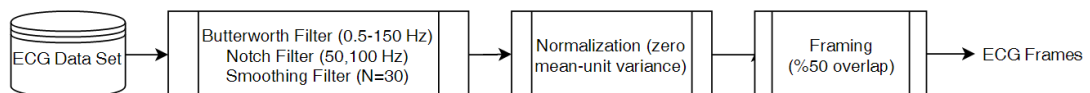
Figure 72: Pretreatment Process

At the first step of the preprocessing stage, ECG signal which hosts various noise components such as powerline noise (50 Hz and its first harmonics), baseline wander, muscle noise. In this process, ECG signals pass through Butterworth filter which has (0.5 Hz-150 Hz cut-off), notch filter (50 Hz and 100 Hz) and smoothing filter.

At the second step, ECG signal is normalized to be zero mean and unit variance as follows

$$X_{norm} = \frac{X - \mu_X}{\sigma_X} \tag{7.1}$$

At the formula, X_{norm}, X, μ_X, and σ_X represents normalized ECG signal, filtered ECG signal, mean value and variance of filtered ECG signal, respectively.

Final step of the preprocessing stage is the framing. At this stage, ECG signal which is normalized with zero-mean and unit variance is separated into frames which has %50 overlap and comprises of five second ECG signals.

7.2 Feature Extraction and Classification Process

At the proposed method in this project, three different feature extraction methods were used for feature extraction from ECG signals. First feature vector set was extracted by using AC/DCT [2] method. Mel-frequency cepstral coefficients (MFCC) which are usually used on speech recognition systems are utilized to extract the second feature vector set. In the project, feature vectors which are AC/DCT and MFCC that consist of 15 coefficients, were used. In additional to this feature vectors, QRS segments were used as a third vector set. R point related to ECG signal is calculated by using Pan-Tompkins QRS detection algorithm [44] which is known in the literature and after that QRS frames were obtained by taking the 200 sample before and after that R points.

In the proposed method, AC/DCT and MFCC feature vector sets which were obtained from the ECG frames in the training set, was classified by using two different LDA classification methods. In other words, LDA classifications have been trained separately by using these AC/DCT and MFCC vector sets. On the other hand, QRS frames which were located in the training set were classified by using 3-NN

(3-Nearest Neighbor) classification method. Euclidean distance measurement was used for the 3-NN classification method.

$$\varepsilon = \sqrt{(f_T - f_{IN})(f_T - f_{IN})^T} \tag{7.2}$$

Here, f_T ve f_{IN} parameters represent ECG frames which have class label, and ECG frames which have not class label, respectively.
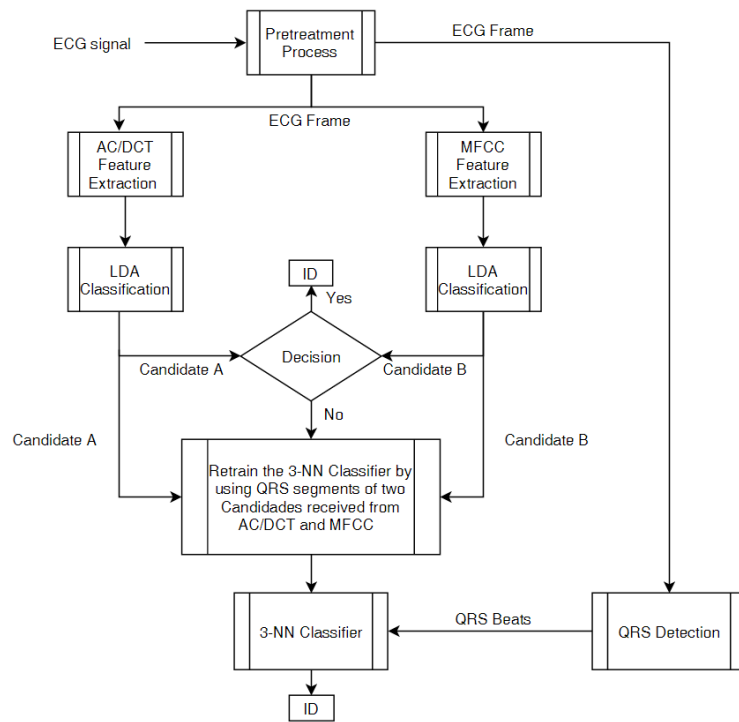
Figure73.a: Block diagram of Proposed ECG Based Biometric Recognition System First Approach
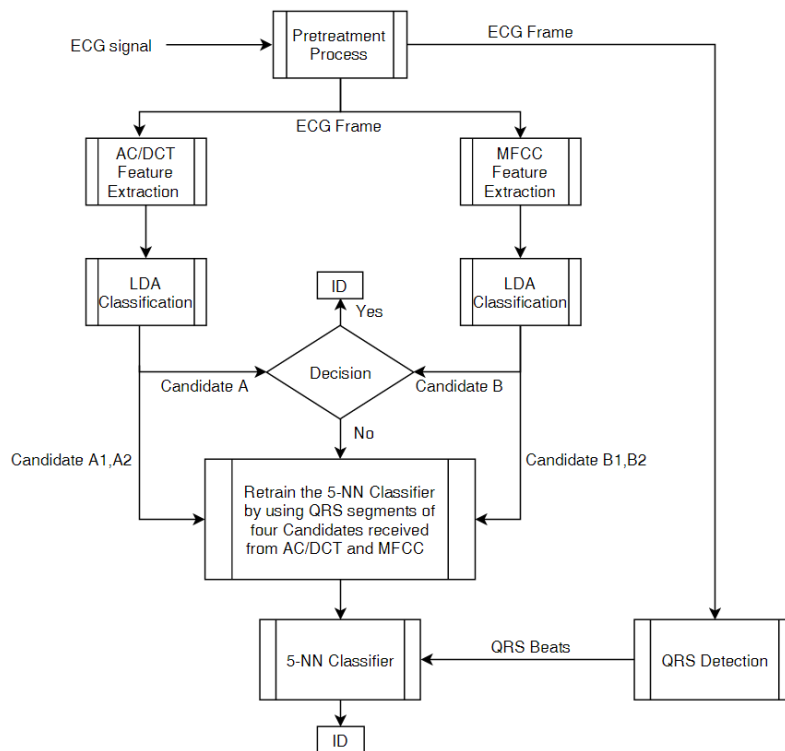
Figure 73.b: Block diagram of Proposed ECG Based Biometric Recognition System Second Approach

In the proposed biometric recognition system, it is based on using three feature vectors which are AC/DCT and MFCC feature vectors, and QRS frames. Firstly AC/DCT, MFCC features are extracted for all the ECG signals from the ECG dataset and two different training set are created for two LDA classifiers. In the first approach, after unknown ECG frame is applied on the system, AC/DCT feature vector is determined for the unknown ECG frame. LDA classifier labeled this feature vector by using AC/DCT features in the training set, and Candidate A is assigned related to unknown ECG frame. MFCC feature vector is also determined for the unknown ECG frame at the same time, and LDA classifier assigned it as Candidate-B by using features in the training set which is obtained before. If both two different LDA classifiers give the same candidates, unknown ECG frame is classified as ID-A or ID-B. Otherwise, 3-NN classifier retrains by using QRS frame which is obtained before, for Candidate A and Candidate B located in the training set. After that QRS frames related to unknown ECG frame is extracted, 3-NN classifier makes a decision between given QRS frames of candidate A and B with QRS frames of unknown ECG by using strategy of majority, and class is assigned and is labeled for the unknown ECG frame. In the second approach, if both two different LDA classifiers don't give the same candidate, QRS frames of first two candidates which is obtained from AC/DCT and QRS frames of first two candidates which is obtained from MFCC is sent to 5-NN Classifier. 5-NN classifier retrains by using QRS frames for candidates A_1, A_2 and candidates B_1, B_2 located in the training set. Then 5-NN classifier makes a decision between QRS frames of candidates A_1, A_2, B_1, B_2 with QRS frames of unknown ECG signal by using Euclidean distance measurement technique, and class is assigned and is labeled for the unknown ECG frame. Block diagram related to first and second approach was shown in the Figure 73.a and 73.b, respectively.

7.3 Experimental Work

7.3.1 ECG Dataset

In the project, ECG dataset is created mostly on the students of Işık University by using the Fingertip ECG device which design is shown in the previous section. 26 students of Işık University which age between 19 to 26 and 4 middle aged person are used for ECG dataset. Unfortunately, one of the ECG signal taken from student showed arrhythmia both fingertip device and patient monitor, so we assume that ECG dataset consists of 29 healthy people and 1 unhealthy person. ECG signals were taken range of 1 minute to 5 minutes at two different weeks for each person. Thus, 30 different ECG signals taken at first week, second week are assigned to training dataset and test dataset, respectively.

7.3.2 Assessment Criteria

Four different statistical criteria's are used to measure the success of classification method. These criteria defined as Sensitivity, Specificity, F_{score}, and Frame Recognition Rate.

Sensitivity is defined as the proportion of positive samples which are correctly identified. On the other hand, the specificity is defined as the proportion of the negative samples which are correctly identified. The sensitivity and the specificity are given as [45]

$$Sensitivity = \frac{TP}{TP + FN} \tag{7.3}$$

$$Specificity = \frac{TN}{TN + FP} \tag{7.4}$$

In the equation above, TP, TN, FP, and FN are defined as True Positive, True Negative, False Positive, and False Negative, respectively.

In other criteria is F_{score} which shows the accuracy of the experiment. It defined as the harmonic mean of the precious and recall, and is given as [45]

$$F_{score} = 2 \times \frac{Precious \times Recall}{Precious + Recall} \tag{7.5}$$

Precious and Recall is calculated as

$$Recall = Sensitivity \tag{7.6}$$

$$Precision = \frac{TP}{TP + FP} \tag{7.7}$$

Final criteria known as Frame Recognition Rate is defined as the ratio between the number of frame correctly identified and the total number of frame for each subject. It is calculated as [45]

$$Frame\ Recognition\ Rate = \frac{N_{TP}}{N_F} \tag{7.8}$$

In this equation, N_{TP} and N_F represent the number of frame correctly identified and the total number of frame for each subject, respectively.

7.3.3 Assessment Result

Proposed method is compared with the AC/DCT [2] and MFCC based methods. First and second approach tested on ECG dataset which consist of the 17 individual's ECG signal taken at different weeks to make an accurate comparison between the proposed methods with the other methods. After increasing the ECG dataset to 30 people, first and second approach then tested on new ECG dataset. Fingertip ECG signals recorded on each person in 1 minute intervals with three times. Then ECG dataset is separated into 3 different folders, and these folders consist of 5 to 22 frame ECG signals. Scores of the first folder was put on the tables below.

ID matrix	1	2	3	4	5	6	7	8	9	10	11	12	13	14	15	16	17	
11	11	0	0	0	0	0	0	0	0	0	0	0	0	0	0	0	0	100,0000
19	0	17	0	0	0	0	0	0	0	0	0	2	0	0	0	0	0	89,4737
22	0	2	18	0	0	0	2	0	0	0	0	0	0	0	0	0	0	81,8182
17	0	0	0	14	0	0	0	0	0	0	0	0	0	0	0	0	3	82,3529
11	0	0	0	0	10	0	0	0	0	0	0	1	0	0	0	0	0	90,9091
11	1	0	0	0	1	6	0	0	0	0	0	1	1	0	0	0	1	54,5455
13	0	0	0	0	0	0	13	0	0	0	0	0	0	0	0	0	0	100,0000
19	0	0	0	0	0	0	5	11	3	0	0	0	0	0	0	0	0	57,8947
22	0	1	0	0	0	0	0	0	21	0	0	0	0	0	0	0	0	95,4545
21	0	0	0	0	0	0	0	0	0	21	0	0	0	0	0	0	0	100,0000
5	0	0	0	0	0	0	0	0	0	0	5	0	0	0	0	0	0	100,0000
21	0	0	0	0	0	0	0	0	0	0	0	21	0	0	0	0	0	100,0000
21	0	0	0	0	0	0	0	0	0	0	0	0	21	0	0	0	0	100,0000
22	0	0	0	0	0	0	0	0	0	0	0	0	0	22	0	0	0	100,0000
21	0	0	0	9	0	0	0	0	0	0	0	0	0	0	12	0	0	57,1429
22	0	0	0	0	0	0	0	0	0	0	0	0	0	0	0	22	0	100,0000
5	0	0	0	0	0	0	0	0	0	0	0	0	0	0	0	0	5	100,0000
																		88,7995

Table 2.a: Contingency matrix which is obtained from only AC/DCT Features for 17 people

81

Table: ID matrix — contingency matrix (rows are person IDs, columns are cluster labels, last column is percentage)

ID matrix	1	2	3	4	5	6	7	8	9	10	11	12	13	14	15	16	17	18	19	20	25	27	30	31	34	35	36	37	38	40	%
11	11	0	0	0	0	0	0	0	0	0	0	0	0	0	0	0	0	0	0	0	0	0	0	0	0	0	0	0	0	0	100,0000
19	0	16	0	0	0	0	0	0	0	0	0	0	0	0	0	0	0	0	0	0	0	0	0	0	0	0	0	0	0	0	84,2105
22	0	1	19	0	0	0	1	0	0	0	0	0	0	0	0	0	0	0	0	0	0	0	0	0	0	0	0	0	0	1	86,3636
17	0	0	0	14	0	0	0	0	0	0	0	0	0	0	0	0	3	0	0	0	0	0	0	0	0	0	0	0	0	0	82,3529
11	0	0	0	0	10	0	0	0	0	0	0	0	1	0	0	0	0	0	0	0	0	0	0	0	0	0	0	0	0	0	90,9091
11	0	0	0	0	2	6	0	0	0	0	0	1	1	0	0	0	0	1	0	0	1	0	0	0	0	0	0	0	0	0	54,5455
13	0	0	0	0	0	0	12	0	0	0	0	0	1	0	0	0	0	0	0	0	0	0	0	0	0	0	0	0	0	0	92,3077
19	0	0	0	0	0	0	5	11	3	0	0	0	0	0	0	0	0	0	0	0	0	0	0	0	0	0	0	0	0	0	57,8947
22	0	0	0	0	0	0	0	0	18	0	0	0	0	0	0	0	0	1	3	0	0	0	0	0	0	0	0	0	0	0	81,8182
21	0	0	0	0	0	0	0	0	0	21	0	0	0	0	0	0	0	0	0	0	0	0	0	0	0	0	0	0	0	0	100,0000
5	0	0	0	0	0	0	0	0	0	0	4	0	0	0	0	0	0	0	0	0	0	0	0	1	0	0	0	0	0	0	80,0000
21	0	0	0	0	0	0	0	0	0	0	0	21	0	0	0	0	0	0	0	0	0	0	0	0	0	0	0	0	0	0	100,0000
21	0	0	0	0	0	0	0	0	0	0	0	0	21	0	0	0	0	0	0	0	0	0	0	0	0	0	0	0	0	0	100,0000
22	0	0	0	0	0	0	0	0	0	0	0	0	0	22	0	0	0	0	0	0	0	0	0	0	0	0	0	0	0	0	100,0000
21	0	0	0	10	0	0	0	0	0	0	0	0	0	0	10	0	0	0	0	0	0	0	0	0	0	0	1	0	0	0	47,6190
22	0	0	0	0	0	0	0	0	0	0	0	0	0	0	0	14	0	0	0	0	0	0	0	0	0	0	8	0	0	0	63,6364
5	0	0	0	0	0	0	0	0	0	0	0	0	0	0	0	0	5	0	0	0	0	0	0	0	0	0	0	0	0	0	100,0000
6	0	0	0	0	0	0	0	0	0	0	0	0	0	0	0	0	0	6	0	0	0	0	0	0	0	0	0	0	0	0	100,0000
13	0	0	0	0	0	0	0	0	0	0	0	0	0	0	0	0	0	0	13	0	0	0	0	0	0	0	0	0	0	0	100,0000
22	0	0	0	0	0	0	0	0	0	0	0	0	0	0	0	0	0	0	0	22	0	0	0	0	0	0	0	0	0	0	100,0000
22	0	0	0	0	0	1	0	0	0	0	0	0	0	0	0	0	0	0	0	0	21	0	0	0	0	0	0	0	0	0	95,4545
7	0	0	0	0	0	0	0	0	0	0	0	0	0	0	0	0	0	0	0	0	0	7	0	0	0	0	0	0	0	0	100,0000
6	0	0	0	0	0	0	0	0	0	0	0	0	0	0	0	0	0	0	0	0	0	0	6	0	0	0	0	0	0	0	100,0000
19	0	0	0	0	0	0	0	0	0	0	0	0	0	0	0	0	0	0	0	0	0	0	0	19	0	0	0	0	0	0	100,0000
21	0	0	0	0	0	0	0	0	0	0	0	0	0	0	0	0	0	0	0	0	0	0	0	0	21	0	0	0	0	0	100,0000
20	0	0	0	0	0	0	0	0	0	0	0	0	0	0	0	0	0	0	0	0	0	0	0	0	0	20	0	0	0	0	100,0000
21	0	0	0	0	0	0	0	0	0	0	0	0	0	0	0	0	0	0	0	0	0	0	0	0	0	0	20	0	0	0	95,2381
22	0	0	0	0	0	0	0	0	0	0	0	0	0	0	0	0	0	0	0	0	0	0	0	0	0	0	0	22	0	0	100,0000
21	0	0	0	0	0	0	0	0	0	0	0	0	0	0	0	0	0	0	0	0	0	0	0	0	0	0	0	0	21	0	100,0000
8	0	0	0	0	0	0	0	0	0	0	0	0	0	0	0	0	0	0	0	0	0	0	0	0	0	0	0	0	0	8	100,0000
																																90,4117

Table 2.b: Contingency Matrix which is obtained from only AC/DCT Features for 30 people

ID matrix	1	2	3	4	5	6	7	8	9	10	11	12	13	14	15	16	17		
11	8	2	0	0	0	0	0	0	0	1	0	0	0	0	0	0	0		72,7273
19	6	7	0	0	0	0	3	0	0	0	0	0	0	2	0	0	1		36,8421
22	2	0	9	0	0	0	3	0	0	0	0	0	0	7	0	0	1		40,9091
17	0	0	0	6	0	0	0	0	0	0	0	0	0	0	1	4	6		35,2941
11	0	0	0	0	11	0	0	0	0	0	0	0	0	0	0	0	0		100,0000
11	0	0	0	0	0	7	0	0	0	0	0	3	0	0	1	0	0		63,6364
13	0	0	0	0	0	0	7	1	4	1	0	0	0	0	0	0	0		53,8462
19	0	1	0	0	0	0	2	14	2	0	0	0	0	0	0	0	0		73,6842
22	0	0	0	0	0	0	0	0	22	0	0	0	0	0	0	0	0		100,0000
21	0	2	0	0	0	0	0	0	0	18	0	0	0	1	0	0	0		85,7143
5	0	0	0	0	0	0	0	0	0	0	5	0	0	0	0	0	0		100,0000
21	0	0	0	0	0	0	1	0	1	0	0	19	0	0	0	0	0		90,4762
21	0	0	0	0	0	0	0	0	0	0	0	0	20	0	0	0	1		95,2381
22	0	0	0	0	0	0	0	0	0	2	0	0	0	20	0	0	0		90,9091
21	0	0	0	0	0	0	0	0	0	0	0	0	0	1	16	3	1		76,1905
22	0	0	0	0	0	0	0	0	0	2	0	0	0	2	0	17	1		77,2727
5	0	1	0	0	0	0	0	0	0	0	0	0	0	0	0	0	4		80,0000
																			74,8671

Table 3.a: Contingency Matrix which is obtained from only MFCC Features for 17 people

83

ID matrix	1	2	3	4	5	6	7	8	9	10	11	12	13	14	15	16	17	18	19	20	25	27	30	31	34	35	36	37	38	40	
11	7	3	0	0	0	0	0	0	0	1	0	0	0	0	0	0	0	0	0	0	0	0	0	0	0	0	0	0	0	0	63,6364
19	5	7	0	0	0	0	2	0	0	0	0	0	0	2	0	0	1	0	0	0	0	0	0	0	0	0	0	0	0	2	36,8421
22	1	0	3	0	0	0	0	0	0	0	0	0	0	0	0	0	0	0	0	12	0	0	0	0	0	0	0	0	0	2	13,6364
17	0	0	0	6	0	0	0	0	0	0	0	0	0	0	1	4	6	0	0	0	0	0	0	0	0	0	0	0	0	0	35,2941
11	0	0	0	0	9	0	0	0	0	0	0	0	0	0	0	0	0	0	0	0	0	0	0	0	0	0	0	0	0	2	81,8182
11	0	0	0	0	0	4	0	0	0	0	0	0	0	0	0	0	0	0	0	0	0	0	0	0	0	0	0	0	0	0	36,3636
13	0	0	0	0	0	0	7	1	4	0	0	0	0	0	0	0	0	0	0	0	0	0	0	0	0	0	0	0	0	0	53,8462
19	0	0	0	0	0	0	3	14	1	0	0	0	0	0	0	0	0	0	0	0	0	0	0	0	0	0	0	0	0	0	73,6842
22	0	0	0	0	0	0	0	0	22	0	0	0	0	0	0	0	0	0	0	0	0	0	0	0	0	0	0	0	0	0	100,0000
21	0	0	0	0	0	0	0	0	0	13	0	0	0	1	0	0	0	0	0	0	0	0	0	0	0	0	5	0	0	0	61,9048
5	0	0	0	0	0	0	0	0	0	0	4	0	0	0	0	0	0	0	1	0	0	0	0	0	0	0	0	0	0	0	80,0000
21	0	0	0	0	0	0	0	0	1	0	0	17	0	0	0	0	0	0	0	0	0	0	0	0	0	0	0	0	0	0	80,9524
21	0	0	0	0	0	0	0	0	0	0	0	0	19	0	0	0	0	0	0	0	0	0	1	1	0	0	0	0	0	0	90,4762
22	0	0	0	0	0	0	0	0	0	0	0	0	0	19	0	0	1	2	0	0	0	0	0	0	0	0	0	0	0	0	86,3636
21	0	0	0	0	0	0	0	0	0	0	0	0	0	0	15	2	1	0	1	0	0	0	0	0	0	0	0	0	0	0	71,4286
22	0	0	0	0	0	0	0	0	0	0	0	0	0	0	0	16	0	0	0	0	0	0	0	0	0	0	1	0	0	0	72,7273
5	0	0	0	0	0	0	0	0	0	0	0	0	0	0	0	0	4	0	0	0	0	0	0	0	0	0	1	0	0	0	80,0000
6	0	0	0	0	0	0	0	0	0	0	0	0	0	0	0	0	0	5	0	0	0	0	0	0	0	0	0	0	0	0	83,3333
13	0	0	0	0	0	0	0	0	0	0	1	0	0	0	1	0	0	0	11	0	0	0	0	0	0	0	0	0	0	0	84,6154
22	0	0	0	0	0	0	0	0	0	0	0	0	0	0	0	0	0	0	0	22	0	0	0	0	0	0	0	0	0	0	100,0000
22	0	0	0	0	0	0	0	0	0	0	0	1	0	0	0	0	0	0	2	0	15	0	0	3	0	1	0	0	0	0	68,1818
7	0	0	0	0	0	0	0	0	0	0	0	0	0	0	0	0	0	0	0	0	0	7	0	0	0	0	0	0	0	0	100,0000
6	0	0	0	0	0	0	0	0	0	0	0	0	0	0	0	0	0	0	0	0	0	0	6	0	0	0	0	0	0	0	100,0000
19	0	0	0	0	0	0	0	0	0	0	3	0	0	0	0	0	0	0	0	0	0	0	0	16	0	0	0	0	0	0	84,2105
21	0	0	0	0	0	0	0	0	0	0	0	0	0	0	0	0	0	0	0	0	0	0	0	0	21	0	0	0	0	0	100,0000
20	0	0	0	0	0	0	0	0	0	0	0	0	0	0	0	0	0	0	0	0	0	1	0	0	0	19	0	0	0	0	95,0000
21	0	2	0	0	0	0	0	0	0	2	0	0	0	0	0	0	0	0	0	0	0	0	0	0	0	0	17	0	0	0	80,9524
22	0	0	0	0	0	0	0	0	0	0	0	0	0	0	0	0	0	0	0	0	0	0	0	0	0	0	0	22	0	0	100,0000
21	0	6	0	0	0	0	0	0	0	0	0	0	0	1	0	0	0	0	1	0	0	0	0	0	0	0	0	0	13	0	61,9048
8	0	0	2	0	0	0	0	0	0	0	0	0	0	0	0	0	0	0	0	0	0	0	0	0	0	0	0	0	0	6	75,0000
																															75,0724

Table 3.b: Contingency Matrix which is obtained from only MFCC Features for 30 people

ID matrix	1	2	3	4	5	6	7	8	9	10	11	12	13	14	15	16	17	
11	11	0	0	0	0	0	0	0	0	0	0	0	0	0	0	0	0	100,0000
19	0	17	0	0	0	0	0	0	0	0	0	2	0	0	0	0	0	89,4737
22	0	1	16	0	0	0	5	0	0	0	0	0	0	0	0	0	0	72,7273
17	0	0	0	14	0	0	0	0	0	0	0	0	0	0	0	1	2	82,3529
11	0	0	0	0	11	0	0	0	0	0	0	0	0	0	0	0	0	100,0000
11	0	0	0	0	0	9	0	0	0	0	0	1	0	0	1	0	0	81,8182
13	0	0	0	0	0	0	13	0	0	0	0	0	0	0	0	0	0	100,0000
19	0	0	0	0	0	0	1	15	3	0	0	0	0	0	0	0	0	78,9474
22	0	0	0	0	0	0	0	0	22	0	0	0	0	0	0	0	0	100,0000
21	0	0	0	0	0	0	0	0	0	21	0	0	0	0	0	0	0	100,0000
5	0	0	0	0	0	0	0	0	0	0	5	0	0	0	0	0	0	100,0000
21	0	0	0	0	0	0	0	0	0	0	0	21	0	0	0	0	0	100,0000
21	0	0	0	0	0	0	0	0	0	0	0	0	21	0	0	0	0	100,0000
22	0	0	0	0	0	0	0	0	0	0	0	0	0	22	0	0	0	100,0000
21	0	0	0	0	0	0	0	0	0	0	0	0	0	0	19	2	0	90,4762
22	0	0	0	0	0	0	0	0	0	0	0	0	0	0	0	22	0	100,0000
5	0	0	0	0	0	0	0	0	0	0	0	0	0	0	0	0	5	100,0000
																		93,8703

Table 4.a: Contingency Matrix which is obtained from first approach for 17 people

Table 4.b: Contingency Matrix which is obtained from first approach for 30 people

ID matrix	1	2	3	4	5	6	7	8	9	10	11	12	13	14	15	16	17	18	19	20	25	27	30	31	34	35	36	37	38	40	
11	11	0	0	0	0	0	0	0	0	0	0	0	0	0	0	0	0	0	0	0	0	0	0	0	0	0	0	0	0	0	100,0000
19	0	16	0	0	0	0	0	0	0	0	0	0	0	0	0	0	0	0	0	0	0	0	0	0	0	0	0	0	0	0	84,2105
22	0	1	18	0	0	0	1	0	0	0	0	2	0	0	0	0	0	0	0	0	0	0	0	0	0	0	0	0	0	0	81,8182
17	0	0	0	14	0	0	0	0	0	0	0	0	0	0	0	1	2	0	0	0	0	0	0	0	0	0	0	0	0	0	82,3529
11	0	0	0	0	11	0	0	0	0	0	0	0	0	0	0	0	0	0	0	0	0	0	0	0	0	0	0	0	0	0	100,0000
11	0	0	0	0	0	6	5	0	0	0	0	0	0	0	0	0	0	0	0	0	0	0	0	0	0	0	0	0	0	0	54,5455
13	0	0	0	0	0	1	12	0	0	0	0	0	0	0	0	0	0	0	0	0	0	0	0	0	0	0	0	0	0	0	92,3077
19	0	0	0	0	0	0	2	14	3	0	0	0	0	0	0	0	0	0	0	0	0	0	0	0	0	0	0	0	0	0	73,6842
22	0	0	0	0	0	0	0	0	20	0	0	0	0	0	0	0	0	0	2	0	0	0	0	0	0	0	0	0	0	0	90,9091
21	0	0	0	0	0	0	0	0	0	21	0	0	0	0	0	0	0	0	0	0	0	0	0	0	0	0	0	0	0	0	100,0000
5	0	0	0	0	0	0	0	0	0	0	4	1	0	0	0	0	0	0	0	0	0	0	0	0	0	0	0	0	0	0	80,0000
21	0	0	0	0	0	0	0	0	0	0	0	21	0	0	0	0	0	0	0	0	0	0	0	0	0	0	0	0	0	0	100,0000
21	0	0	0	0	0	0	0	0	0	0	0	0	21	0	0	0	0	0	0	0	0	0	0	0	0	0	0	0	0	0	100,0000
22	0	0	0	0	0	0	0	0	0	0	0	0	0	22	0	0	0	0	0	0	0	0	0	0	0	0	0	0	0	0	100,0000
21	0	0	0	0	0	0	0	0	0	0	0	0	0	0	19	2	0	0	0	0	0	0	0	0	0	0	0	0	0	0	90,4762
22	0	0	0	0	0	0	0	0	0	0	0	0	0	0	0	19	0	0	0	0	0	0	0	0	0	0	3	0	0	0	86,3636
5	0	0	0	0	0	0	0	0	0	0	0	0	0	0	0	0	5	0	0	0	0	0	0	0	0	0	0	0	0	0	100,0000
6	0	0	0	0	0	0	0	0	0	0	0	0	0	0	0	0	0	6	0	0	0	0	0	0	0	0	0	0	0	0	100,0000
13	0	0	0	0	0	0	0	0	0	0	0	0	0	0	0	0	0	1	12	0	0	0	0	0	0	0	0	0	0	0	92,3077
22	0	0	0	0	0	0	0	0	0	0	0	0	0	0	0	0	0	0	0	22	0	0	0	0	0	0	0	0	0	0	100,0000
22	0	0	0	0	0	0	0	0	0	0	0	0	0	0	0	0	0	0	0	0	20	0	0	0	0	0	0	0	0	0	90,9091
7	0	0	0	0	0	0	0	0	0	0	0	0	0	0	0	0	0	0	0	0	0	7	0	0	0	0	0	0	0	0	100,0000
6	0	0	0	0	0	0	0	0	0	0	0	0	0	0	0	0	0	0	0	0	0	0	6	0	0	0	0	0	0	0	100,0000
19	0	0	0	0	0	0	0	0	0	0	0	0	0	0	0	0	0	0	0	0	0	0	0	19	0	0	0	0	0	0	100,0000
21	0	0	0	0	0	0	0	0	0	0	0	0	0	0	0	0	0	0	0	0	0	0	0	0	21	0	0	0	0	0	100,0000
20	0	0	0	0	0	0	0	0	0	0	0	0	0	0	0	0	0	0	0	0	0	0	0	0	0	20	0	0	0	0	100,0000
21	0	0	0	0	0	0	0	0	0	1	0	0	0	0	0	0	0	0	0	0	0	0	0	0	0	0	20	0	0	0	95,2381
22	0	0	0	0	0	0	0	0	0	0	0	0	0	0	0	0	0	0	0	0	0	0	0	0	0	0	0	22	0	0	100,0000
21	0	1	0	0	0	0	0	0	0	0	0	0	0	0	0	0	0	0	0	0	0	0	0	0	0	0	0	0	20	0	95,2381
8	0	0	0	0	0	0	0	0	0	0	0	0	0	0	0	0	0	0	0	0	0	0	0	0	0	0	0	0	0	8	100,0000
																															93,0120

ID matrix	1	2	3	4	5	6	7	8	9	10	11	12	13	14	15	16	17	
11	11	0	0	0	0	0	0	0	0	0	0	0	0	0	0	0	0	100,0000
19	0	19	0	0	0	0	0	0	0	0	0	0	0	0	0	0	0	100,0000
22	0	0	16	0	0	0	6	0	0	0	0	0	0	0	0	0	0	72,7273
17	0	0	0	16	0	0	0	0	0	0	0	0	0	0	0	0	1	94,1176
11	0	0	0	0	11	0	0	0	0	0	0	0	0	0	0	0	0	100,0000
11	0	0	0	1	0	9	0	0	0	0	0	1	0	0	0	0	0	81,8182
13	0	0	0	0	0	0	13	0	0	0	0	0	0	0	0	0	0	100,0000
19	0	0	0	0	0	0	3	15	1	0	0	0	0	0	0	0	0	78,9474
22	0	0	0	0	0	0	0	0	22	0	0	0	0	0	0	0	0	100,0000
21	0	0	0	0	0	0	0	0	0	21	0	0	0	0	0	0	0	100,0000
5	0	0	0	0	0	0	0	0	0	0	5	0	0	0	0	0	0	100,0000
21	0	0	0	0	0	0	0	0	0	0	0	21	0	0	0	0	0	100,0000
21	0	0	0	0	0	0	0	0	0	0	0	0	21	0	0	0	0	100,0000
22	0	0	0	0	0	0	0	0	0	0	0	0	0	22	0	0	0	100,0000
21	0	0	0	0	0	0	0	0	0	0	0	0	0	0	20	0	1	95,2381
22	0	0	0	0	0	0	0	0	0	0	0	0	0	0	0	22	0	100,0000
5	0	0	0	0	0	0	0	0	0	0	0	0	0	0	0	0	5	100,0000
																		95,4617

Table 5.a: Contingency Matrix which is obtained from second approach for 17 people

ID matrix	1	2	3	4	5	6	7	8	9	10	11	12	13	14	15	16	17	18	19	20	25	27	30	31	34	35	36	37	38	40	
11	11	0	0	0	0	0	0	0	0	0	0	0	0	0	0	0	0	0	0	0	0	0	0	0	0	0	0	0	0	0	100,0000
19	0	19	0	0	0	0	0	0	0	0	0	0	0	0	0	0	0	0	0	0	0	0	0	0	0	0	0	0	0	0	100,0000
22	0	1	19	0	0	0	2	0	0	0	0	0	0	0	0	0	0	0	0	0	0	0	0	0	0	0	0	0	0	0	86,3636
17	0	0	0	16	0	0	0	0	0	0	0	0	0	0	0	0	1	0	0	0	0	0	0	0	0	0	0	0	0	0	94,1176
11	0	0	0	0	11	0	0	0	0	0	0	0	0	0	0	0	0	0	0	0	0	0	0	0	0	0	0	0	0	0	100,0000
11	0	0	0	0	0	9	0	0	2	0	0	0	0	0	0	0	0	0	0	0	0	0	0	0	0	0	0	0	0	0	81,8182
13	0	0	0	0	0	0	13	0	0	0	0	0	0	0	0	0	0	0	0	0	0	0	0	0	0	0	0	0	0	0	100,0000
19	0	0	0	0	0	0	4	13	2	0	0	0	0	0	0	0	0	0	0	0	0	0	0	0	0	0	0	0	0	0	68,4211
22	0	0	0	0	0	0	0	1	21	0	0	0	0	0	0	0	0	0	0	0	0	0	0	0	0	0	0	0	0	0	95,4545
21	0	0	0	0	0	0	0	0	0	21	0	0	0	0	0	0	0	0	0	0	0	0	0	0	0	0	0	0	0	0	100,0000
5	0	0	0	0	0	0	0	0	0	0	4	0	0	0	0	0	1	0	0	0	0	0	0	0	0	0	0	0	0	0	80,0000
21	0	0	0	0	0	0	0	0	0	0	0	21	0	0	0	0	0	0	0	0	0	0	0	0	0	0	0	0	0	0	100,0000
21	0	0	0	0	0	0	0	0	0	0	0	0	21	0	0	0	0	0	0	0	0	0	0	0	0	0	0	0	0	0	100,0000
22	0	0	0	0	0	0	0	0	0	0	0	0	0	22	0	0	0	0	0	0	0	0	0	0	0	0	0	0	0	0	100,0000
21	0	0	0	0	0	0	0	0	0	0	0	0	0	0	19	0	2	0	0	0	0	0	0	0	0	0	0	0	0	0	90,4762
22	0	0	0	0	0	0	0	0	0	0	0	1	0	0	0	21	0	0	0	0	0	0	0	0	0	0	0	0	0	0	95,4545
5	0	0	0	0	0	0	0	0	0	0	0	0	0	0	0	0	5	0	0	0	0	0	0	0	0	0	0	0	0	0	100,0000
6	0	0	0	0	0	0	0	0	0	0	0	0	0	0	0	0	0	6	0	0	0	0	0	0	0	0	0	0	0	0	100,0000
13	0	0	0	0	0	0	0	0	0	0	0	0	0	0	0	0	0	0	13	0	0	0	0	0	0	0	0	0	0	0	100,0000
22	0	0	0	0	0	0	0	0	0	0	0	0	0	0	0	0	0	0	0	22	0	0	0	0	0	0	0	0	0	0	100,0000
22	0	0	0	0	0	0	0	0	0	0	0	0	0	0	0	0	0	0	0	0	21	0	0	0	0	0	1	0	0	0	95,4545
7	0	0	0	0	0	0	0	0	0	0	0	0	0	0	0	0	0	0	0	0	0	7	0	0	0	0	0	0	0	0	100,0000
6	0	0	0	0	0	0	0	0	0	0	0	0	0	0	0	0	0	0	0	0	0	0	6	0	0	0	0	0	0	0	100,0000
19	0	0	0	0	0	0	0	0	0	0	0	0	0	0	0	0	0	0	0	0	0	0	0	19	0	0	0	0	0	0	100,0000
21	0	0	0	0	0	0	0	0	0	0	0	0	0	0	0	0	0	0	0	0	0	0	0	0	21	0	0	0	0	0	100,0000
20	0	0	0	0	0	0	0	0	0	0	0	0	0	0	0	0	0	0	0	0	0	0	0	0	0	20	0	0	0	0	100,0000
21	0	0	0	0	0	0	0	0	0	0	0	0	0	0	0	0	0	0	0	0	0	0	0	0	0	0	21	0	0	0	100,0000
22	0	0	0	0	0	0	0	0	0	0	0	0	0	0	0	0	0	0	0	0	0	0	0	0	0	0	0	22	0	0	100,0000
21	2	0	0	0	0	0	0	0	0	0	0	0	0	0	0	0	0	0	0	0	0	0	0	0	0	0	0	0	19	0	90,4762
8	0	0	0	0	0	0	0	0	0	0	0	0	0	0	0	0	0	0	0	0	0	0	0	0	0	0	0	0	0	8	100,0000
																															95,9346

Table 5.b: Contingency Matrix which is obtained from second approach for 30 people

Contingency Matrix for the first, second approach, only AC/DCT method and only MFCC method are given in tables above. Each row of the matrix shows the known class, and column of the matrix shows the detected class. Elements on the diagonal of the matrix show the number of correctly predicted frame for each class. As shown in the table 2, the ECG frames which are located in the test dataset, are mostly arranged in the correct classes. Frame recognition rates related to each person that located in test dataset for the proposed method and the other methods are represented in Table 6.

ID	Number of Windows	Window Recognition Rate			
		ACDCT	MFCC	Proposed Approach-1	Proposed Approach-2
1	11	100,0000	72,7273	100,0000	100,0000
2	19	89,4737	36,8421	89,4737	100,0000
3	22	81,8182	40,9091	72,7273	72,7273
4	17	82,3529	35,2941	82,3529	94,1176
5	11	90,9091	100,0000	100,0000	100,0000
6	11	54,5455	63,6364	81,8182	81,8182
7	13	100,0000	53,8462	100,0000	100,0000
8	19	57,8947	73,6842	78,9474	78,9474
9	22	95,4545	100,0000	100,0000	100,0000
10	21	100,0000	85,7143	100,0000	100,0000
11	5	100,0000	100,0000	100,0000	100,0000
12	21	100,0000	90,4762	100,0000	100,0000
13	21	100,0000	95,2381	100,0000	100,0000
14	22	100,0000	90,9091	100,0000	100,0000
15	21	57,1429	76,1905	90,4762	95,2381
16	22	100,0000	77,2727	100,0000	100,0000
17	5	100,0000	80,0000	100,0000	100,0000
	Average	88,7995	74,8671	93,8703	95,4617

Table 6.a: Frame Recognition Rates between Proposed Method and Others for 17 people

		Window Recognition Rate			
ID	Number of Windows	ACDCT	MFCC	Proposed Approach-1	Proposed Approach-2
1	11	100,0000	63,6364	100,0000	100,0000
2	19	84,2105	36,8421	84,2105	100,0000
3	22	86,3636	13,6364	81,8182	86,3636
4	17	82,3529	35,2941	82,3529	94,1176
5	11	90,9091	81,8182	100,0000	100,0000
6	11	54,5455	36,3636	54,5455	81,8182
7	13	92,3077	53,8462	92,3077	100,0000
8	19	57,8947	73,6842	73,6842	68,4211
9	22	81,8182	100,0000	90,9091	95,4545
10	21	100,0000	61,9048	100,0000	100,0000
11	5	80,0000	80,0000	80,0000	80,0000
12	21	100,0000	80,9524	100,0000	100,0000
13	21	100,0000	90,4762	100,0000	100,0000
14	22	100,0000	86,3636	100,0000	100,0000
15	21	47,6190	71,4286	90,4762	90,4762
16	22	63,6364	72,7273	86,3636	95,4545
17	5	100,0000	80,0000	100,0000	100,0000
18	6	100,0000	83,3333	100,0000	100,0000
19	13	100,0000	84,6154	92,3077	100,0000
20	22	100,0000	100,0000	100,0000	100,0000
25	22	95,4545	68,1818	90,9091	95,4545
27	7	100,0000	100,0000	100,0000	100,0000
30	6	100,0000	100,0000	100,0000	100,0000
31	19	100,0000	84,2105	100,0000	100,0000
34	21	100,0000	100,0000	100,0000	100,0000
35	20	100,0000	95,0000	100,0000	100,0000
36	21	95,2381	80,9524	95,2381	100,0000
37	22	100,0000	100,0000	100,0000	100,0000
38	21	100,0000	61,9048	95,2381	90,4762
40	8	100,0000	75,0000	100,0000	100,0000
	Average	90,4117	75,0724	93,0120	95,9346

Table 6.b: Frame Recognition Rates between Proposed Method and Others for 30 people

AC/DCT and MFCC are depended on the heart beat variability of the person. Although ECG signal of each person is taken in the same condition, heart beat rate can change in time depending on individual activities in each day. Excessively increases or decreases in the heart beat rates reduce the recognition rate of AC/DCT and MFCC based recognition systems. Because of these, AC/DCT and MFCC features are needed to combine with an ECG based biometric recognition systems which include temporal and amplitude features. In proposed method, AC/DCT and MFCC features are combined with features which include QRS beats. In the given

Table 3, it can be seen that, proposed method increases the frame recognition rate for each person who located in test dataset.

Sensitivity, Specificity, F_{score} , and Frame Recognition Rate were presented in Table 4 for both AC/DCT, MFCC based methods and proposed method. First approach achieves the average frame recognition rate of %94 for 17 people while the AC/DCT and MFCC methods provide the frame recognition rate of %89 and %75, individually. Second approach improved the recognition rate and its average frame recognition rate is %95 for 17 people. Increasing the database caused small percentage of decreasing in recognition rate. This time, average recognition rate of first approach was %93 for 30 people while the frame recognition rate of AC/DCT and MFCC methods were %90, and %75, respectively. Frame recognition rate of second approach increased to %96 for 30 people. The performance evaluation on the given parameters in Table 7 between the other methods and proposed approaches are illustrated in Figure 61.

Methods	Sensitivity	Specificity	F$_{SCORE}$	Average Recognition Rate
ACDCT	0,8834	0,9927	0,8834	88,7995
MFCC	0,7420	0,9839	0,7420	74,8671
Proposed Approach-1	0,9329	0,9958	0,9329	93,8703
Proposed Approach-2	0.9505	0.9969	0.9505	95,4617

Table 7.a: Comparison of the Classification Performance between the Proposed
Method with Others for 17 people

Methods	Sensitivity	Specificity	F$_{SCORE}$	Average Recognition Rate
ACDCT	0,8982	0,9965	0,8982	90,4117
MFCC	0,7454	0,9912	0,7454	75,0724
Proposed Approach-1	0,9308	0,9976	0,9308	93,0120
Proposed Approach-2	0,9593	0,9986	0,9593	95,9346

Table 7.b: Comparison of the Classification Performance between the Proposed
Method with Others for 30 people

Chapter 8

Discussions and Conclusions

In this project, ECG based biometric recognition system was presented. The proposed method depends on QRS information of ECG signals combined with AC/DCT features, MFCC features. %93 and %96 average frame recognition rates were achieved from experimental work of first and second approach, respectively. It can be seen that second approach shows %3 improvements over first approach. If AC/DCT [2] and MFCC based recognition rate are compared with the proposed methods, approximately % 15 improvements are seen to be achieved.

In this project, Fingertip ECG circuit which measures the channel 1 ECG signal had been used for extraction the signal from body. The reason of using fingertip ECG circuit was; to achieve a portable recognition system. However, because of using two fingers, muscular noise which interfering the ECG signal increased, and it caused lower recognition rate.

Dataset firstly is constructed with ECG signal of 17 people, then it increased to 30 people, and it is used for evaluation of biometric recognition system. Increasing the size of the dataset was seen that decrease the recognition rate. Therefore, ECG based biometric systems should not be used alone. It can be used with speech and retina recognition system to increase the recognition rate. It is known that speech, retina, or fingerprint of a person can easily be taken without realizing by using high resolution camera, and they can used to trick the recognition systems. However, ECG signal can't be taken without being noticed nor applied it directly to the system. For this reason, it is very important to increase the security. Therefore, the works in written below are proposed to increase the recognition rate of our system.

- Surface of the ECG electrode should to be extended, and redesign for palm to reduce the muscular noise and hand movements.
- Combined with speech, retina or fingerprint recognition system to increase the reliability.
- Change the LDA classification method with SVM (Support Vector Machine) and GMM (Gaussian Mixture Model) classification method.
- Reconstruct ECG database by using new device.

References

[1]   Jain K., Ross A., and Prabhakar S., "An Introduction to Biometric Recognition," *IEEE Transactions on Circuits and Systems for Video Technology*, 14, 1, 4–20, (2004).

[2]   Wang Y., Agrafioti F., Hatzinakos D., and Plataniotis K. N., "Analysis of Human Electrocardiogram for Biometric Recognition," *EURASIP Journal on Advances in Signal Processing*, 2008, 1-11, (2008).

[3]   Fang C. and Chan H. L., "Human Identification by Quantifying Similarity and Dissimilarity in Electrocardiogram Phase Space," *Elsevier, Pattern Recognition*, 42, 9, 1824-1831, (2009).

[4]   Wübbeler G., Stavridis M., Kreiseler D., Bousseljot R.D., and Elster C., "Verification of Humans Using Electrocardiogram," *Elsevier, Pattern Recognition Letters*, 28, 1172-1175, (2007).

[5]   Biel L., Pettersson O., Philipson L., and Wide P., "ECG Analysis: A New Approach in Human Identification," *IEEE Transactions on Instrumentation and Measurement*, 50, 3, 808–812, (2001).

[6]   Irvine J. M., Wiederhold B. K., Gavshon L. W., et al., "*Heart Rate Variability: A New Biometric for Human Identification*," *The International Conference on Artificial Intelligence* (*IC-AI '01*), Las Vegas, Nev, USA, (2001), pp:1106–1111.

[7]   Shen T. W., Tompkins W. J., and Hu Y. H., "One-lead ECG for Identity Verification," *The 2nd Joint Engineering in Medicine and Biology, 24th Annual Conference and the Annual Fall Meeting of the Biomedical Engineering Society* (*EMBS/BMES '02*), Houston, Tex, USA, (2002) , pp: 62–63.

[8]   Israel S. A., Scruggs W. T., Worek W. J., and Irvine J.M., "Fusing Face and ECG for Personal Identification," *The 32nd Applied Imagery Pattern Recognition Workshop (AIPR'03)*, Washington, DC, USA, (2003), pp: 226–231.

[9] Israel S. A., Irvine J. M., Cheng A., Wiederhold M. D., and Wiederhold B.K., "ECG to Identify Individuals," *Pattern Recognition*, 38, 1, 133–142, (2005).

[10] Shen T. W., "Biometric Identity Verification Based on Electrocardiogram (ECG)," (Ph.D. dissertation), University of Wisconsin, Madison, Wis, USA, (2005).

[11] Shen T.W., "Quartile Discriminant Measurement (QDM) Method for ECG Biometric Feature Selection," *International Symposium of Biomedical Engineering*, Taiwan, (2006), No. 10394.

[12] Chan A. D. C., Hamdy M. M., Badre A., and Badee V., "Wavelet Distance Measure for Person Identification Using Electrocardiograms," *IEEE Transactions on Instrumentation and Measurement*, 57, 2, 248-253, (2008).

[13] Chuang-Chien C., Chou-Min C., and Chih-Yu H., "A Novel Personal Identity Verification Approach Using a Discrete Wavelet Transform of the ECG Signal," *International Conference on Multimedia and Ubiquitous Engineering (MUE 2008)*, Busan, Korea, (2008), pp. 201–206.

[14] Irvine J. M., Israel S. A., Scruggs W. T., and Worek W. J., "EigenPulse: Robust Human Identification from Cardiovascular Function," *Pattern Recognition*, 41, 11, 3427-3435, (2008).

[15] Fatemian S.Z., and Hatzinakos D., "A New ECG Feature Extractor for Biometric Recognition," *The 16th International Conference on Digital Signal Processing (DSP 2009)*, Santorini, Greece, (2009), pp: 1-6.

[16] Li M. and Narayanan S., "Robust ECG Biometrics by Fusing Temporal and Cepstral Information," *International Conference on Pattern Recognition*, İstanbul, Turkey, (2010), pp: 1326-1329.

[17] Sufi F., Khalil I., and Habib I., "Polynomial Distance Measurement for ECG Based Biometric Authentication," *Security and Communication Networks*, 3, 4, 303-319, (2010).

[18] Loong J.L.C., Subari K.S., Besar R., Abdullah M.K., "A New Approach to ECG Biometric Systems: A Comparitive Study between LPC and WPD Systems," *World Academy of Science Engineering and Technology*, 68, 759-764, (2010).

[19] Ting C. M. and Salleh S. H., "ECG Based Personal Identification Using Extended Kalman Filter," *10th Int. Conf. on Information Sciences Signal Processing and Their Applications*, (2010), pp. 774–777.

[20] Sufi F. and Khalil I., Faster Person Identification Using Compressed ECG in Time Critical Wireless Telecardiology Applications," *Journal of Network and Computer Applications*, 34, 1, 282-293, (2011).

[21] Shen T. W., Tompkins W. J., and Hu Y. H., "Implementation of a One-lead ECG Human Identification System on a Normal Population," *Journal of Engineering and Computer Innovations*, 2, 1, 12-21, (2011).

[22] Safie S. I., Soraghan J J., and Petropoulakis L., "Electrocardiogram (ECG) Biometric Authentication Using Pulse Active Ratio (PAR)," *IEEE Transactions on Information Forensics and Security*, 6, 4, 1315-1322, (2011).

[23] Chen C. K., Lin C. L., and Chiu Y. M., "Individual Identification Based on Chaotic Electrocardiogram Signals," *The 6th IEEE Conference on Industrial Electronics and Applications*, Beijing, China, (2011) pp: 1771-1776.

[24] B. Vuksanovic and M.Alhamdi, "Analysis of Human Electrocardiogram for Biometric Recognition Using Analytic and AR Modeling Extracted Parameters," International Journal of Information and Electronics Engineering, Vol. 4, No. 6, November 2014

[25] O.Boumbarov, Y. Velchev, S.Sokolov, "Personal Biometric Identification Based on ECG Features, " Ministry and Education Science Bulgaria, NSF Grant By-TH-202/2006-, Multimodal biometric analysis:methods and algorithms

[26] Noureddine Belgacem, Fethi Bereksi-Reguig,"Person Identification System Based on Electrocardiogram Signal Using LabVIEW," International Journal on Computer Science and Engineering 4.6 (Jun 2012): 974-981.

[27] Zhidong Zhao, Lei Yang, Diandian Chen, Yi Luo ,"A Human ECG Identification System Based on Ensemble Empirical Mode Decomposition, " *Sensors 2013, 13(5), 6832-6864; doi:10.3390/s130506832*

[28] Manal. M. Tantawi, Kenneth Revett, Abdel-Badeeh Salem, Mohamed F. Tolba,"A wavelet feauture extraction method for electrocardiogram (ECG)-based biometric recognition ," Signal, Image and Processing September 2015, Volume 9, Issues 6, pp 1271-1280

[29] Nathan M. Kesto, "Electrocardiography Circuit Design ," lecture notes http://www.egr.msu.edu/classes/ece480/capstone/spring13/group03/documents /ElectrocardiographyCircuitDesign.pdf

[30] Dr Dallas Price, " *How to read an Electrocardiogram (ECG). Part One: Basic principles of the ECG. The normal ECG,* "Consultant Cardiologist, St Mary's Hospital, Isle of Wight, UK

[31] *Alex Wong, Kong-Pang Pun, Yuan-Ting Zhang and Chiu-Sing Choy,* An ECG measurement IC using driven-right-leg circuit

[32] Michael R. Neuman, "Biopotential Amplifiers, " lecture notes
https://ay1415.moodle.wisc.edu/prod/pluginfile.php/74584/mod_resource/content/1/Ch06-MI4e-7-11-08.pdf

[33] Texas Instruments, "*Active Filter Design Techniques notes*"
http://www.ti.com/lit/ml/sloa088/sloa088.pdf

[34] Vedat Tavşanoğlu, "*Digital Filter Design*," lecture notes

[35] MIKROELECTRONIKA, "*Basic Concepts of Digital Filtering,*" e-boo k
http://learn.mikroe.com/ebooks/digitalfilterdesign/chapter/basic-concepts-of-digital-filtering/

[36] "The Engineering Project, Complete Tutorial on Proteus ISIS and ARES, "
http://www.theengineeringprojects.com/2013/03/a-complete-tutorial-on-how-to-use.html

[37] Plessey Semiconductor, Electric Potential Integrated Circuit
http://www.saelig.com/supplier/plessey/PS25201A.pdf

[38] Analog Devices instrumentation amplifier, AD627BRZ datasheet
http://www.analog.com/media/en/technical-documentation/data-sheets/AD627.pdf

[39] Texas Instruments operational amplifier, OPA2379 datasheet
http://www.ti.com.cn/general/cn/docs/lit/getliterature.tsp?genericPartNumber=opa379&fileType=pdf

[40] MICROCHIP microcontroller, dsPIC30f3011 datasheet
http://ww1.microchip.com/downloads/en/DeviceDoc/70141c.pdf

[41] Huang X., Acero A., and Hon H.W., "*Spoken Language Processing: A Guide to Theory, Algorithm, and System Development,*" Prentice-Hall, ISBN: 0-13-022616-5, 2001.

[42] Bishop C.M., "Pattern Recognition and Machine Learning," Springer, ISBN-13: 978-0387-31073-2, 2006.

[43] Cunningham P. And Delany S. J., "k-Nearest Neighbour Classifiers," *Technical Report, University College Dublin*, UCD-CSI-2007-4, Mach 27, 2007

[44] Pan J. and Tompkins W. J., "A Real-Time QRS Detection Algorithm," *IEEE Transactions on Biomedical Engineering*, vol. 32, no.3, pp. 230-236, 1985.

[45] Hakan Gurkan, Umit Guz and B.S. Yarman, "A novel Biometric Authentication Approach Using Electrocardiogram Signals", 35th Annual International IEEE EMBS Conference, February 4 2013

[46] Butterworth Lowpass Filter Frequency Response, https://tr.wikipedia.org/wiki/Butterworth_filtre#/media/File:Butterworth_Filter _Orders.svg

[47] Gain and group delay of a fifth-order type I Chebyshev filter, https://en.wikipedia.org/wiki/Chebyshev_filter#/media/File:Chebyshev5_Gain Delay.png

[48] XP IA0503D DC-DC Voltage Converter datasheet http://www.xppower.com/Portals/0/pdfs/SF_IA.pdf

[49] USB Serial Adapter FT232rl datasheet http://www.ftdichip.com/Support/Documents/DataSheets/ICs/DS_FT232R.pdf

[50] Multicomp 7.37 Mhz crystal datasheet, http://www.farnell.com/datasheets/1661828.pdf

[51] CEL Photocoupler PS2501 datasheet, http://www.cel.com/pdf/datasheets/ps2501.pdf

[52] Lippincott and Wilkins , Wolters Kluwen Heart, "ECG Strip Ease - An Arrhythmia Interpretation Workbook "

Appendix A

Selection of Microcontroller
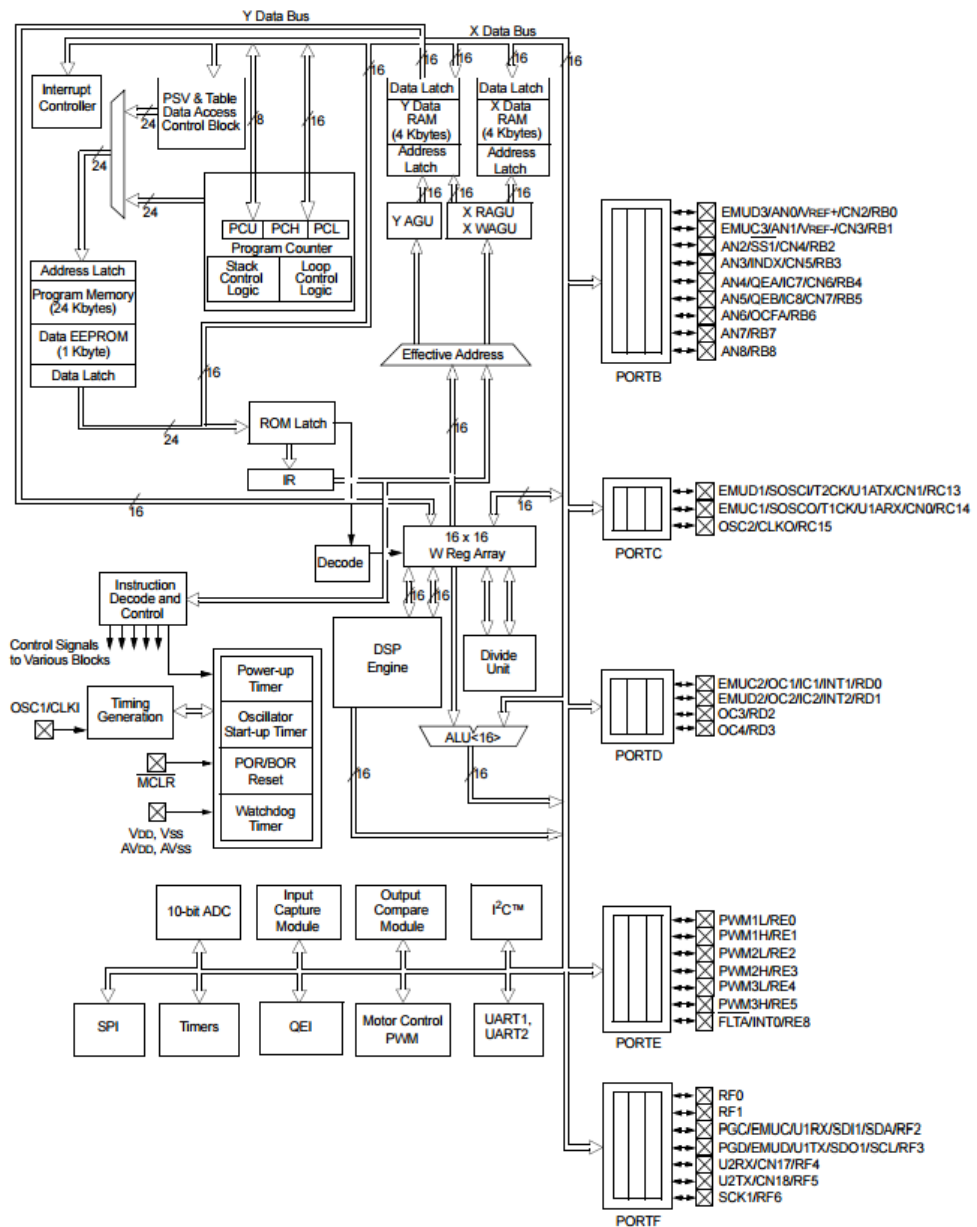
Figure 74: Block Diagram of dsPIC30f3011 Microcontroller [40]

Microchip dspic30f3011 microcontroller is 44-pin device and it has thirty output pins which are 3 pins PORTC, 9 pins PORTB and 7 pins PORTE, 4 pin PORTD ,and 7 pin PORTF. dsPIC30f3011 have five I/O port, twenty nine interrupt (3 external interrupt sources, 8 users selectable priority levels for each interrupt source ,4 processor trap sources), and nine 10 bits A/D input channels. dspic30f3011 can be programmed by using Micro C, JAL, ASM, CCS C programming languages. The purpose of choosing the dsPIC30F3011 is mainly being low cost product among the other dsPICs can be found easily in Turkey, and in MicroC there are filter methods for dsPIC products.

Basic configuration of dsPIC30F3011

44-Pin TQFP
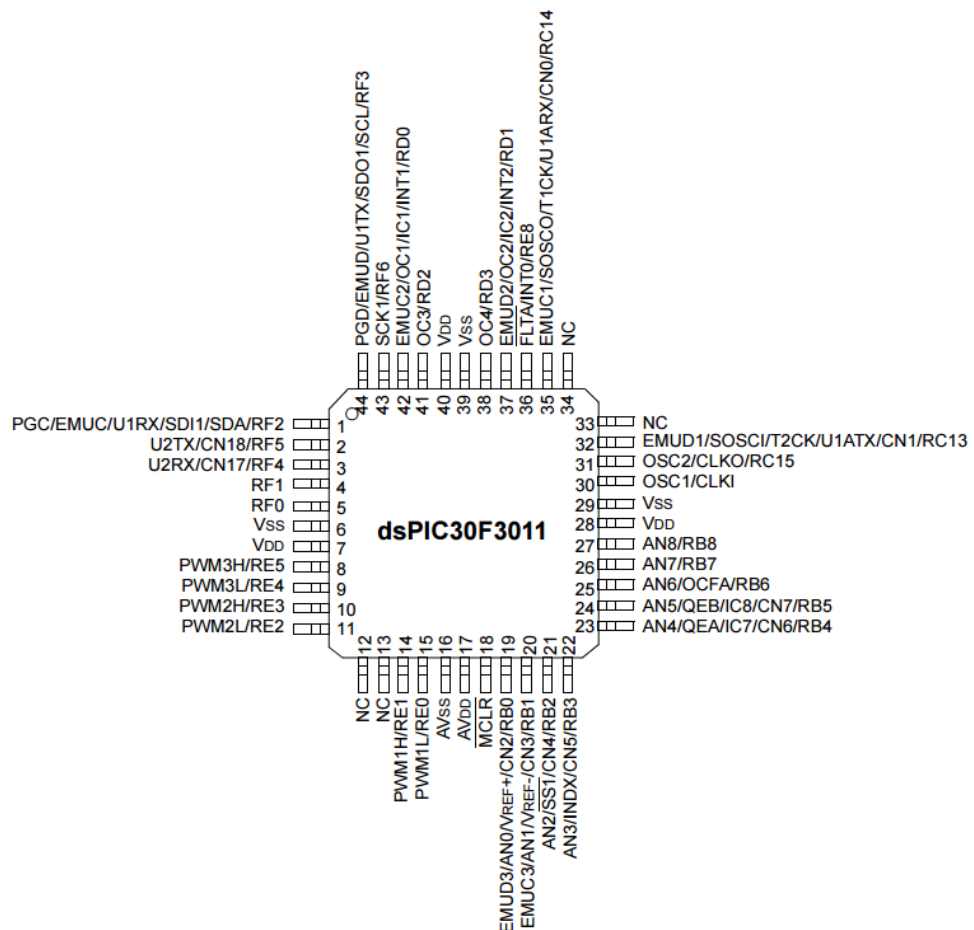
Figure 75: Pin Diagram of dsPIC30F3011 Microcontroller **[40]**

First it is needed to be known that dsPICs are microcontroller and all of microcontroller such as motherboard of a PC needs a processor. dsPIC30F3011 also needs a processor, and RC combination as an oscillator or crystal oscillator which is specifically produced for microcontroller can be used.

Crystal oscillators are kept in a metal case and have two pins. These two pins are connected to the OSC1, OSC2 ports of dsPIC and 30 pF ceramic capacitors whose other end is connected to ground needs to be attached on pins of the crystal oscillator. 7.37 MHz crystal is used on dsPIC oscillation pins. In dsPIC, there are PLL 2, PLL 4, PLL 8 and PLL 16 options which increase the microprocessor's working frequency by multiplying the external clock (oscillator) with 2, 4, 8 or 16. dsPIC30F3011 microcontroller's maximum clock frequency can be 120 MHz by using 7.37 MHz with PLL 16 option. 120 MHz (120/4= 30 MIPs) clock frequency was used to increase the speed of digital filters functions in the MicroC program.
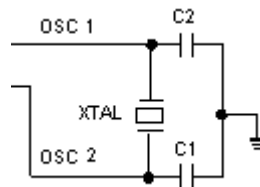
Figure 76: Basic configuration of Microcontrollers **[40]**

RC circuit can be used as an oscillator. In applications when precision isn't necessary, RC oscillator can be used to decreasing the cost of the circuit. However frequency of RC oscillators depends on the calculations. The value of resistor and capacitor are needed to be calculated with respect to power supply voltage which is applied on them. No matter which frequency applied to dsPIC with RC oscillators, in order to get a clock to work microcontroller, clock of oscillator must divided by four. If 4 Mhz frequency is applied with RC oscillators, PIC senses it as 1 MIPs frequency. That means that only one command of the ASM language is being processed in 1usec (1/1000000) by PIC.
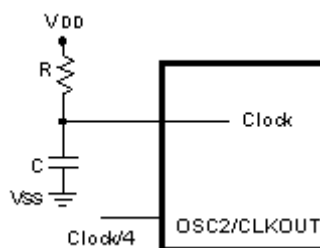

Figure 77: Basic configuration of Microcontrollers **[40]**

dsPIC30F3011 microcontroller's 7th, 17th, 28th, and 40th pins are VDD which should be connected to voltage source in the range of 2.5 Volt to 5.5 Volt. dsPIC30F3011 microcontroller's 6th, 16th, 29th and 39th pins are VSS which should be connected to ground.

dsPIC has a reset pin which named as MCLR. For dsPIC30F3011 working, MCLR pin is needed to be connected to power supply with 10 K resistor. When MCLR pin of the dsPIC connect to ground, the program of the PIC won't work because of getting reset.

Microcontroller has also several sources of resets

1- Power on Reset: Reset during power on (POR)
2- Reset during sleep regime
3- Reset when Watch dog timer overflow
4- Reset by using CLRWDT command
5- Brown out reset: BOR does automatically reset the chip when the power coming to microcontroller isn't sufficient to work

These reset sources can be changed manually while programming to microcontroller. In most of the applications, Brown out reset and Watch dog reset are closed not to reset the dsPIC when there are other devices which draining the current the most [40].

Appendix C

Amplifier

C.1 Operational Amplifier

Op-Amps (Operational Amplifier) are high gain electronic voltage amplifier with a different input. It can use for produce an output potential with respect to ground which is hundreds or thousands of times larger than the potential difference between inputs of op-amp. Op-amps are consists of identical transistors and resistors in a package which is shown as
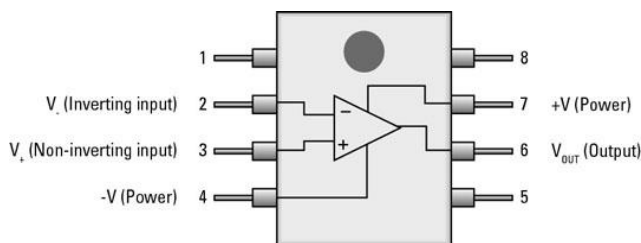

Figure 78: Op-amp Block diagram **[39]**	Figure 79: Smd Package **[39]**

There are many package types like SOIC-8, SOT-32, DIP-8, VSSOP etc. SOIC-8 package type was used to minimize the circuit board. Except DIP package, the other package types are known as surface-mount component. They are directly soldered on the board without drilling hole on the surface. For this reasons, these components make the circuit small.

C.1.1 Op-amp Selection
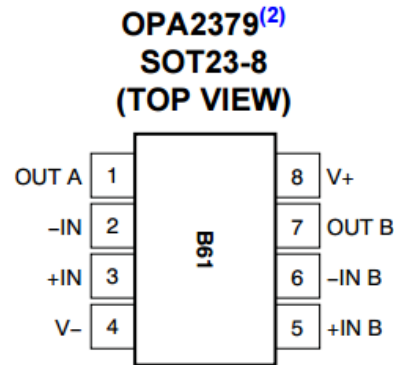
Figure 80: Component Side (Top View) of OPA2379   **[39]**

OPA2379 (SOIC-8 package type) chip which in one package there are 2 operational amplifier, is used in the project.

Specifications of the OPA2379 are [40]

- Low noise 2.8 μV_{pp} $(0.1\ Hz - 10\ Hz)$
- $80\ nV/\sqrt{Hz}$ of wideband noise
- 100 dB CMRR
- Wide Supply Voltage Range: 1.8 V – 5.5 V

It has single-supply operational capability which means negative voltage for doing low pass and high pass analog filtering are not needed to be given. But there is a disadvantage of single supply operational amplifier which is; if an analog bandreject filter is wanted to be done, it won't work with single supply mode. To do an analog band-reject filter, double supply op-amp is need to be chosen and positive and negative voltages on op-amp have to be given. If it don't, bandreject filters' frequency response will not match with the calculated result.

C.2 Instrumentation Amplifier

Instrumentation amplifiers are types of differential amplifier which consist of input buffer op-amp, that eliminate the need of input impedance matching, so this makes the amplifier especially suitable to use of precise measurement. They have also additional characteristics such as low DC offset, low noise, high CMRR (common mode rejection ratio), high open-loop gain and high input impedance. They are used when high precision, accuracy and stability are needed. Instrumentation Amplifier consists of identical op-amps and identical resistors which is shown below [32]
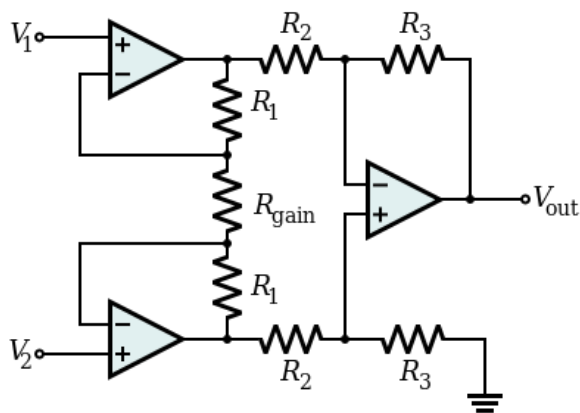
Figure 81: Basic Schematic of Instrumentation Amplifier   **[32]**

The gain calculation for the Instrumentation amplifier above is [38]

$$\frac{V_{out}}{V_2 - V_1} = \left(1 + \frac{2R_1}{R_{gain}}\right)\frac{R_3}{R_2} \tag{C.1}$$

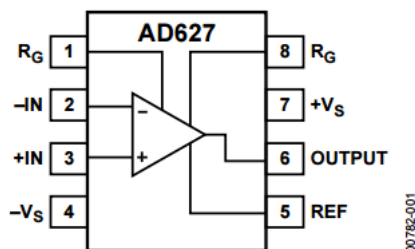## C.2.1 Instrumentation Amplifier Selection

Figure 1. 8-Lead PDIP (N) and SOIC_N (R)

Figure 82: Component Side (Top View) of AD627   **[38]**

AD627BRZ is used for instrumentation amplifier (SOIC-8 package type) because of high accuracy dc performance, high common mode rejection ratio, and high gain. Specifications of the AD627BRZ are [38]

- *Low noise* $38 \, nV/\sqrt{Hz} \, at \, 1Khz$
- 83 dB CMRR
- Wide Supply Voltage Range: $(\pm 2.2 \, V - \pm 18 \, V)$
- Easy to calculate gain

If we look at the schema of the AD627, there are pins named RG which determines the instrumentation amplifier gain by changing the resistor value attached on RG points.

Gain calculation for AD627 is shown on its datasheet as

$$V_{out} = [V_{in}(+) - V_{in}(-)]x(5 + 200k\Omega/R_G) + \; V_{ref}$$

(C.2)

$$R_G = 200k\Omega/(Gain - 5)$$

(C.3)

Recommended Values of Gain Resistors

Desired Gain	1% Standard Table Value of R_G	Resulting Gain
5	∞	5.00
6	200 kΩ	6.00
7	100 kΩ	7.00
8	68.1 kΩ	7.94
9	51.1 kΩ	8.91
10	40.2 kΩ	9.98
15	20 kΩ	15.00
20	13.7 kΩ	19.60
25	10 kΩ	25.00
30	8.06 kΩ	29.81
40	5.76 kΩ	39.72
50	4.53 kΩ	49.15
60	3.65 kΩ	59.79
70	3.09 kΩ	69.72
80	2.67 kΩ	79.91
90	2.37 kΩ	89.39
100	2.1 kΩ	100.24
200	1.05 kΩ	195.48
500	412 Ω	490.44
1000	205 Ω	980.61

Table 8: Recommended Values of Gain Resistors for AD627 Instrumentation Op-amp **[38]**

It can be seen in the formula above, minimum achievable gain is 5. Changing the resistor value of Rg will determine the gain of the AD627BRZ. Despite of maximum gain determined as 1000, the 500 gain value should not be exceeded. The more the gain is increased, the more instrumentation amplifier will be unstable.

107

Appendix D

Other Circuit Components

D.1 DC-DC Isolated Voltage Regulator

It converts 5 Volt DC voltages into +3.3 volt and -3.3 volt in order to supply the op-amp positive and negative pins. Also, situation of over DC input voltage and over DC input current condition; it can isolate input and output voltage not to harm patients while patients are holding the circuit.
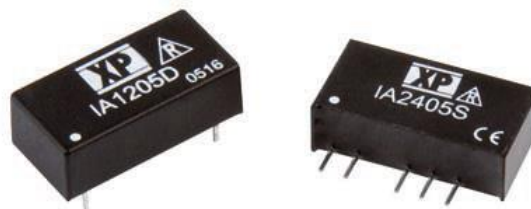

Figure 83: DC-DC Isolated Voltage Regulator **[48]**

D.2 FT232RL USB Serial Adapter

It is an adapter that simple and inexpensive way to convert dsPIC Serial Port to USB connection. It does not need external crystal, has an integreted EEPROM (internal memory) for Device ID. FT232RL chips provide 2 data input lines which are RxD and TxD that are connected to dsPIC UART ports. USB port can provide 5 volt 500 mA power for both FT232RL and microcontroller without any need of voltage converter. PC recognize the FT232RL as virtual COM port in device manager, so this makes easy to send and receive data by using serial port commands both PC and microcontroller side.
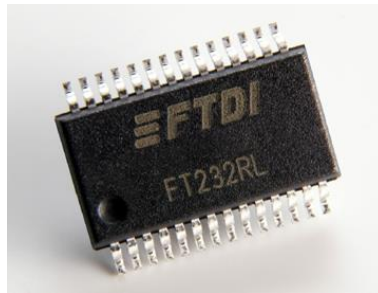
Figure 84: FT232RL USB Serial Adapter **[49]**

D.3 Crystal Oscillator

It is an electronic oscillator circuit which uses mechanical resonance of vibrating crystal to create a precise frequency for microcontroller. They work like microprocessor for microcontroller. Most common frequencies are 4 MHz, 7.37 MHz, 8 MHz, 12 MHz, 16 MHz, 20 MHz, and 40 MHz.
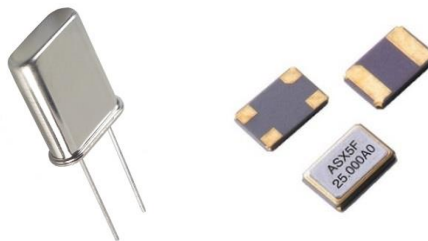

Figure 85: Crystal Oscillator **[50]**

D.4 SMD LED

It is a semiconductor component which converts applied voltage to light. It has two pins (anode and cathode). There are many package types of SMD LEDs such as 0402 metric, 0603 metric, 1005 metric, 1608 metric etc. I used 1608 metric (0603 imperial) SMD LEDs and resistors in ECG circuit.

Figure 86: SMD LED

D.5 SMD Capacitor

Capacitors are known as components which store electrical energy temporarily in an electric field. The sizes of capacitors vary widely according to the amount of load it carries. The forms of capacitors also vary with different specifications. For designing analog filtering, Non-polarized capacitors are used for increasing life of circuit. There is a fact that if polarized capacitor is attached with reverse polarization, no matter how low voltage is given, it will break the capacitor after a while later.

Figure 87 : SMD Capacitor

D.6 Opto-coupler

Optocoupler is also known as opto-isolator, photocoupler or optical isolator. It is electronic component which transfers electrical signals to the light emitting diode or transistor by using light. It is used for isolating noise on opto-coupler's transistor side. Most common type of opto-couplers consist of LED, phototransistor and photodiode.The figure below is an example of analog opto-coupler.
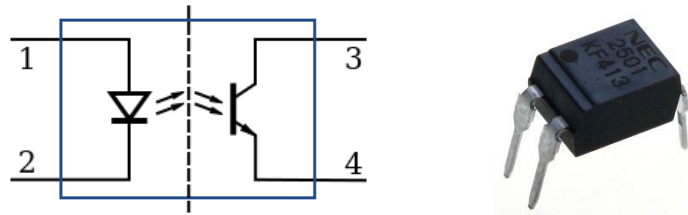
Figure 88: Analog Opto-coupler [**51**]

Appendix E

Normalized Denominator Polynomials in Factored Form

n (order)	Normalized Denominator Polynomials in Factored Form
1	$(1+s)$
2	$(1+1.414s+s^2)$
3	$(1+s)(1+s+s^2)$
4	$(1+0.765s+s^2)(1+1.848s+s^2)$
5	$(1+s)(1+0.618s+s^2)(1+1.618s+s^2)$
6	$(1+0.518s+s^2)(1+1.414s+s^2)(1+1.932s+s^2)$
7	$(1+s)(1+0.445s+s^2)(1+1.247s+s^2)(1+1.802s+s^2)$
8	$(1+0.390s+s^2)(1+1.111s+s^2)(1+1.663s+s^2)(1+1.962s+s^2)$
9	$(1+s)(1+0.347s+s^2)(1+s+s^2)(1+1.532s+s^2)(1+1.879s+s^2)$
10	$(1+0.313s+s^2)(1+0.908s+s^2)(1+1.414s+s^2)(1+1.782s+s^2)(1+1.975s+s^2)$

Table 9: Butterworth Polynomials in Factored Form [**33**]

Appendix F

EPIC Ultra High Impedance ECG Sensor

PS25201A ECG sensors are the product of Plessey Semiconductors Electric Potential Integrated Circuit (EPIC). It is an ultra-high impedance solid state ECG sensor. It is used as a dry contact with no need for potentially dangerous low impedance circuit across the heart. Its resolution is as good as disposable wet electrodes [37].

Specifications are

- 20 $G\Omega$ Ultra high input resistance
- Dry-contact capacitive coupling
- Input capacitance as low as 15 pF
- Lower cut-off frequency point is 0.2 Hz
- Higher cut-off frequency point is 10 KHz
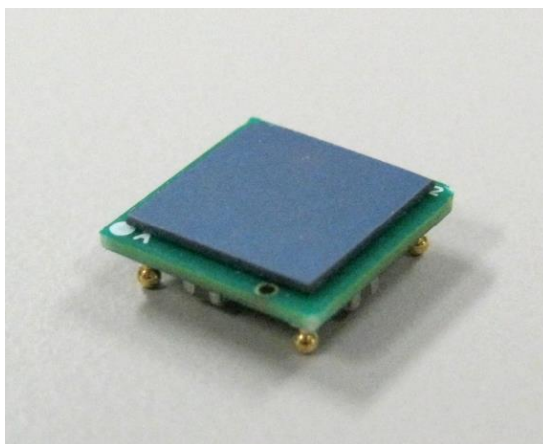- Operates with bipolar power supply from $\pm 2.4\,V$ to $\pm 4.0\,V$
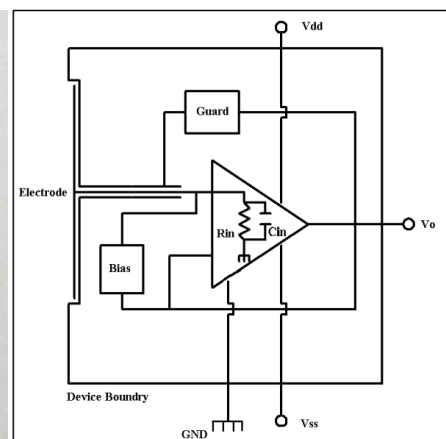

Figure 89: PS25201A ECG Sensor [**37**]   Figure 90: Internal Circuit of ECG Sensor [**37**]

Characteristics	Value			Units	Conditions
	Min.	Typ.	Max.		
Supply voltage	±2.4		±4.0	V	Bipolar supply, Gnd=0V
Supply current	1.5	2.5	3.5	mA	
Effective input resistance		20		GΩ	
Effective input capacitance		15		pF	
Voltage Gain (Av)		50			
Coupling capacitance		250		pF	Sensor to skin
Lower -3dB point		0.20		Hz	Set by internal DC signal rejection network – coupling capacitor 250pF
Upper -3dB point		10.0		kHz	
Noise		tbd			

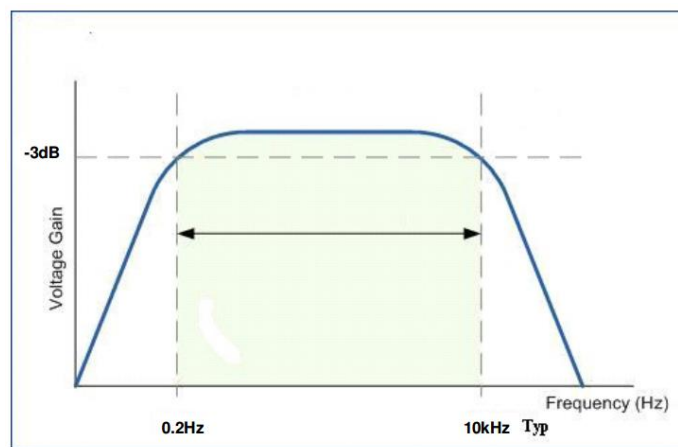Table 10: Electrical Characteristic of ECG Sensor **[37]**

Figure 91: Bode plot of EPIC ECG Sensor **[37]**

From the bode plot of ECG Sensor, it can be said that ECG Sensor has an internal 0.2 Hz highpass filter and 10 KHz lowpass filter.

114

Curriculum Vitae

Gökhan Güven was born on 20th December 1989 in İstanbul, Turkey. He received his BS degree in Electrical and Electronics Engineering in 2014. Since 2014, he had worked as a research assistant at the department of Electronics Engineering of Işık University from 2014 to 2016.